

## Frequent truncating mutations of *STAG2* in bladder cancer

David A Solomon<sup>1,2</sup>, Jung-Sik Kim<sup>1</sup>, Jolanta Bondaruk<sup>3</sup>, Shahrokh F Shariat<sup>4,5,18</sup>, Zeng-Feng Wang<sup>6</sup>, Abdel G Elkahlon<sup>7</sup>, Tomoko Ozawa<sup>8</sup>, Julia Gerard<sup>1</sup>, DaZhong Zhuang<sup>4</sup>, Shizhen Zhang<sup>3</sup>, Neema Navai<sup>9</sup>, Arlene Siefker-Radtke<sup>10</sup>, Joanna J Phillips<sup>2</sup>, Brian D Robinson<sup>4,11</sup>, Mark A Rubin<sup>4,11</sup>, Björn Volkmer<sup>12</sup>, Richard Hautmann<sup>13</sup>, Rainer Küfer<sup>14</sup>, Pancras C W Hogendoorn<sup>15</sup>, George Netto<sup>16</sup>, Dan Theodorescu<sup>17</sup>, C David James<sup>8</sup>, Bogdan Czerniak<sup>3</sup>, Markku Miettinen<sup>6</sup> & Todd Waldman<sup>1</sup>

**Here we report the discovery of truncating mutations of the gene encoding the cohesin subunit *STAG2*, which regulates sister chromatid cohesion and segregation, in 36% of papillary non-invasive urothelial carcinomas and 16% of invasive urothelial carcinomas of the bladder. Our studies suggest that *STAG2* has a role in controlling chromosome number but not the proliferation of bladder cancer cells. These findings identify *STAG2* as one of the most commonly mutated genes in bladder cancer.**

Inactivating mutations of the cohesin complex gene *STAG2* have recently been identified in human cancer and were demonstrated to cause chromosome segregation defects and aneuploidy<sup>1–3</sup>. To identify additional tumor types with inactivation of the *STAG2* gene, we screened 2,214 human tumors by immunohistochemistry using a monoclonal antibody to *STAG2* that binds at the C terminus of the protein. As the *STAG2* gene is on the X chromosome, complete genetic inactivation of *STAG2* requires only a single mutational event. Virtually all tumor-derived *STAG2* mutations discovered so far are truncating (for example, nonsense, frameshift or splice site) and lead to absence of the C-terminal epitope and, therefore, loss of expression as detected by immunohistochemistry with the monoclonal antibody<sup>1</sup>. *STAG2* was robustly expressed specifically in the nucleus in all non-neoplastic tissues studied (examples shown in **Supplementary Figs. 1 and 2**).

We discovered that 52 of 295 urothelial carcinomas of the bladder (18%) had complete loss of *STAG2* expression (**Supplementary Fig. 3**

and **Supplementary Table 1**). Occasional loss of *STAG2* expression was also found in several other tumor types (**Supplementary Figs. 4–6**). Urothelial carcinomas that had negative staining for *STAG2* included tumors with a wide range of stages and grades, from low-grade, non-invasive papillary tumors to high-grade, muscle-invasive tumors. In each case with loss of *STAG2* expression, non-neoplastic stroma and endothelial cells retained expression, demonstrating the somatic nature of *STAG2* loss in these tumors. *STAG2*-negative bladder tumors stained positively with antibodies to the constitutively expressed nuclear protein Ini-1, demonstrating intact immunoreactivity for other nuclear antigens (**Supplementary Fig. 7**). In the vast majority of cases, all tumor cells were negative for *STAG2* expression; however, in a small number of cases (2/52), there was evidence of mosaicism (intratumoral heterogeneity), with some regions of the tumor retaining expression of *STAG2* (**Supplementary Fig. 8**). Whereas tumors with complete loss of *STAG2* suggest that inactivation occurred as an early, initiating event in these cases, the small number of mosaic tumors suggests that *STAG2* can occasionally be inactivated during the early progression stage of urothelial tumorigenesis.

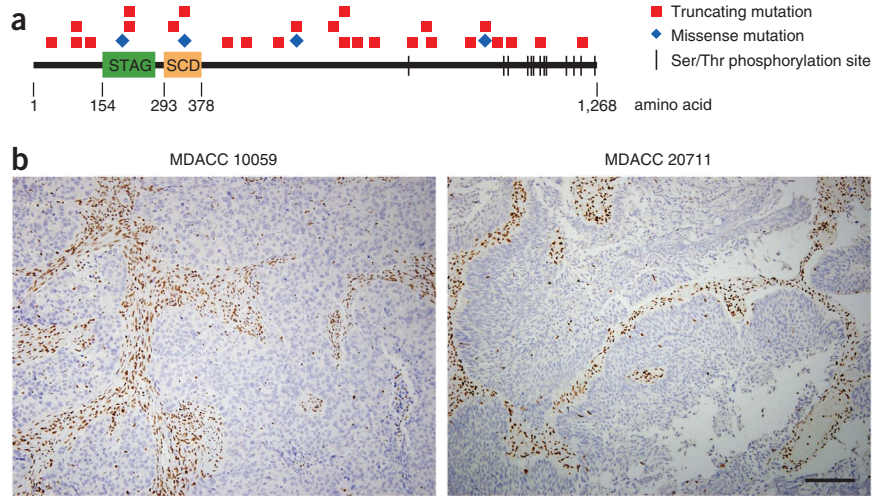
To determine the mechanism underlying the loss of *STAG2* expression, we used Sanger sequencing to analyze the *STAG2* gene in genomic DNA purified from an independent cohort of 111 primary urothelial carcinomas of various grades and stages (clinicopathological characteristics of the tumors are given in **Supplementary Table 2**). We identified 25 mutations in 23 of the cases, with 2 samples each harboring 2 independent mutations (**Fig. 1a** and **Supplementary Table 3**). Apart from known SNPs, no synonymous mutations were identified. Twenty-one of the 25 mutations resulted in premature truncation of the encoded protein, including 5 nonsense, 6 splice-site and 10 frameshift mutations (**Supplementary Fig. 9**). All mutations were shown to be somatic in samples with matched constitutional DNA (8 samples; **Supplementary Table 3**). Mutations were identified in 9 of 25 (36%) pTa non-invasive papillary carcinomas, 6 of 22 (27%) pT1 superficially invasive carcinomas and 8 of 64 (13%) pT2–pT4 muscle-invasive carcinomas. Tumors with truncating *STAG2* mutations were negative for *STAG2* expression via immunohistochemistry (examples are shown in **Fig. 1b** and **Supplementary Fig. 10**). Tumors with missense mutations retained expression of *STAG2* by immunohistochemistry, demonstrating that immunohistochemistry

<sup>1</sup>Department of Oncology, Lombardi Comprehensive Cancer Center, Georgetown University School of Medicine, Washington, DC, USA. <sup>2</sup>Department of Pathology, University of California, San Francisco, San Francisco, California, USA. <sup>3</sup>Department of Pathology, University of Texas MD Anderson Cancer Center, Houston, Texas, USA. <sup>4</sup>Department of Urology, Weill Cornell College of Medicine, New York, New York, USA. <sup>5</sup>Division of Medical Oncology, Weill Cornell College of Medicine, New York, New York, USA. <sup>6</sup>Laboratory of Pathology, National Cancer Institute, Bethesda, Maryland, USA. <sup>7</sup>Cancer Genetics Branch, National Human Genome Research Institute, Bethesda, Maryland, USA. <sup>8</sup>Department of Neurological Surgery, University of California, San Francisco, San Francisco, California, USA. <sup>9</sup>Department of Urology, University of Texas MD Anderson Cancer Center, Houston, Texas, USA. <sup>10</sup>Genitourinary Medical Oncology, University of Texas MD Anderson Cancer Center, Houston, Texas, USA. <sup>11</sup>Department of Pathology, Weill Cornell College of Medicine, New York, New York, USA. <sup>12</sup>Department of Urology, Hospital Kassel, Kassel, Germany. <sup>13</sup>Department of Urology, University Hospital Ulm, Ulm, Germany. <sup>14</sup>Department of Urology, Hospital Am Eichert, Göppingen, Germany. <sup>15</sup>Department of Pathology, Leiden University Medical Center, Leiden, The Netherlands. <sup>16</sup>Department of Pathology, Johns Hopkins University School of Medicine, Baltimore, Maryland, USA. <sup>17</sup>Department of Surgery, University of Colorado Cancer Center, University of Colorado School of Medicine, Aurora, Colorado, USA. <sup>18</sup>Present address: Department of Urology, Medical University of Vienna, Vienna, Austria. Correspondence should be addressed to T.W. (waldmant@georgetown.edu).

Received 19 March; accepted 18 September; published online 13 October 2013; doi:10.1038/ng.2800

**Figure 1** Frequent truncating mutations of *STAG2* in urothelial carcinoma of the bladder. (a) Diagram of the *STAG2* protein with the locations shown for the alterations in urothelial carcinomas identified in this study. STAG, stromal antigen domain; SCD, stromal in conserved domain.

(b) Examples of complete somatic loss of *STAG2* expression by immunohistochemistry in two urothelial carcinomas harboring truncating mutations of *STAG2* (nonsense mutation in MDACC 10059 and canonical splice acceptor mutation in MDACC 20711; **Supplementary Fig. 10**). Expression is retained within the non-neoplastic fibrovascular stroma in each case. Scale bar, 100  $\mu$ m.



does not identify the ~15% of *STAG2*-mutant tumors with missense mutations of the gene (**Supplementary Fig. 11**). Truncating mutations were also observed in 5 of 32 urothelial carcinoma cell lines (**Supplementary Fig. 12**). Tumors and cell lines with *STAG2* mutations frequently had concurrent p53 overexpression or mutation (**Supplementary Fig. 13** and **Supplementary Table 3**).

Next, we performed molecular cytogenetic analysis on 12 primary urothelial carcinomas with *STAG2* mutations and 12 stage-matched tumors with wild-type *STAG2*. Genomic DNA was interrogated using Affymetrix CytoScan HD Arrays, and chromosomal gains and losses were scored for each sample (**Supplementary Figs. 14** and **15** and **Supplementary Table 4**). Nine of the 12 *STAG2*-mutant tumors studied had overt aneuploidy, with up to 35 clonal chromosomal aberrations in a single tumor, whereas 3 tumors with *STAG2* mutations did not contain detectable chromosomal aberrations. Ten of the 12 tumors with wild-type *STAG2* also contained chromosomal copy number aberrations, demonstrating that there are other pathways whose perturbation also leads to aneuploidy in bladder cancer.

We then constructed a *STAG2*-expressing lentivirus and infected UM-UC-3, UM-UC-14 and VM-CUB-3 cells, three urothelial carcinoma cell lines with truncating mutations of *STAG2* (**Fig. 2a** and **Supplementary Fig. 16**). Ectopic re-expression of *STAG2* had no adverse effect on cellular proliferation or *in vivo* growth when cells were injected into mice as subcutaneous xenografts (**Fig. 2b** and **Supplementary Fig. 16**). Ectopic re-expression of *STAG2* did not overtly reduce the degree of aneuploidy (**Supplementary Fig. 17**), perhaps because, once aneuploidy is established, it is thought to be

largely self-sustaining. In contrast, depletion of wild-type *STAG2* via lentivirally expressed short hairpin RNA (shRNA) led to a distinct alteration in the modal chromosome number of RT4 urothelial carcinoma cells (**Fig. 2c,d** and **Supplementary Fig. 18**). Taken together, these functional experiments provide support for the hypothesis that *STAG2* may have a role in controlling chromosomal stability but not in the proliferation of bladder cancer cells.

We next determined the status of *STAG2* expression in a panel of 34 papillary non-muscle-invasive urothelial carcinomas treated by transurethral resection with a median follow-up of 54 months (clinicopathological features of these tumors are given in **Supplementary Table 5**). In this cohort, loss of *STAG2* expression was significantly associated with increased disease-free survival ( $P = 0.05$ ; **Supplementary Fig. 19**). Only 1 of 8 of the *STAG2*-deficient carcinomas (12%) recurred (as a non-invasive carcinoma), whereas 15 of 26 of the *STAG2*-expressing carcinomas (58%) recurred (2 recurred as invasive carcinomas, and 4 metastasized).

We then determined the status of *STAG2* expression in a clinically annotated panel of 349 invasive urothelial carcinomas treated by radical cystectomy with a median follow-up of 130 months (clinicopathological features of these tumors are given in **Supplementary Table 6**). In these invasive tumors, loss of *STAG2* expression was significantly associated ( $P = 0.03$ ) with increased frequency of metastasis to the lymph node. Immunohistochemistry analysis of paired primary tumors and lymph node metastases demonstrated that loss of *STAG2*

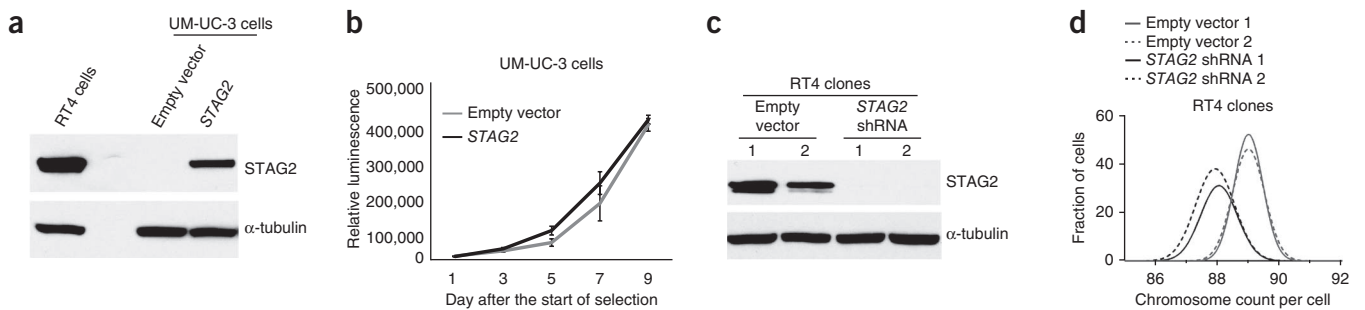


**Figure 2** Effects of *STAG2* inactivation on proliferation and chromosomal stability in urothelial cancer cells. (a) Protein blot showing lentiviral re-expression of wild-type *STAG2* in UM-UC-3 cells, which harbor an endogenous truncating mutation in *STAG2*. The level of re-expression is comparable to the endogenous level of *STAG2* protein in RT4 cells, which have a wild-type *STAG2* gene. (b) Proliferation of pooled UM-UC-3 clones infected with either empty lentivirus or lentivirus expressing *STAG2* after 5 d of selection in puromycin, measured via CellTiter-Glo assay. Error bars, s.d. (c) Protein blot showing the expression of endogenous *STAG2* in individual clones of RT4 cells after infection with either empty lentivirus or lentivirus expressing *STAG2* shRNA. (d) Gaussian distribution plots depicting chromosome numbers per cell in the individual RT4 cell clones in c. Chromosome counts for 100 cells were determined in metaphase spreads for each clone. Individual chromosome numbers are listed in **Supplementary Figure 18**.

expression occurred in the primary tumor before lymphovascular invasion (**Supplementary Fig. 20**). Loss of *STAG2* expression was also associated with increased risk of disease recurrence ( $P = 0.04$ ) and with cancer-specific mortality ( $P = 0.04$ ; **Supplementary Fig. 21**). The biological basis for the different effects of *STAG2* expression on the clinical outcomes of non-muscle-invasive papillary carcinomas versus muscle-invasive carcinomas is currently unknown.

Bladder cancer is the fifth most common human malignancy in the United States, with approximately 74,000 new cases diagnosed each year and approximately 15,000 deaths<sup>4</sup>. Bladder cancer is thought to arise via two different pathways—from papillary lesions that frequently recur but only 15–20% of which progress to muscle invasion and from flat dysplastic lesions (carcinoma *in situ*) that directly progress to muscle invasion without a papillary precursor lesion. The majority of bladder cancers are papillary non-invasive tumors; clinical management of these tumors poses a serious dilemma because it is not currently possible to prospectively determine whether a tumor will recur or progress to invasion.

It is notable that *STAG2* mutations occur and are most common in early-stage bladder cancers, including non-invasive papillary carcinomas. As such, we suggest that *STAG2* mutation is an early event in bladder tumorigenesis. Furthermore, our data suggest that the major mechanism for *STAG2* inactivation in bladder cancer is somatic truncating (~85%) and missense (~15%) mutations (rather than homozygous deletion or promoter hypermethylation), as all *STAG2*-deficient cell lines and primary tumors studied harbored truncating mutations in the gene.

Whether mutations in *STAG2* are a direct cause of aneuploidy in human cancer is currently a source of controversy because a subset of *STAG2*-deficient acute myeloid leukemias and urothelial carcinomas appear to be diploid (refs. 2,5 and **Supplementary Table 4**). Despite these surprising observations, there are several lines of evidence supporting a direct role for *STAG2* inactivation in aneuploidy in cancer. In yeast, mutation of cohesin complex genes causes aberrant chromosome segregation and aneuploidy<sup>6,7</sup>. Recently, a mouse harboring genetic inactivation of *Stag1*, a homolog of *Stag2*, was generated that has increased aneuploidy due to chromosome segregation defects<sup>8</sup>. Targeted inactivation of *STAG2* in HCT116 colon cancer cells and depletion of *STAG2* in RT4 bladder cancer cells leads to alterations in modal chromosome number (ref. 1 and **Fig. 2d**). Also, ectopic expression of *STAG2* has no adverse effect on cellular proliferation or *in vivo* growth (**Fig. 2b** and **Supplementary Fig. 16**), and targeted correction of endogenous mutant *STAG2* in two cancer cell lines resulted in no significant change in global gene expression profiles, arguing against a role for *STAG2* in controlling signaling pathways, cellular proliferation, apoptosis or other transformation-associated processes<sup>1</sup>.

Finally, this discovery has potentially important clinical applications, as a major problem in the treatment of bladder cancer has been

the identification of those 15–20% of papillary tumors that will recur and progress to invasion versus the 80–85% that will not. Here we report that *STAG2* is mutationally inactivated in more than one-third of papillary non-invasive bladder tumors and that these tumors with *STAG2* loss rarely recur or progress, perhaps explaining the difference in the frequencies of *STAG2* inactivation in non-invasive urothelial carcinomas (36%) compared to in invasive urothelial carcinomas (16%). As the immunohistochemical assay for loss of *STAG2* expression is robust and routine clinical sequencing of tumors is imminent, the discovery reported here may have near-term implications for the clinical management of patients with bladder cancer.

## METHODS

Methods and any associated references are available in the [online version of the paper](#).

**Accession codes.** Scanned array images and processed data sets have been deposited in the Gene Expression Omnibus (GEO) under accession [GSE41581](#).

*Note: Any Supplementary Information and Source Data files are available in the online version of the paper.*

## ACKNOWLEDGMENTS

We thank B. Vogelstein for assistance in acquiring samples and preparing genomic DNA. This work was supported by US National Institutes of Health grants R01CA169345, R01CA159467 and R21CA143282 to T.W., by the MD Anderson Cancer Center Bladder Cancer SPORE grant P50CA091846 and by the Intramural Research Program of the National Human Genome Research Institute, US National Institutes of Health.

## AUTHOR CONTRIBUTIONS

D.A.S., J.-S.K., J.B., S.F.S., C.D.J., B.C., M.M. and T.W. designed research. D.A.S., J.-S.K., J.B., Z.-F.W., A.G.E., T.O., J.G., D.Z., S.Z. and J.J.P. performed research. J.B., S.F.S., D.Z., M.A.R., B.V., R.H., R.K., P.C.W.H., G.N., D.T., B.C. and M.M. contributed new reagents and analytic tools. D.A.S., J.-S.K., S.F.S., A.G.E., N.N., A.S.-R., B.D.R., C.D.J., M.M. and T.W. analyzed data. D.A.S., S.F.S. and T.W. wrote the manuscript.

## COMPETING FINANCIAL INTERESTS

The authors declare competing financial interests: details are available in the [online version of the paper](#).

Reprints and permissions information is available online at <http://www.nature.com/reprints/index.html>.

- Solomon, D.A. *et al. Science* **333**, 1039–1043 (2011).
- Walter, M.J. *et al. N. Engl. J. Med.* **366**, 1090–1098 (2012).
- Cancer Genome Atlas Research Network. *Nature* **474**, 609–615 (2011).
- Howlander, N. *et al. SEER Cancer Statistics Review, 1975–2009 (Vintage 2009 Populations)*, [http://seer.cancer.gov/csr/1975\\_2009\\_pops09/](http://seer.cancer.gov/csr/1975_2009_pops09/), based on November 2011 SEER data submission.
- Welch, J.S. *et al. Cell* **150**, 264–278 (2012).
- Michaelis, C., Ciosk, R. & Nasmyth, K. *Cell* **91**, 35–45 (1997).
- Rao, H. *et al. Nature* **410**, 955–959 (2001).
- Remeseiro, S. *et al. EMBO J.* **31**, 2076–2089 (2012).

## ONLINE METHODS

**Tumor specimens.** Of the 2,214 tumor samples screened by immunohistochemistry and described in **Supplementary Table 1**, 1,848 were anonymized, well-characterized tumor samples assembled into multitumor blocks each containing 5–50 cases, as described previously<sup>9,10</sup>. The remainder of the 366 samples described in **Supplementary Table 1** were from (i) a Ewing sarcoma tumor microarray created from resection specimens at Leiden University Medical Center containing 21 informative cases spotted in triplicate, (ii) ovarian cancer tumor microarray OV1921 from US Biomax containing 76 informative cases spotted in duplicate, (iii) bladder cancer tumor microarray BL1002 from US Biomax containing 37 informative cases spotted in duplicate, (iv) bladder cancer tumor microarray BLC1501 from US Biomax containing 70 informative cases spotted in duplicate, (v) bladder cancer tumor microarray BL1921 from US Biomax containing 79 informative cases spotted in duplicate and (vi) a bladder cancer tumor microarray created from resection specimens at the MD Anderson Cancer Center containing 83 informative cases<sup>11</sup>.

For DNA sequencing, genomic DNA was prepared from snap-frozen, treatment-naïve urothelial carcinomas resected at the MD Anderson Cancer Center and the Johns Hopkins University Hospital. The clinicopathological characteristics of these tumors are described in **Supplementary Table 2**.

For the outcomes study described in **Supplementary Figure 19**, a clinically annotated tumor microarray containing 34 cases of papillary non-muscle-invasive urothelial carcinoma of the bladder from individuals treated with transurethral resection was assessed for STAG2 status by immunohistochemistry. Creation and validation of this tumor microarray has been described previously<sup>11</sup>.

For the outcomes study described in **Supplementary Figure 21**, a clinically annotated tumor microarray created from 349 consecutive individuals treated with radical cystectomy for invasive urothelial carcinoma of the bladder between 1988 and 2003 at a single center was assessed for STAG2 status by immunohistochemistry. Creation and validation of these tumor microarrays has been described previously<sup>12</sup>. No subject received preoperative systemic chemotherapy or radiotherapy, and no subject had known metastatic disease at the time of surgery. Postoperatively, subjects were generally seen at least three times in year 1, semiannually in year 2 and annually thereafter. Diagnostic imaging of the upper tract and chest radiography were performed at least annually or as clinically indicated. Individuals identified as having died of urothelial carcinoma had progressive, disseminated and often symptomatic metastases at death. All specimens were collected from properly consented patients at all participating sites in accordance with the institutional review board-approved study.

**Immunohistochemistry.** A mouse monoclonal antibody to STAG2 from Santa Cruz Biotechnology (clone J-12, sc-81852) was used at a dilution of 1:100. A mouse monoclonal antibody to p53 from Dako (clone DO-7, M7001) was used at a 1:25 dilution. Immunostaining was performed in an automated immunostainer (Leica Bond-Max) following heat-induced antigen retrieval for 30 min in high pH epitope retrieval buffer (Bond-Max). Primary antibody was applied for 30 min, and Bond-Max polymer was applied for 15 min. Diaminobenzidine was used as the chromogen, and samples were counterstained with hematoxylin. Samples in which both the tumor and normal cells failed to stain for STAG2 were considered antigenically non-viable and were excluded from the analysis.

**DNA sequencing.** Individual exons of *STAG2* were PCR amplified from genomic DNA using the conditions and primer pairs described by Solomon *et al.*<sup>1</sup>. PCR products were purified using the Exo/SAP method followed by a Sephadex spin column. Sequencing reactions were performed using BigDye v3.1 (Applied Biosystems) using an M13F primer and were analyzed on an Applied Biosystems 3730xl capillary sequencer. Sequences were analyzed using Mutation Surveyor (SoftGenetics). Traces with putative mutations were reamplified and sequenced from both tumor and matched normal DNA from blood when available.

**Protein blots.** Primary antibodies used were STAG2 clone J-12 (Santa Cruz Biotechnology, sc-81852) and  $\alpha$ -tubulin Ab-2 clone DM1A (Neomarkers). Protein was isolated from 32 human urothelial carcinoma cell lines in RIPA buffer, resolved by SDS-PAGE and immunoblotted following standard biochemical techniques.

**Molecular cytogenetics.** Genomic DNA purified from 24 snap-frozen primary urothelial carcinomas was interrogated with Affymetrix CytoScan HD Arrays according to the manufacturer's instructions. Scanned array images and processed data sets have been deposited in GEO (data set [GSE41581](#)). CEL files were generated from scanned array image files by Affymetrix GeneChip Command Console software and were imported into Affymetrix Chromosome Analysis Suite v1.2.2 software. Copy number data files (CYCHP files) were generated using ChAS Analysis Files for CytoScan HD Array version NA32.1 (hg19) as a reference.

**STAG2 lentiviral expression and shRNA depletion.** To create a *STAG2*-expressing lentivirus, human *STAG2* cDNA corresponding to CCDS14607 was synthesized (Genscript), cloned into the lentiviral expression vector pLJM1 (Addgene) and packaged by cotransfection of 293T cells (ATCC) with lentiviral helper plasmids pHR'CMV8.2 $\Delta$ R and pCMV-VSV-G as previously described<sup>13</sup>. Virus-containing conditioned medium was harvested 48 h after transfection, filtered and used to infect recipient cells in the presence of 8  $\mu$ g/ml polybrene. Infected cells were selected with 2  $\mu$ g/ml puromycin until all mock-infected cells were dead and were then maintained in puromycin. Identification and validation of lentiviral *STAG2* shRNA constructs have been described previously<sup>5</sup>.

**CellTiter-Glo proliferation assays.** Proliferation of pooled clones of *STAG2*-mutant urothelial cancer cells infected with empty lentiviral vector or with lentiviral vector expressing *STAG2* was performed using the CellTiter-Glo Luminescent Cell Proliferation Assay (Promega) according to the manufacturer's instructions.

**Subcutaneous xenograft growth assays.** Three million cells from pooled clones of UM-UC-3 cells infected with either empty lentiviral vector or with lentiviral vector expressing *STAG2*, after puromycin selection, were injected subcutaneously into the flanks of 5- to 6-week-old female athymic mice (*nu/nu* genotype, BALB/c background; Simonsen Laboratories;  $n = 10$ ). Tumor volume was measured three times weekly starting on day 13 after injection. Mice were housed and fed under aseptic conditions, and all animal research was approved by the University of California, San Francisco Institutional Animal Care and Use Committee.

**Chromosome counting.** Cultured cells were treated with 0.02  $\mu$ g/ml colcemid for 55 min at 37 °C. Cells were then trypsinized and centrifuged for 7 min at 200g, and the cell pellet was resuspended in warmed hypotonic solution and incubated at 37 °C for 11 min. Swollen cells were centrifuged, and the pellet was resuspended in 8 ml of Carnoy's fixative (3:1 methanol:glacial acetic acid). After incubation in fixative at room temperature for 96 min, the cell suspension was centrifuged and washed twice in Carnoy's fixative. After the final centrifugation, cells were resuspended in 1 to 3 ml of freshly prepared fixative to produce an opalescent cell suspension. Drops of the final cell suspension were placed on clean slides and air dried. Slides were stained with a 1:3 mixture of Wright's stain and 0.06 M phosphate buffer for 4–10 min, washed with tap water for 5 s and then air dried. One hundred cells in metaphase were examined for chromosome count in a blinded fashion.

**Statistical analysis.** Analyses were performed with SPSS 17 (SPSS, IBM). Differences in variables with a continuous distribution across categories were assessed using the Mann-Whitney *U* test (two categories) and the Kruskal-Wallis test (three and more categories). The Fisher's exact test and the  $\chi^2$  test were used to evaluate the association between categorical variables. Univariable recurrence and cancer-specific survival probabilities were estimated using the Kaplan-Meier method, and differences were assessed using the log-rank test. All tests are two-sided, and a *P* value of 0.05 was set to be statistically significant.

9. Miettinen, M. *Appl. Immunohistochem.* **20**, 410–412 (2012).

10. Miettinen, M. *et al. Am. J. Surg. Pathol.* **36**, 629–639 (2012).

11. Kim, J.H. *et al. Lab. Invest.* **85**, 532–549 (2005).

12. Rink, M. *et al. Urol. Oncol.* doi:10.1016/j.urolonc.2012.06.011 (1 September 2012).

13. Solomon, D.A. *et al. Cancer Res.* **68**, 10300–10306 (2008).

# Supplementary Materials

## Frequent truncating mutations of STAG2 in bladder cancer

David A. Solomon, Jung-Sik Kim, Jolanta Bondaruk, Shahrokh F. Shariat, Zeng-Feng Wang, Abdel G. Elkahloun, Tomoko Ozawa, Julia Gerard, DaZhong Zhuang, Shizhen Zhang, Neema Navai, Arleen Siefker-Radtke, Joanna J. Phillips, Brian D. Robinson, Mark A. Rubin, Björn Volkmer, Richard Hautmann, Rainer Küfer, Pancras C. W. Hogendoorn, George Netto, Dan Theodorescu, C. David James, Bogdan Czerniak, Markku Miettinen, and Todd Waldman

### **Contents**

Supplementary Figures 1-21

Supplementary Tables 1 and 4-6\*

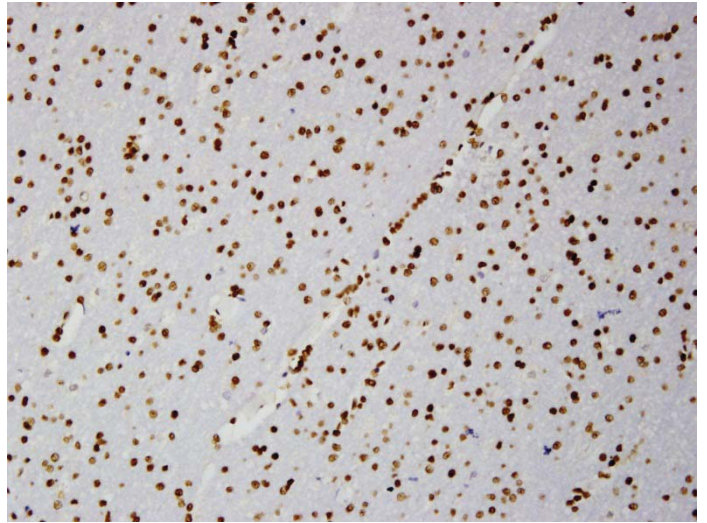
\* Supplementary Tables 2 and 3 are available as separate .xlsx files for downloading.

# Supplementary Figure 1

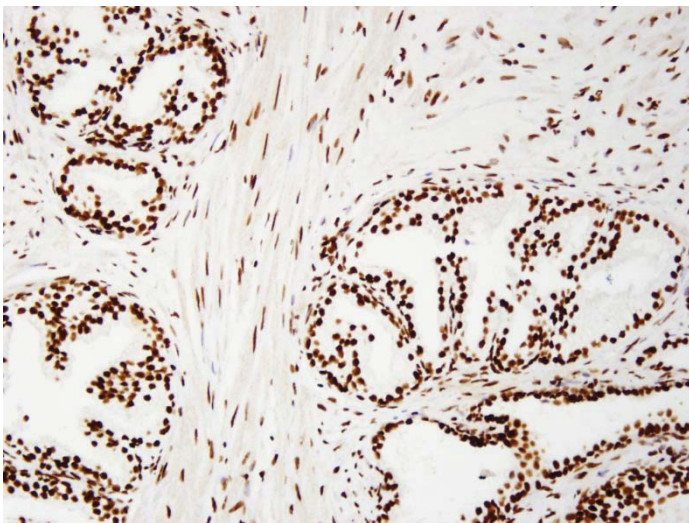
appendix



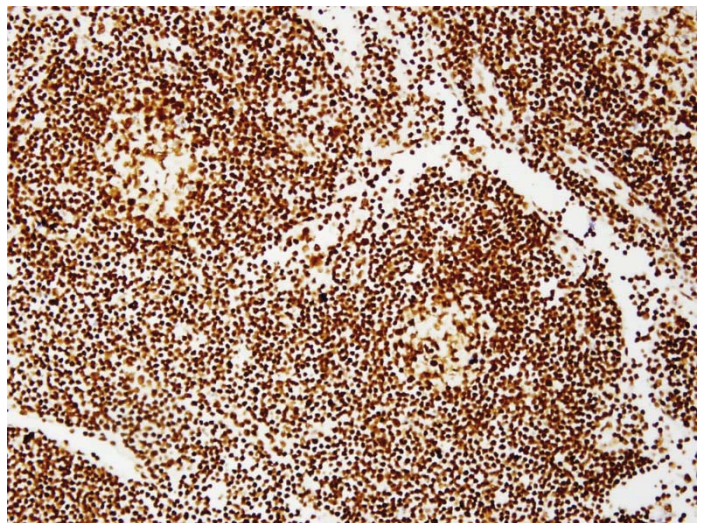
brain



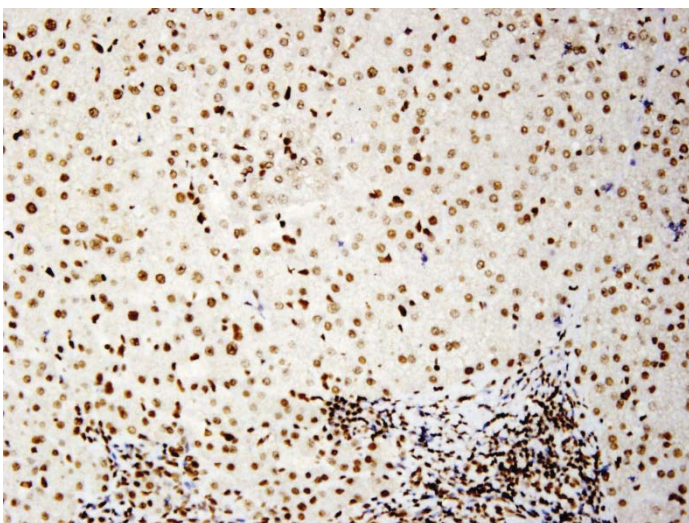
prostate



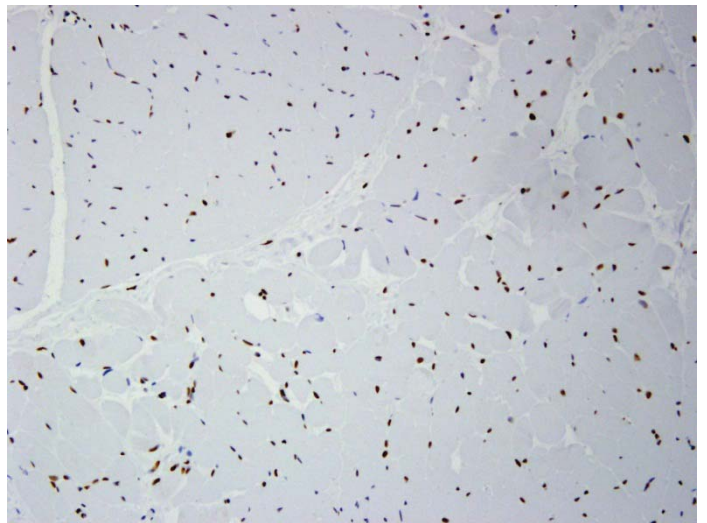
lymph node



liver

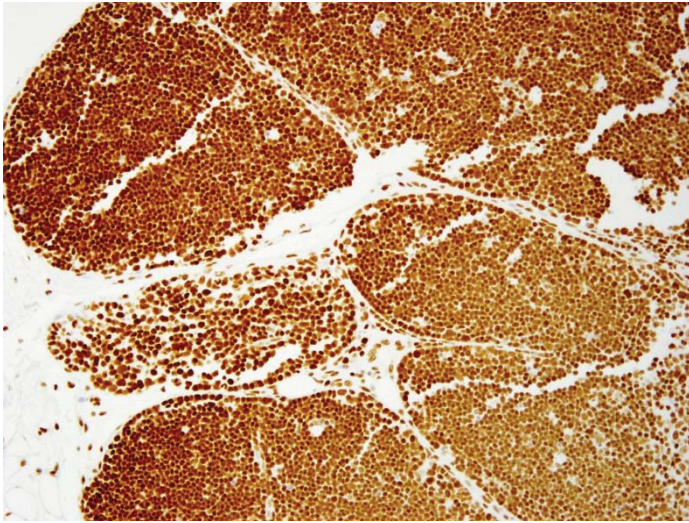


skeletal muscle

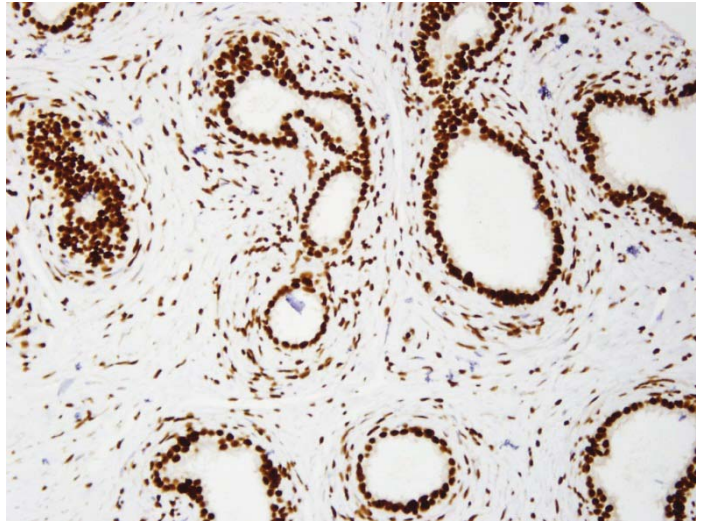


## Supplementary Figure 1 continued

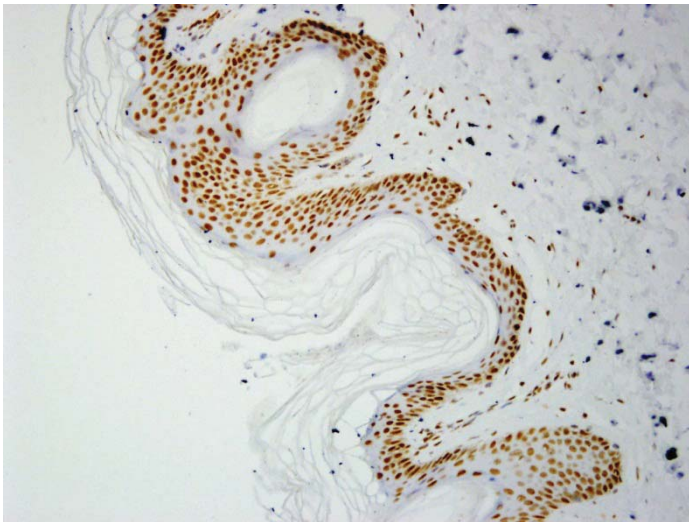
thymus



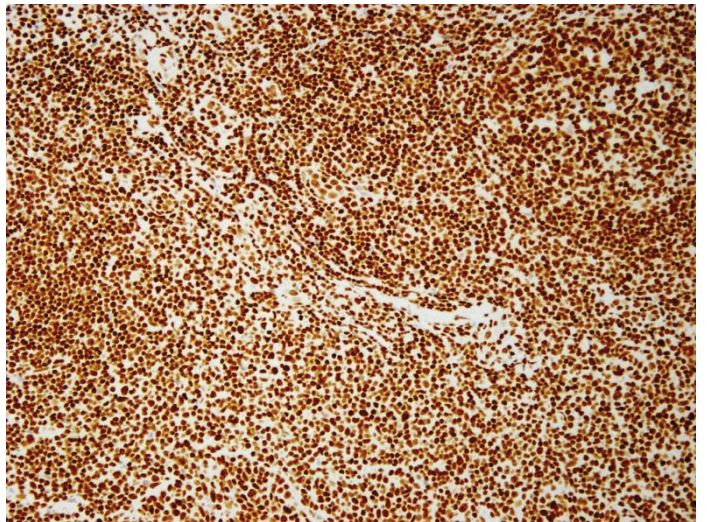
testis



skin

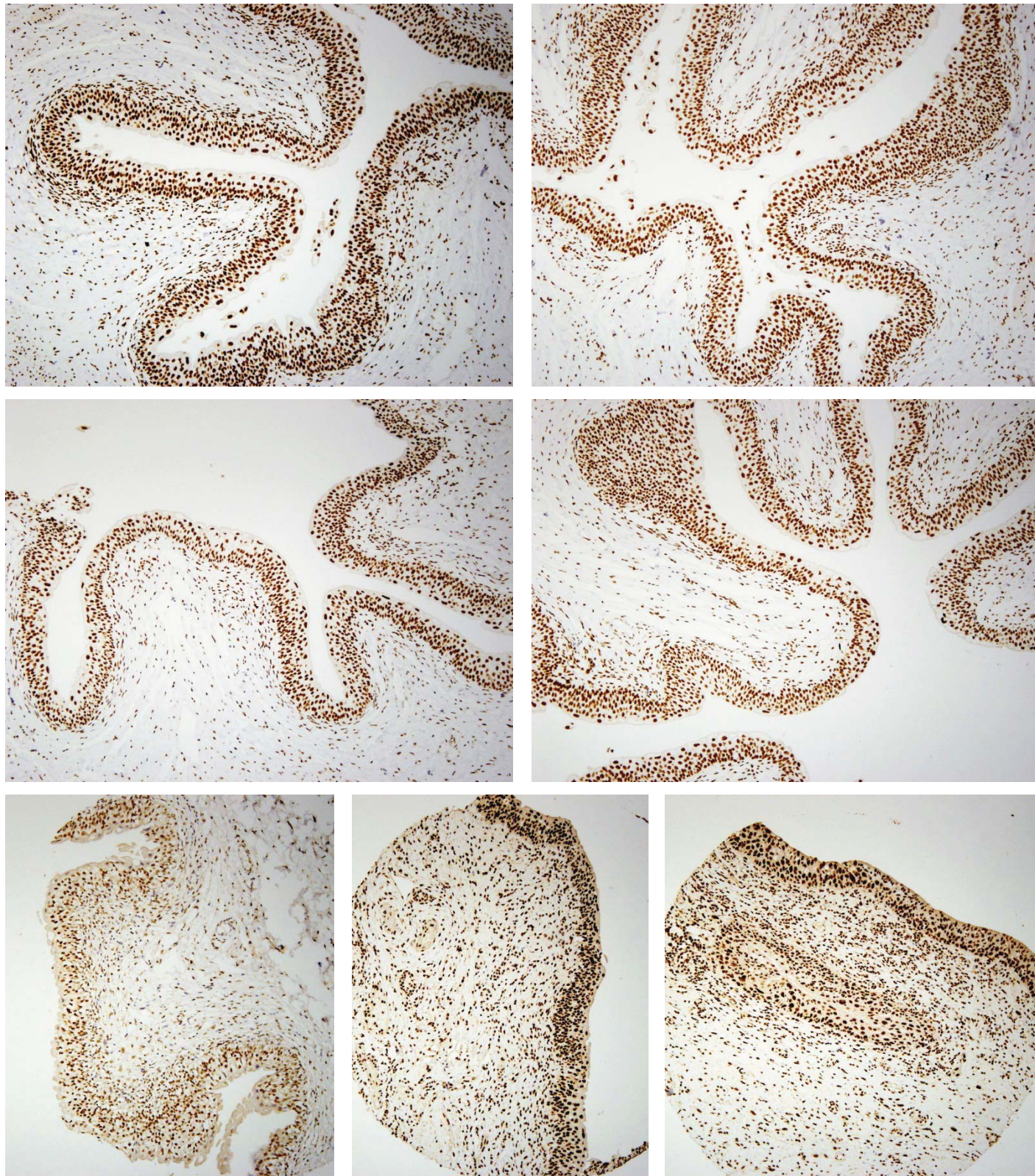


tonsil



**Supplementary Figure 1.** STAG2 is robustly expressed in all normal human tissues examined. Representative images of STAG2 immunohistochemistry on normal non-neoplastic tissues from various organs.

## Supplementary Figure 2

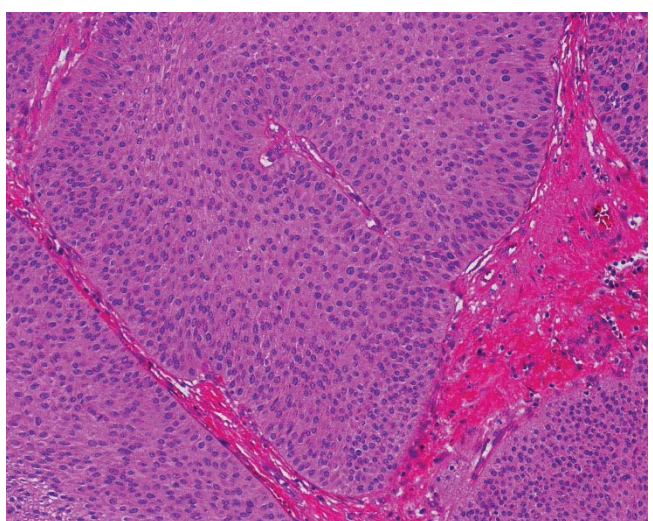
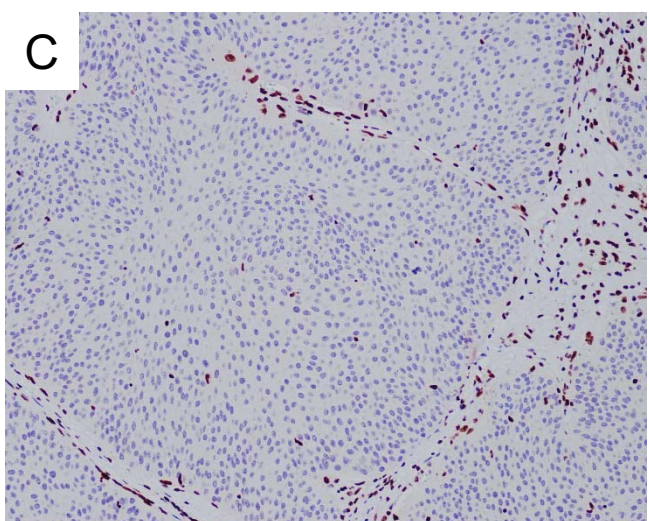
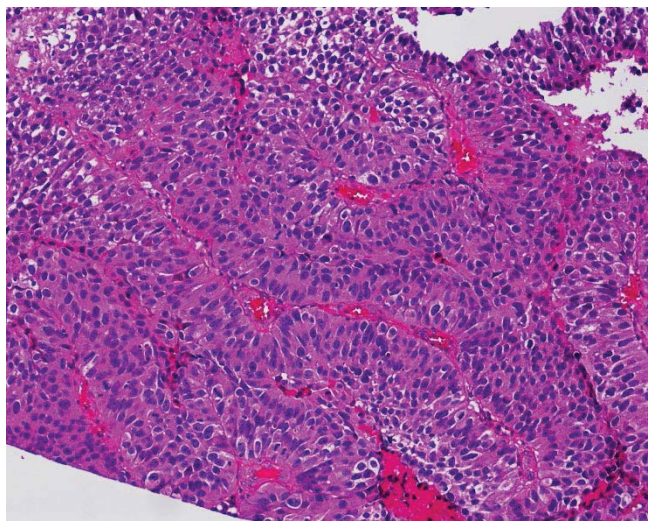
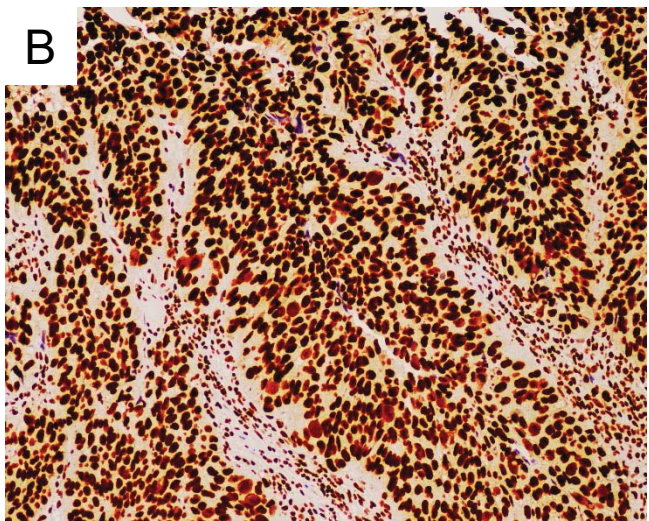
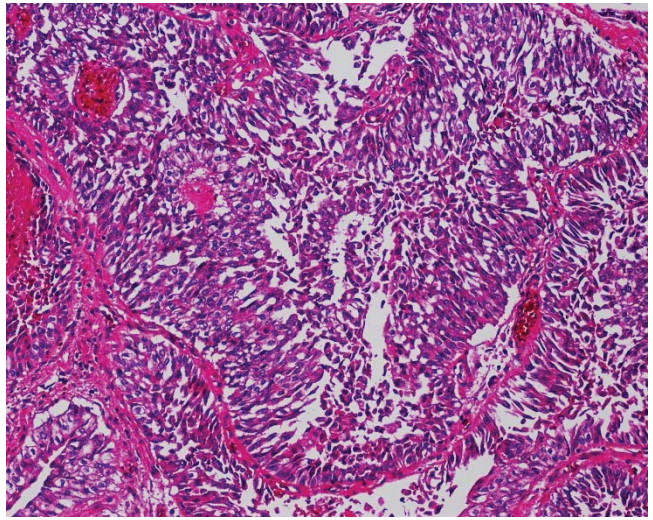
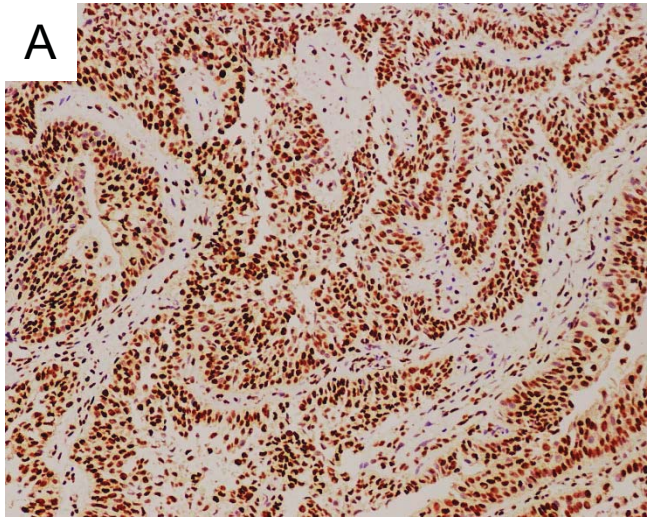


**Supplementary Figure 2.** STAG2 is robustly expressed in normal human urothelium. Representative images of STAG2 immunohistochemistry on normal non-neoplastic urothelium from several patients.

Supplementary Figure 3

STAG2

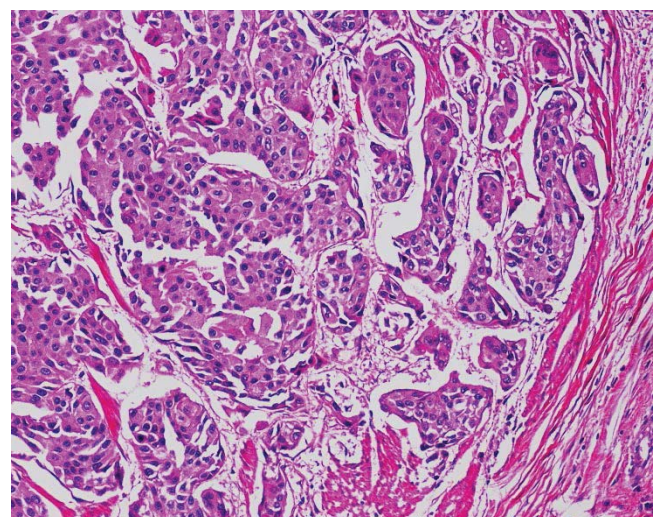
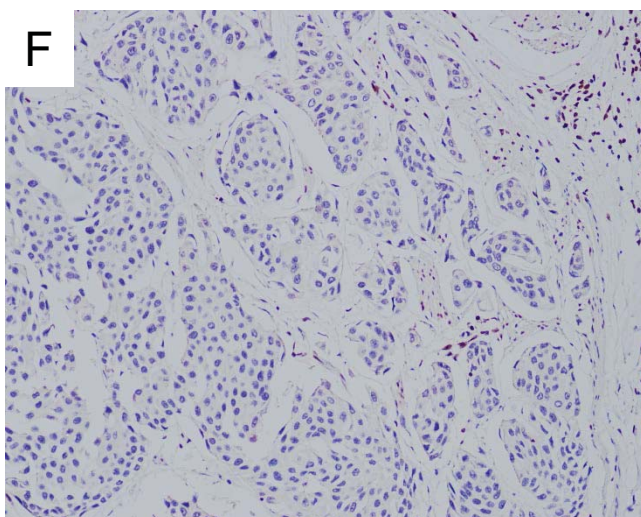
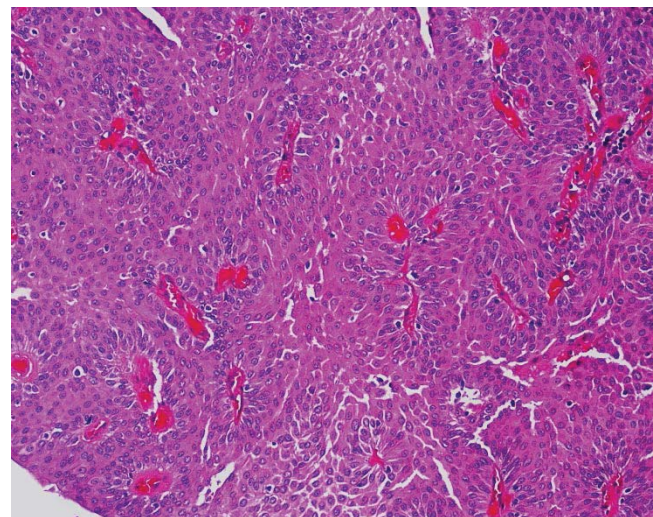
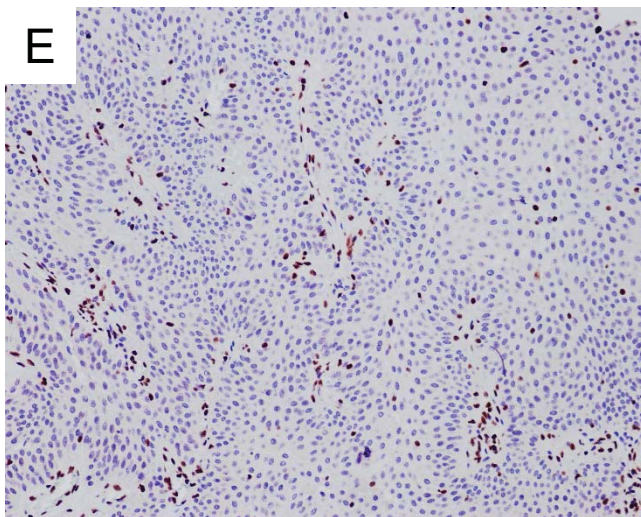
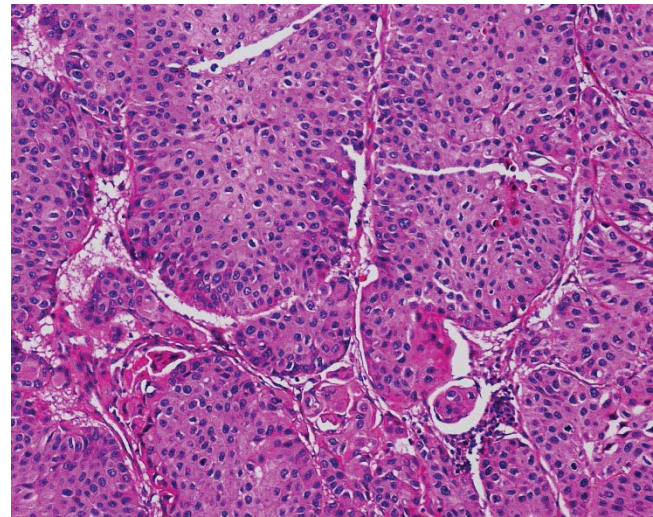
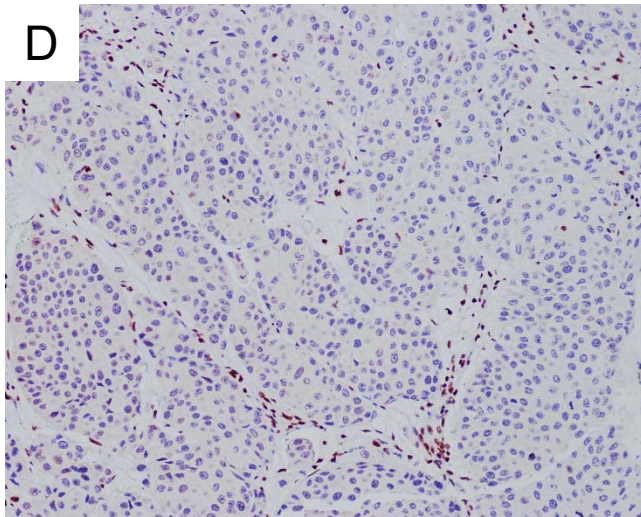
H&E



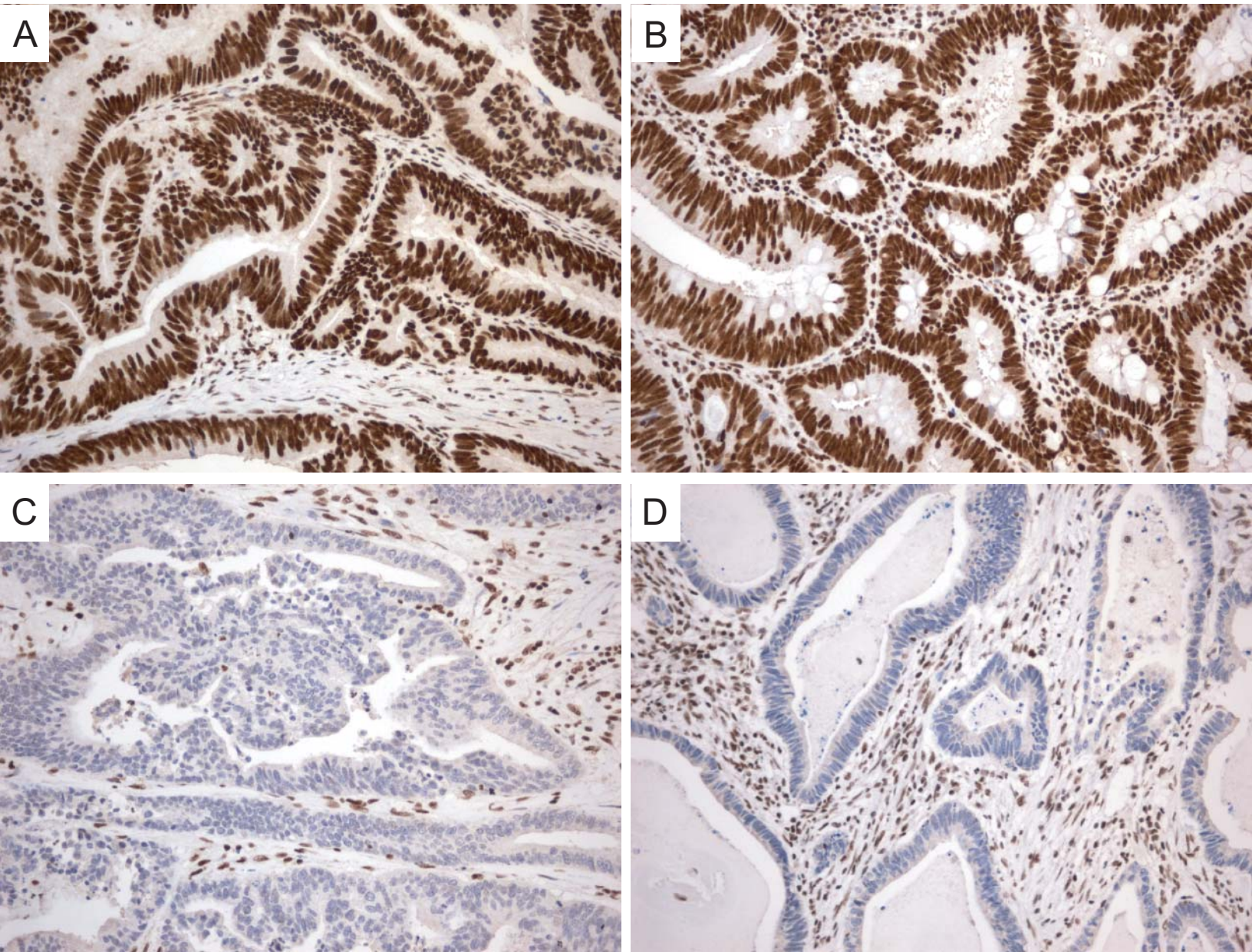
## Supplementary Figure 3 continued

STAG2

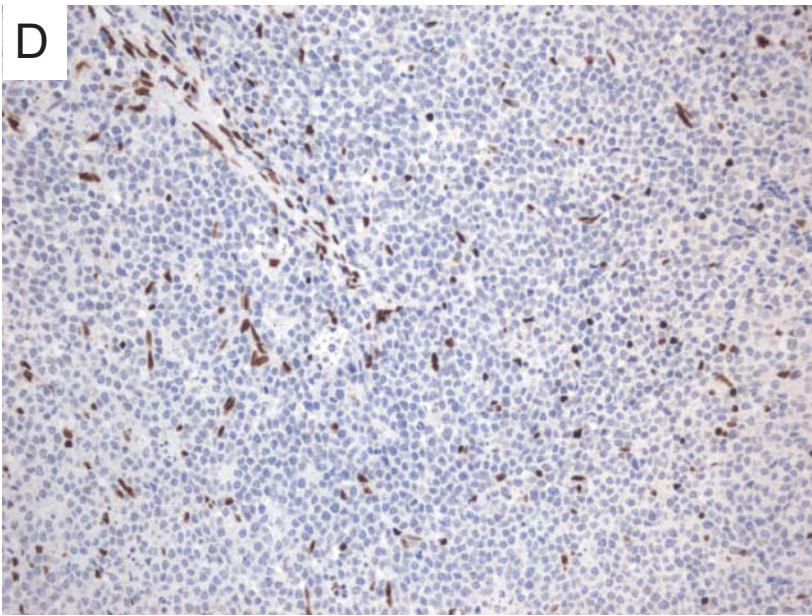
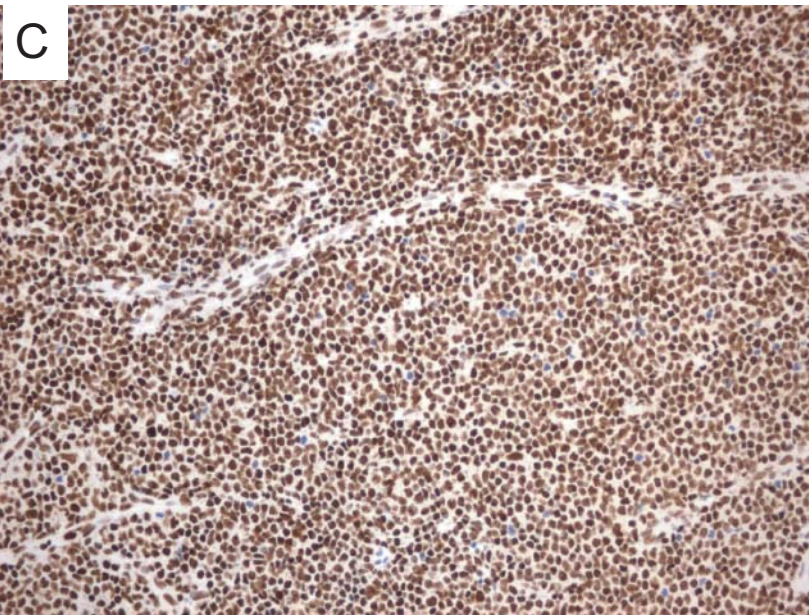
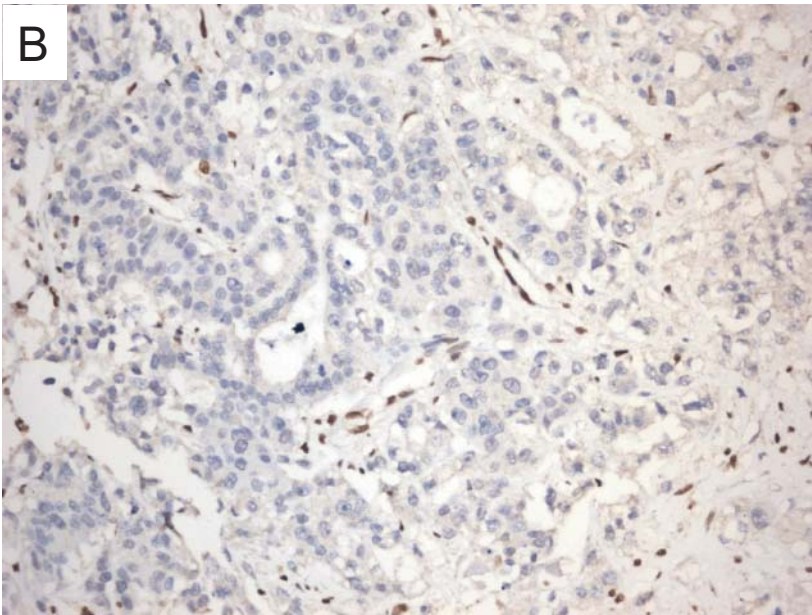
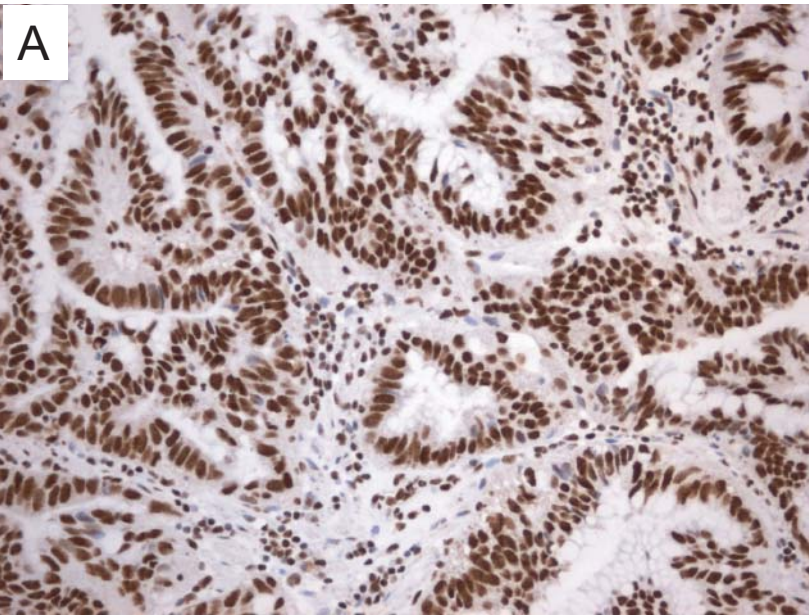
H&E



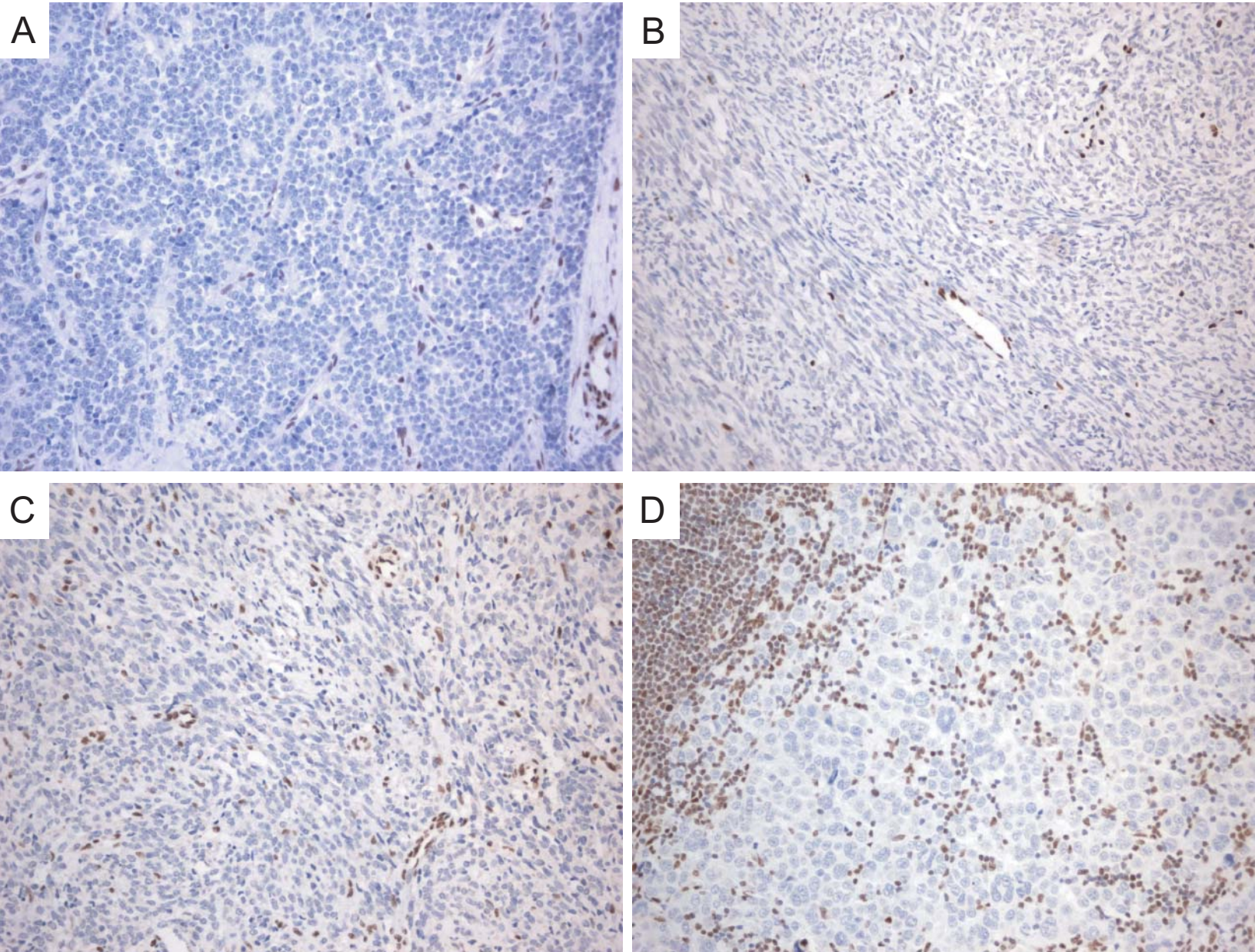
**Supplementary Figure 3.** STAG2 expression is lost in a subset of urothelial carcinomas of the bladder. Shown are two urothelial carcinomas with retained expression of STAG2 (A-B) and four urothelial carcinomas with complete loss of STAG2 expression (C-F) by immunohistochemistry.



**Supplementary Figure 4.** STAG2 expression is lost in a small subset of colorectal adenocarcinomas. Shown are two adenocarcinomas with retained expression of STAG2 (A and B), and two adenocarcinomas with complete loss of STAG2 expression (C and D) by immunohistochemistry.



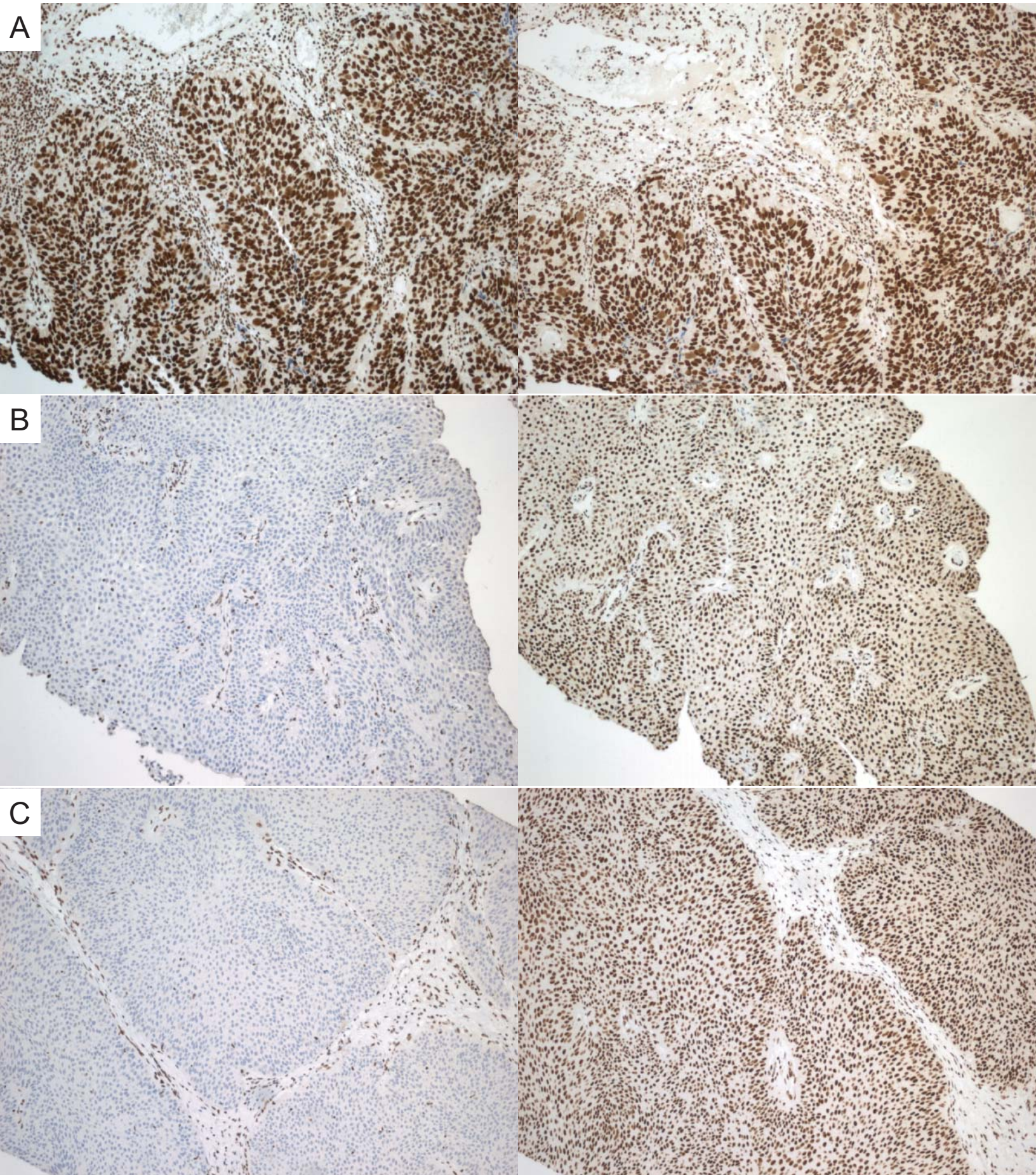
**Supplementary Figure 5.** STAG2 immunohistochemistry of a STAG2-expressing and a STAG2-deficient gastric adenocarcinoma (A-B), and a STAG2-expressing and STAG2-deficient acute myelogenous leukemia (C-D).



**Supplementary Figure 6.** Loss of STAG2 expression in a Ewing's sarcoma (A), uterine leiomyosarcoma (B), malignant peripheral nerve sheath tumor (C), and melanoma metastasis to a lymph node (D).

STAG2

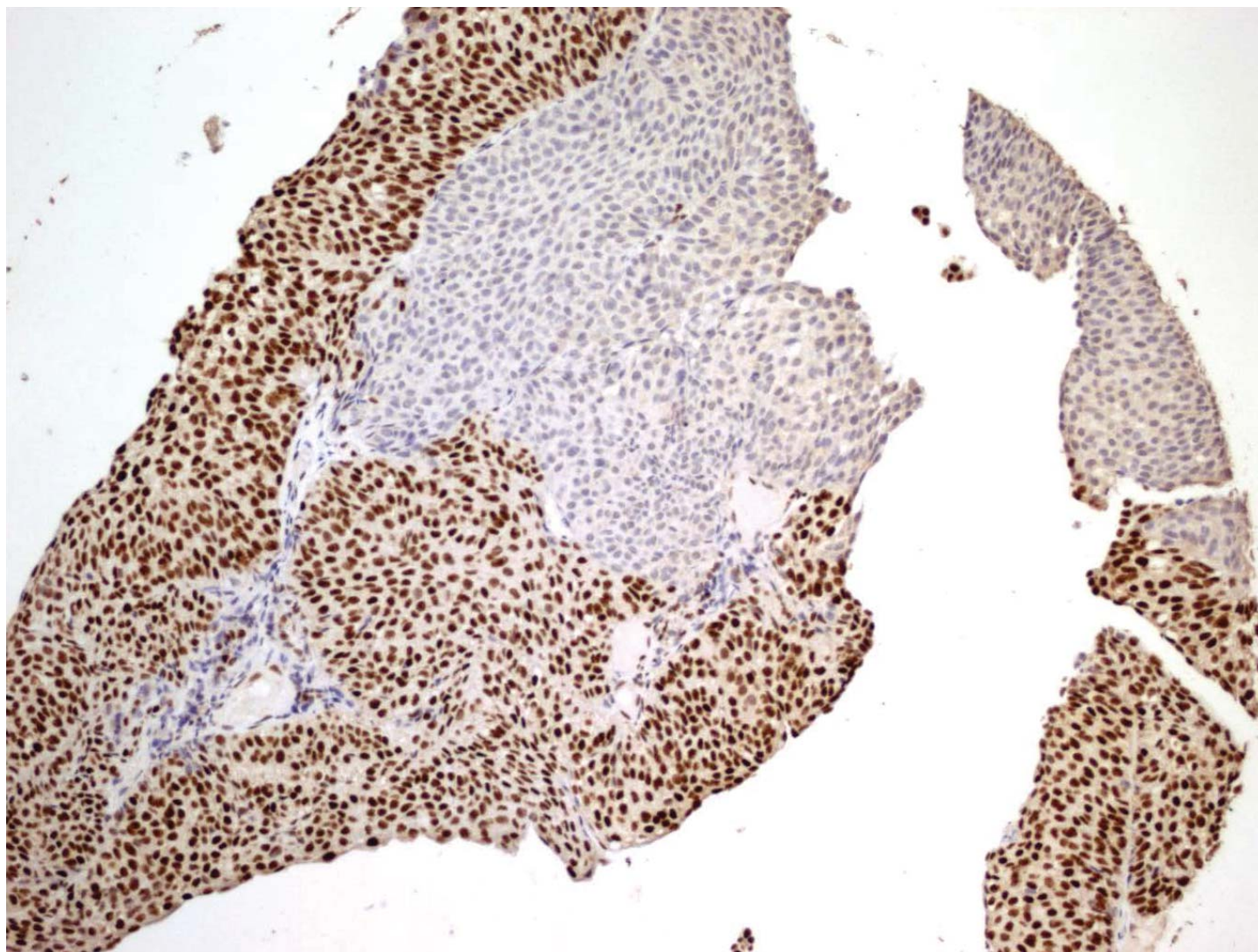
Ini-1



**Supplementary Figure 7.** Immunohistochemistry for the constitutively expressed chromatin remodeling protein Ini-1 (also known as SNF5 or BAF47) shows robust expression in both STAG2 expressing (A) and STAG2-deficient (B,C) urothelial carcinomas demonstrating that STAG2-negative tumors are antigenically intact.

A

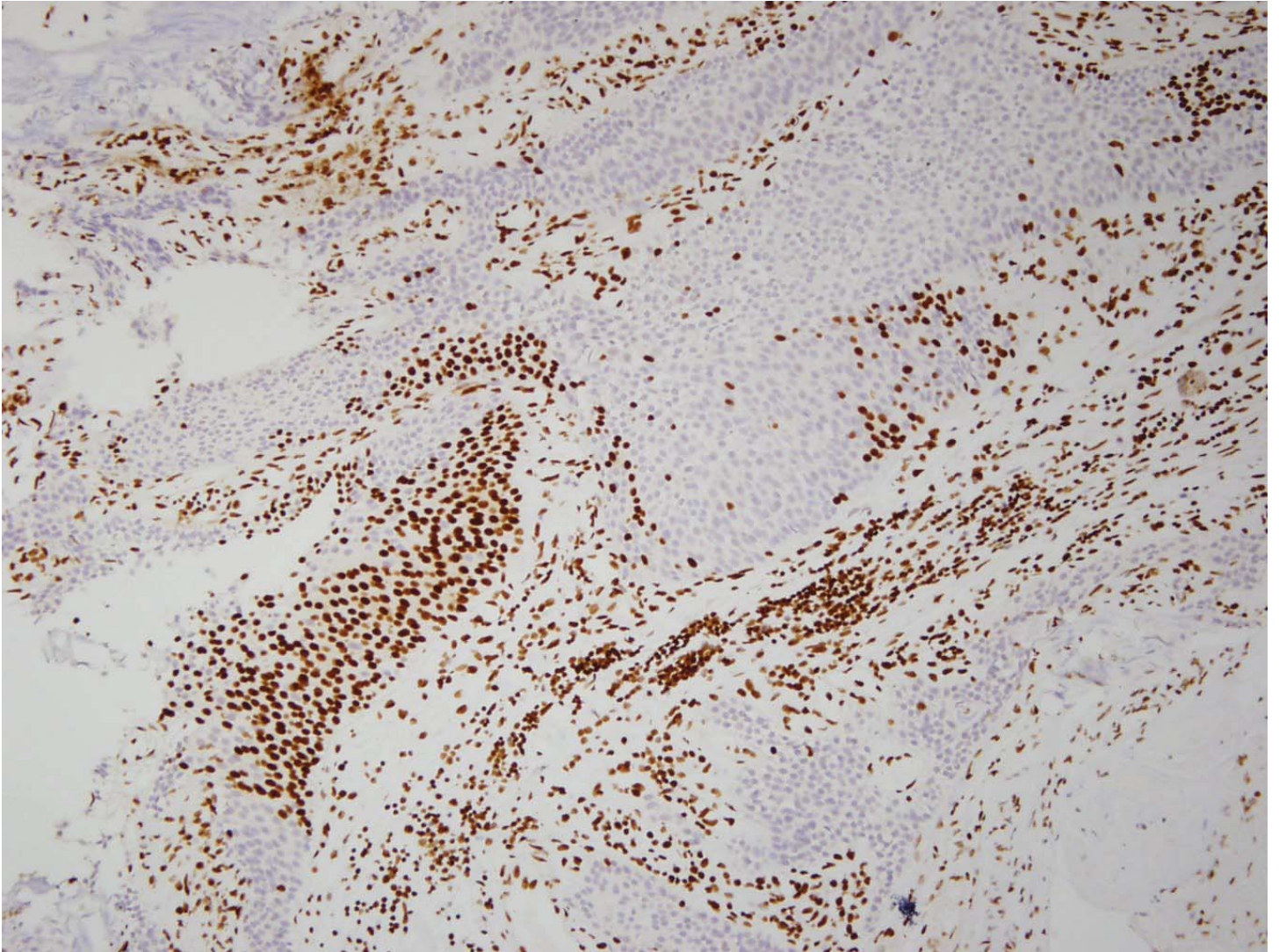
BL1921 B8 – region of mosaicism within tumor



Supplementary Figure 8 continued

B

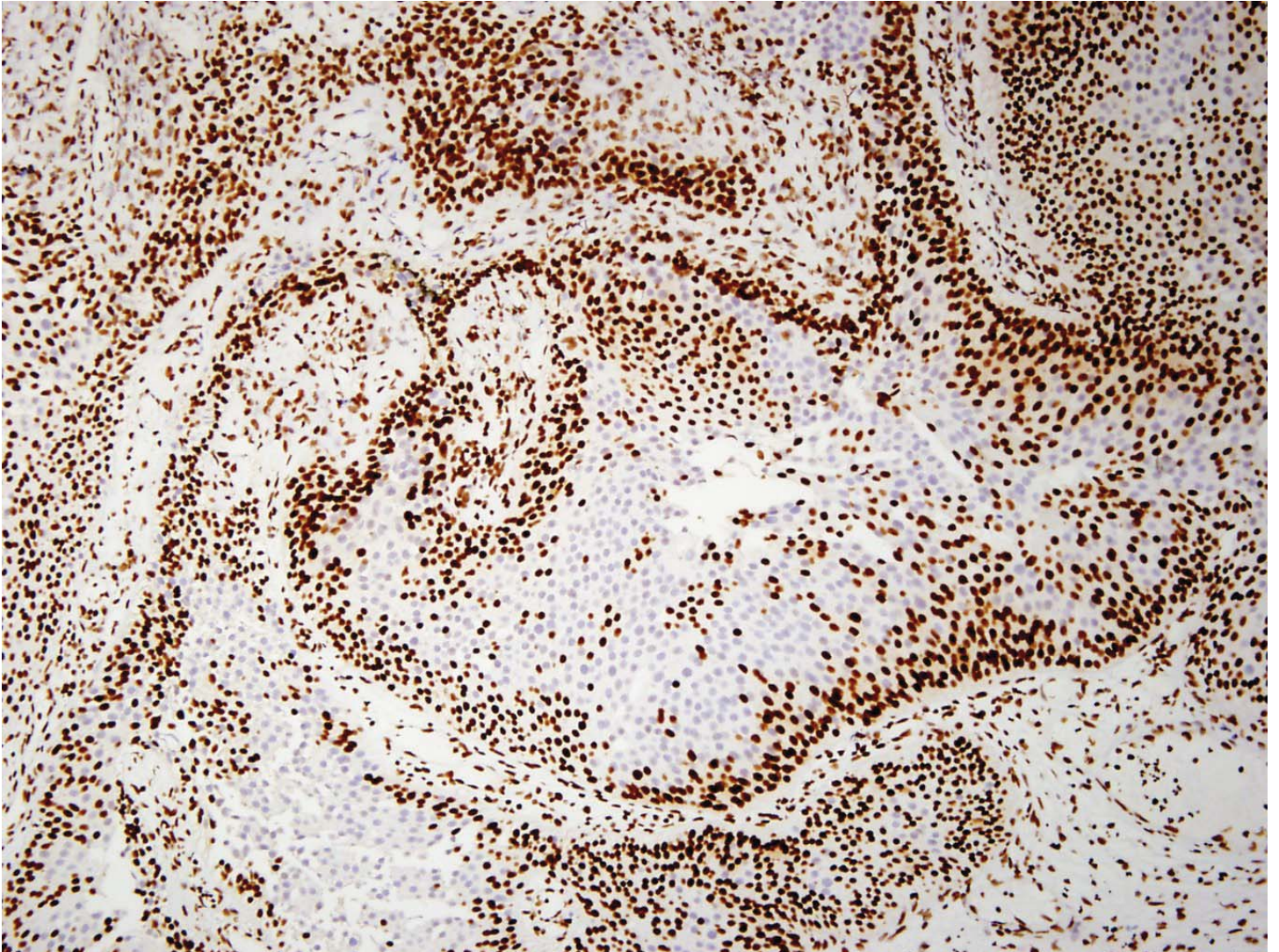
MDACC 20099 – one region of mosaicism within tumor



Supplementary Figure 8 continued

C

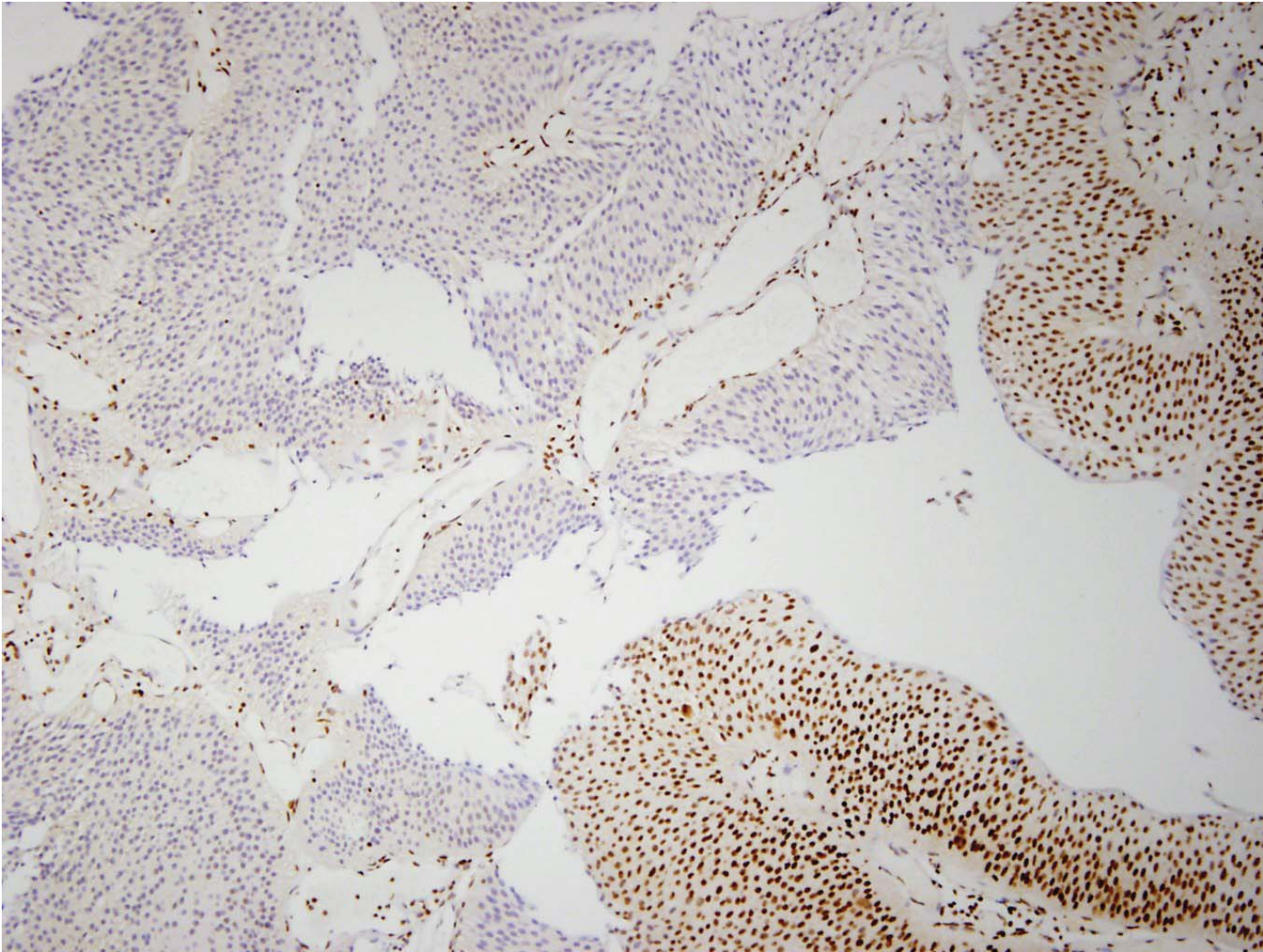
MDACC 20099 – additional region of mosaicism within tumor



Supplementary Figure 8 continued

D

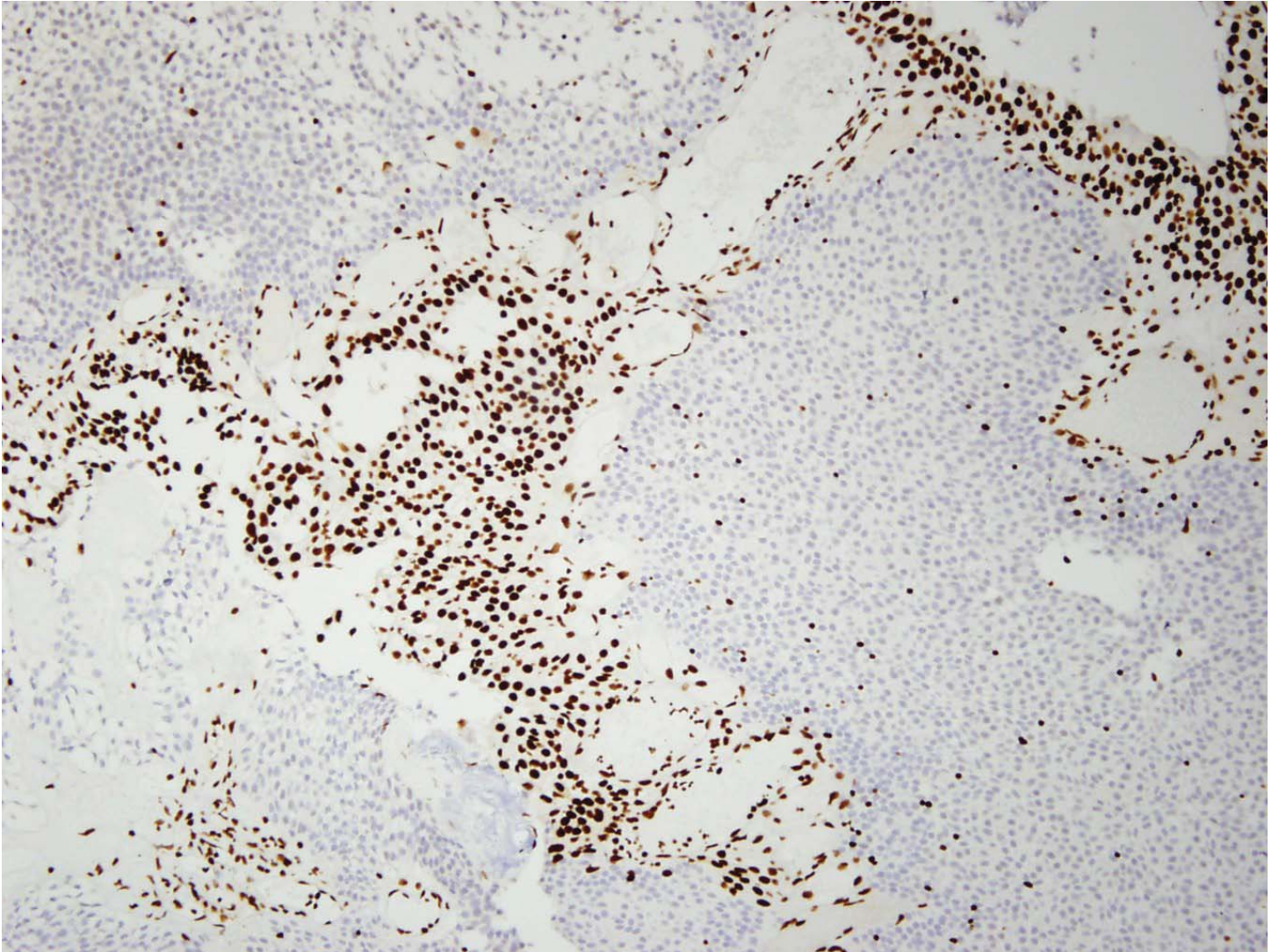
MDACC 20167 – region of mosaicism within tumor



## Supplementary Figure 8 continued

E

MDACC 20654 – region of mosaicism within tumor

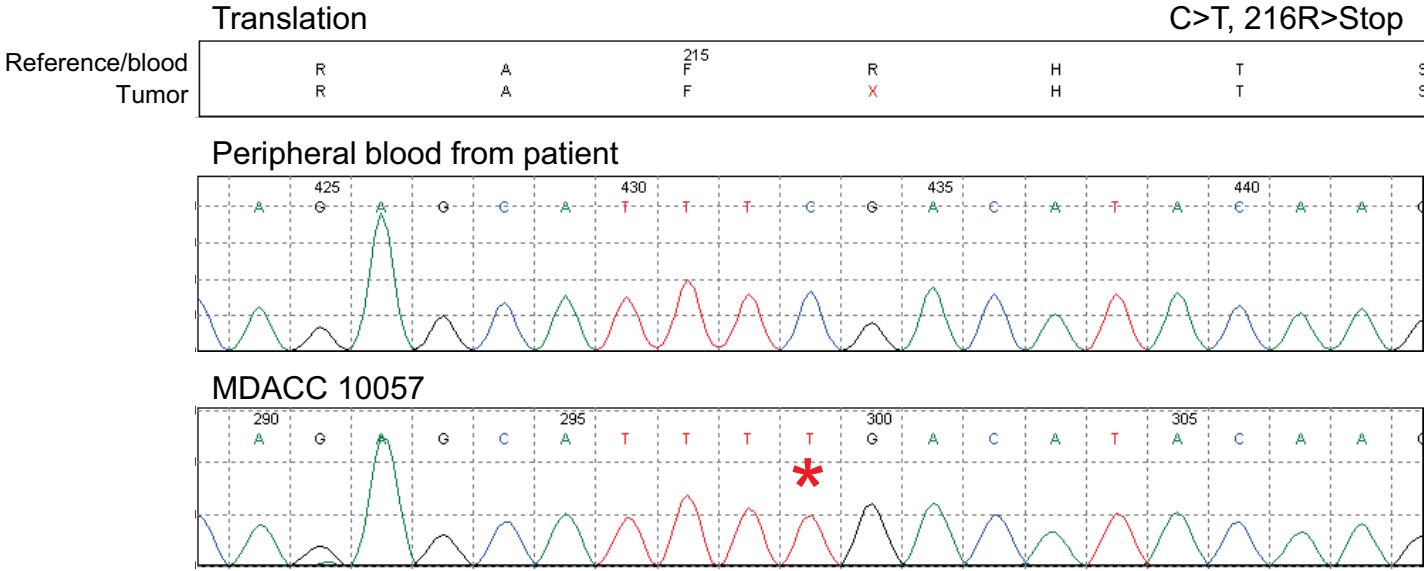


**Supplementary Figure 8.** Examples of mosaic STAG2 loss within urothelial carcinomas.

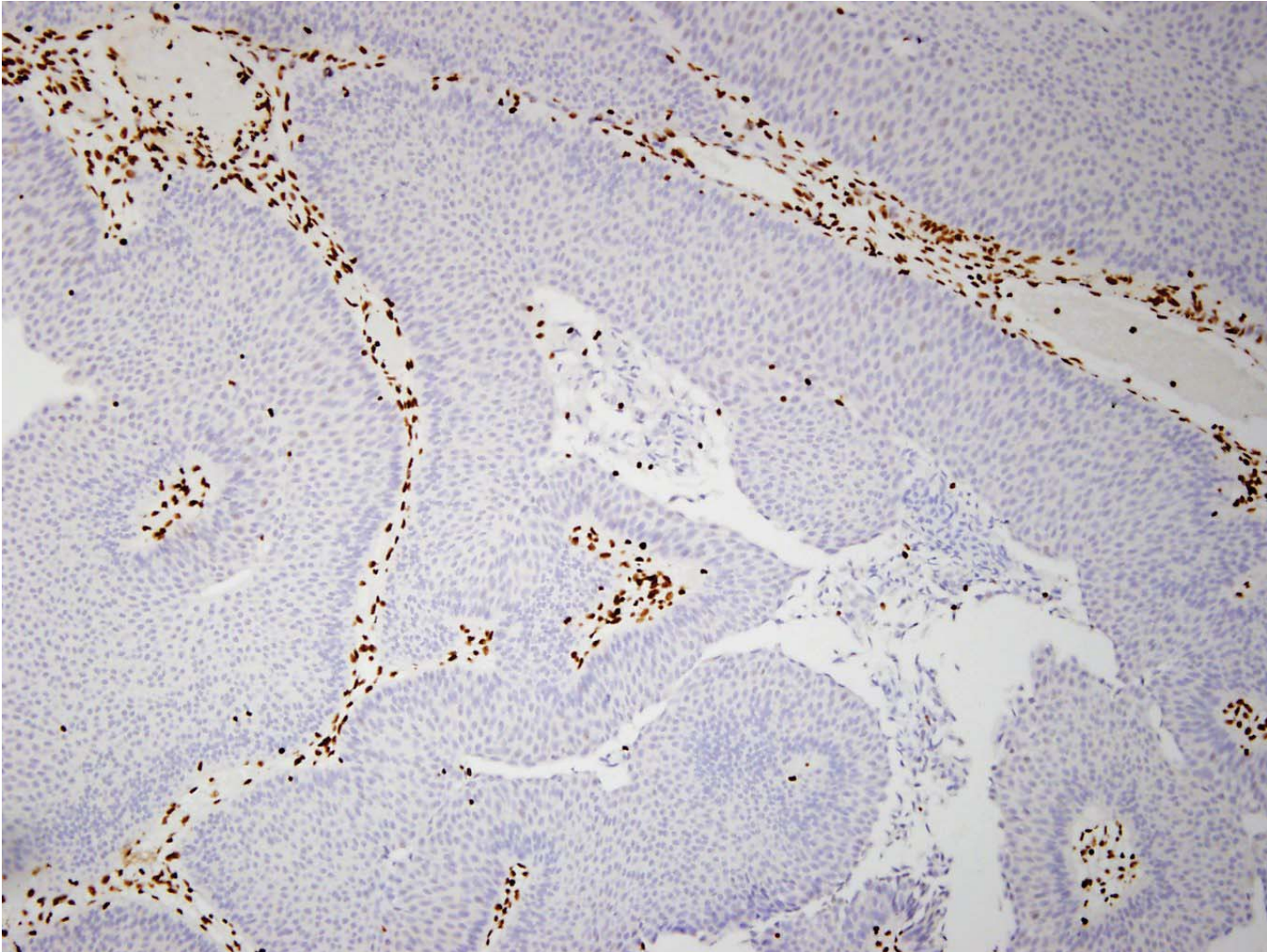


# Supplementary Figure 10

A

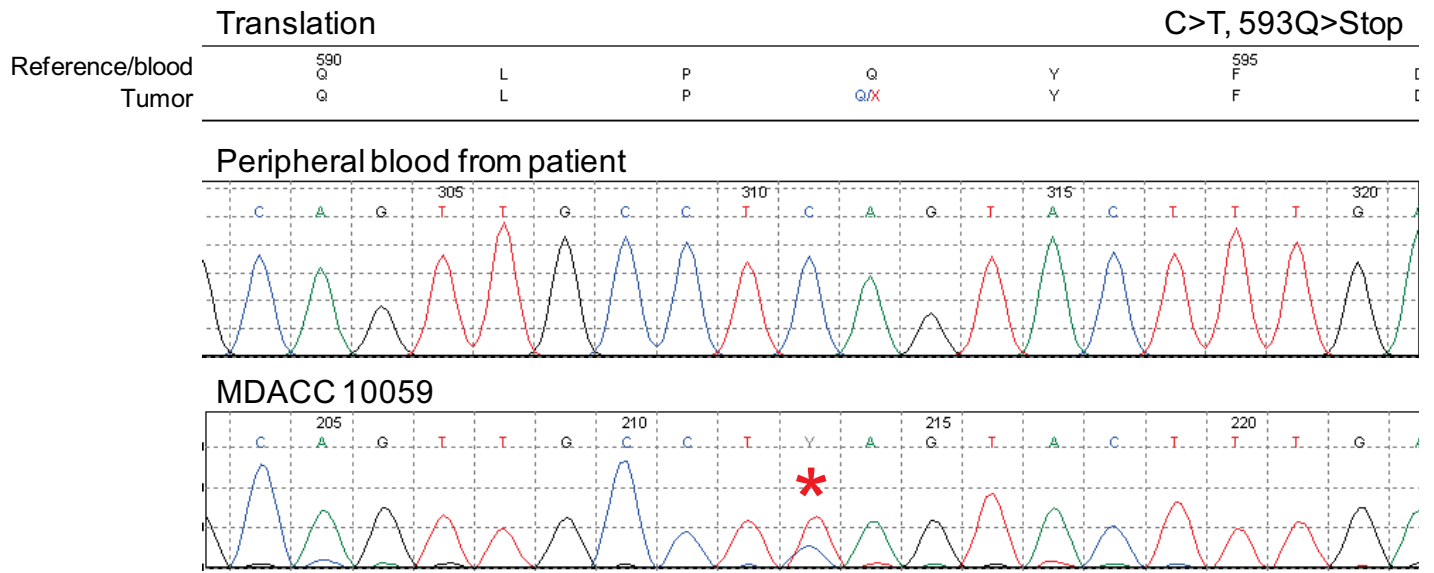


MDACC 10057

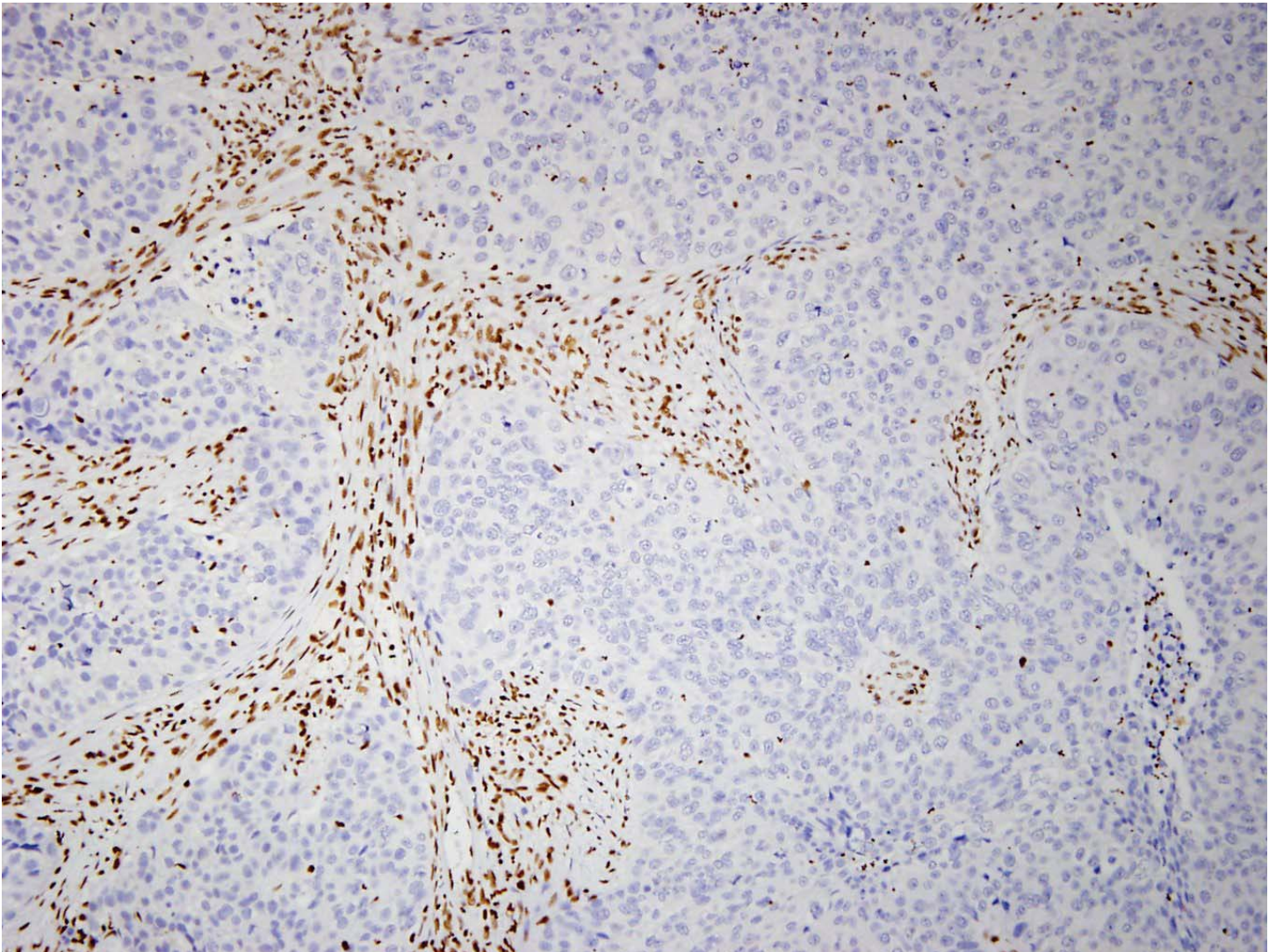


# Supplementary Figure 10 continued

B

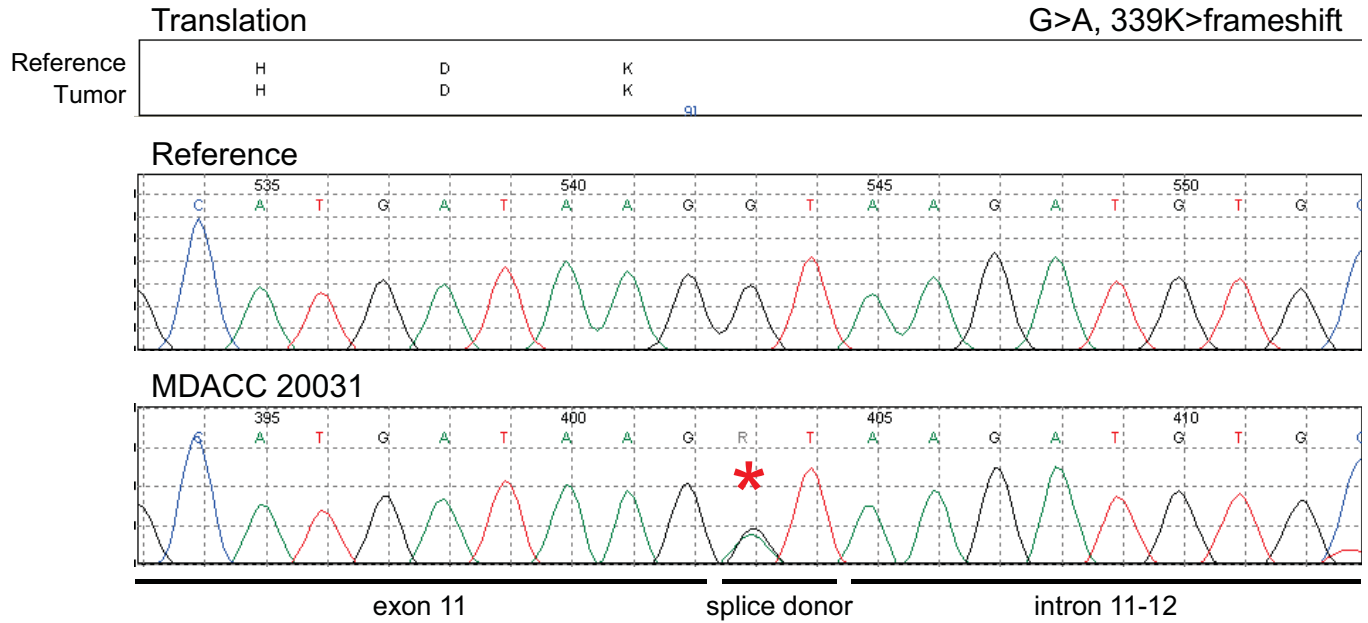


MDACC 10059

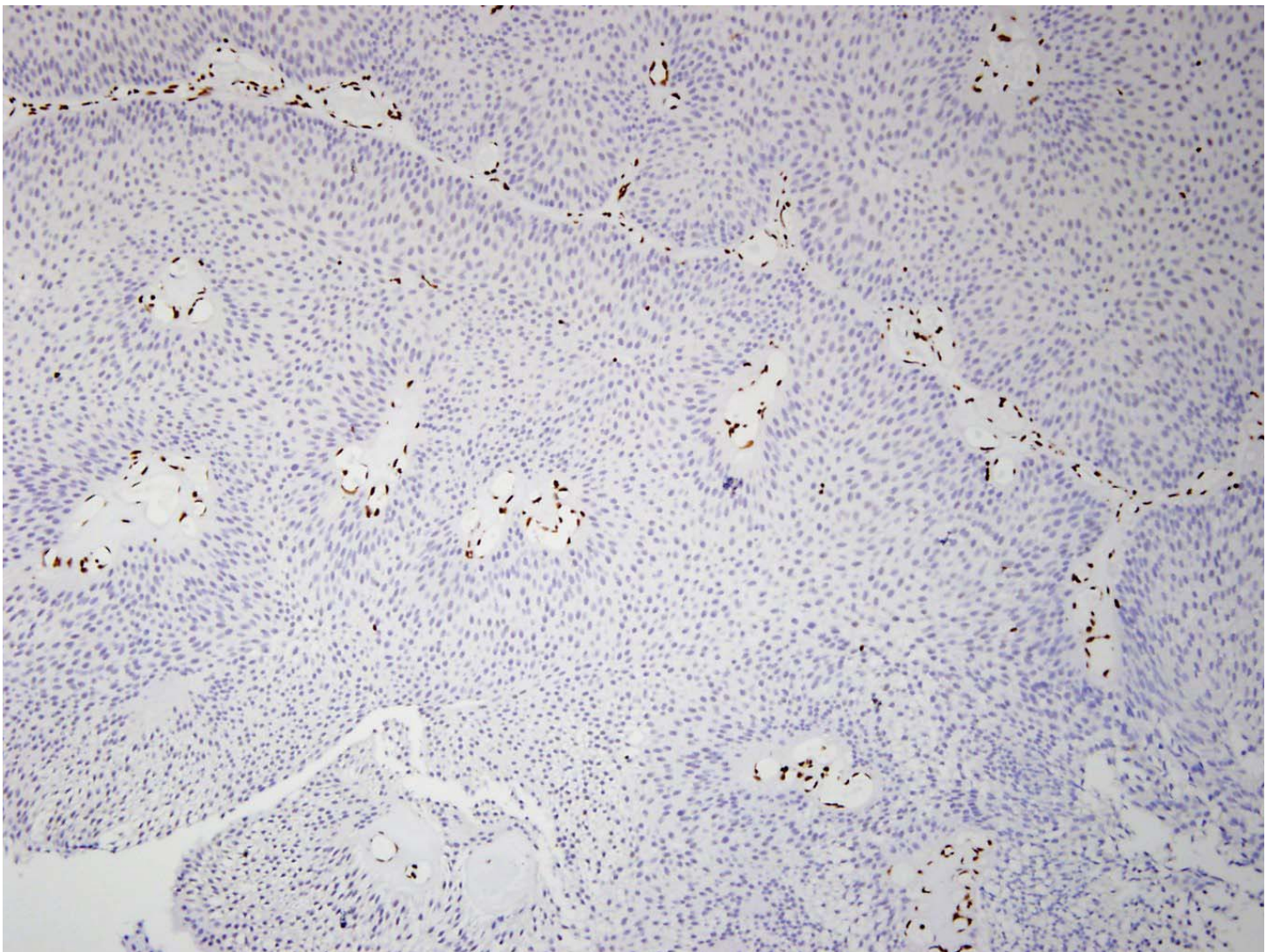


# Supplementary Figure 10 continued

## C

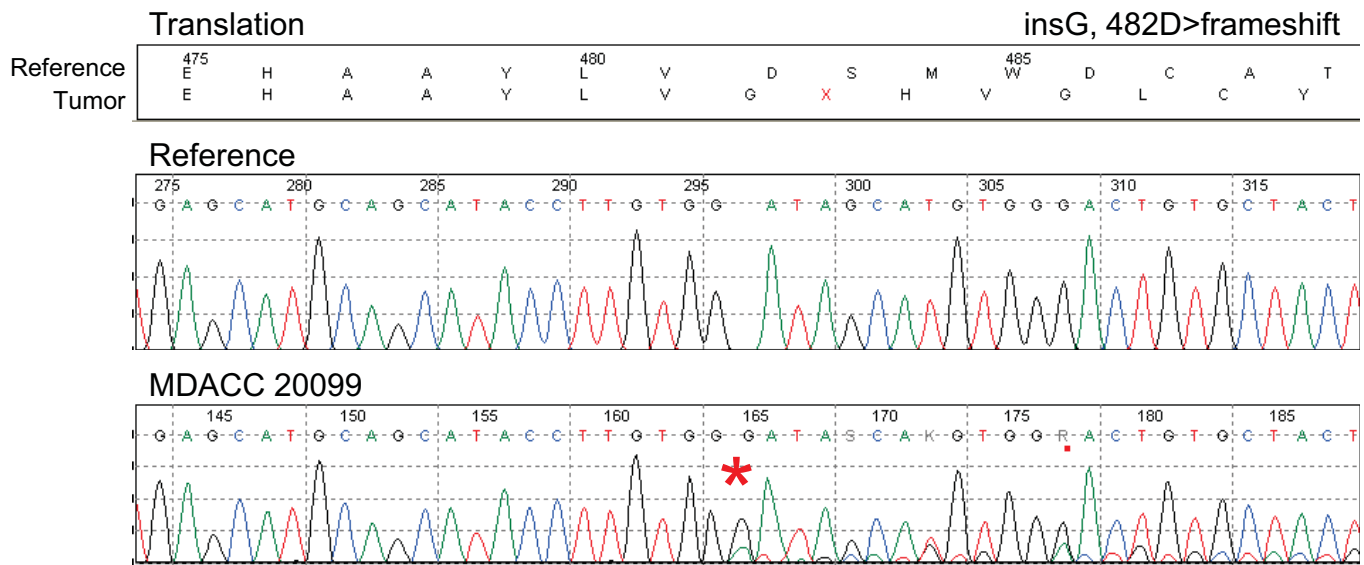


### MDACC 20031

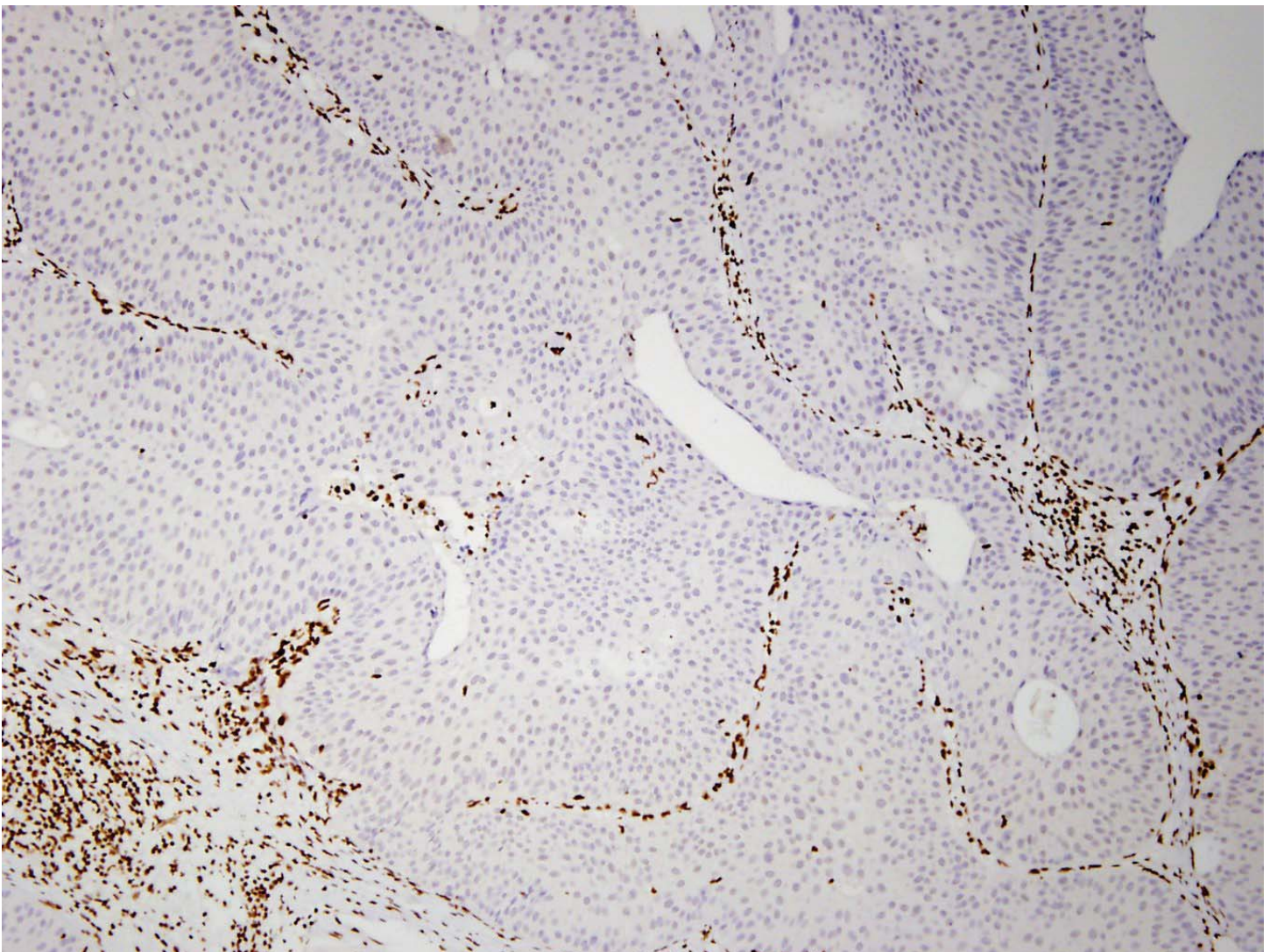


# Supplementary Figure 10 continued

D

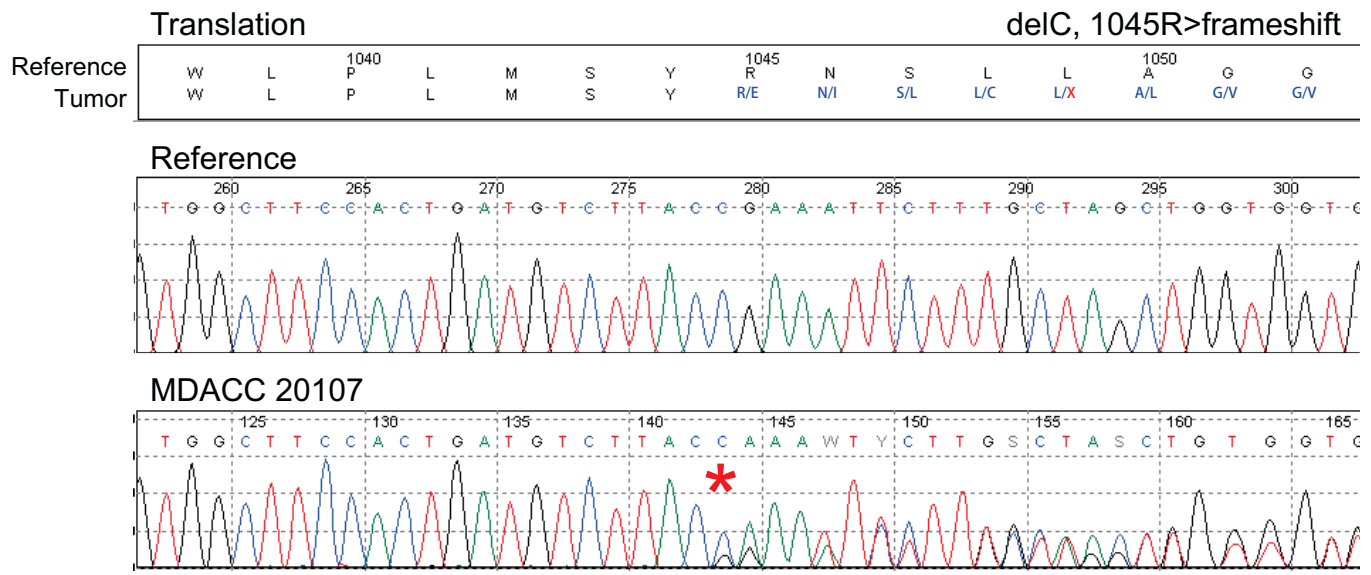


MDACC 20099

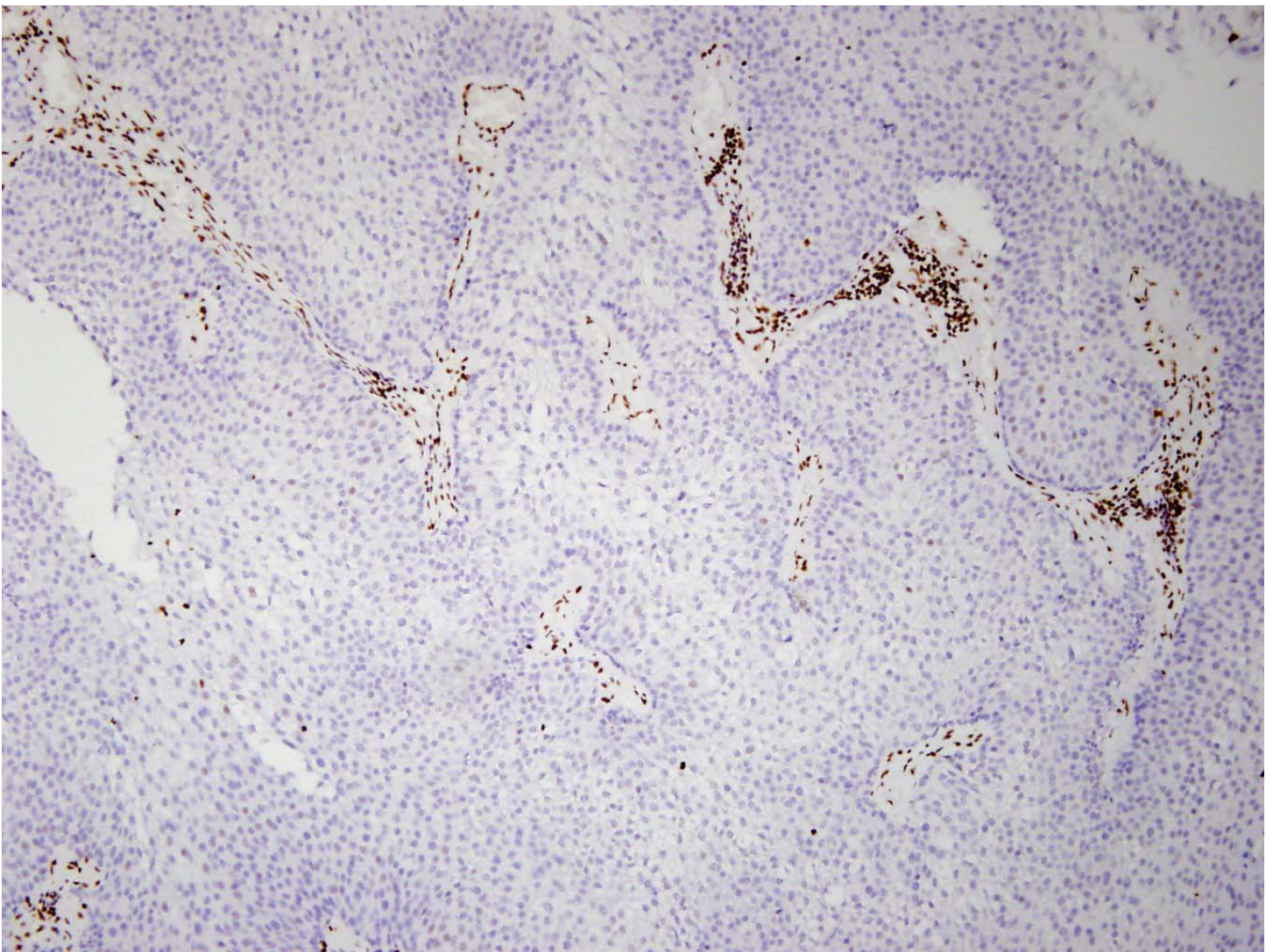


# Supplementary Figure 10 continued

E

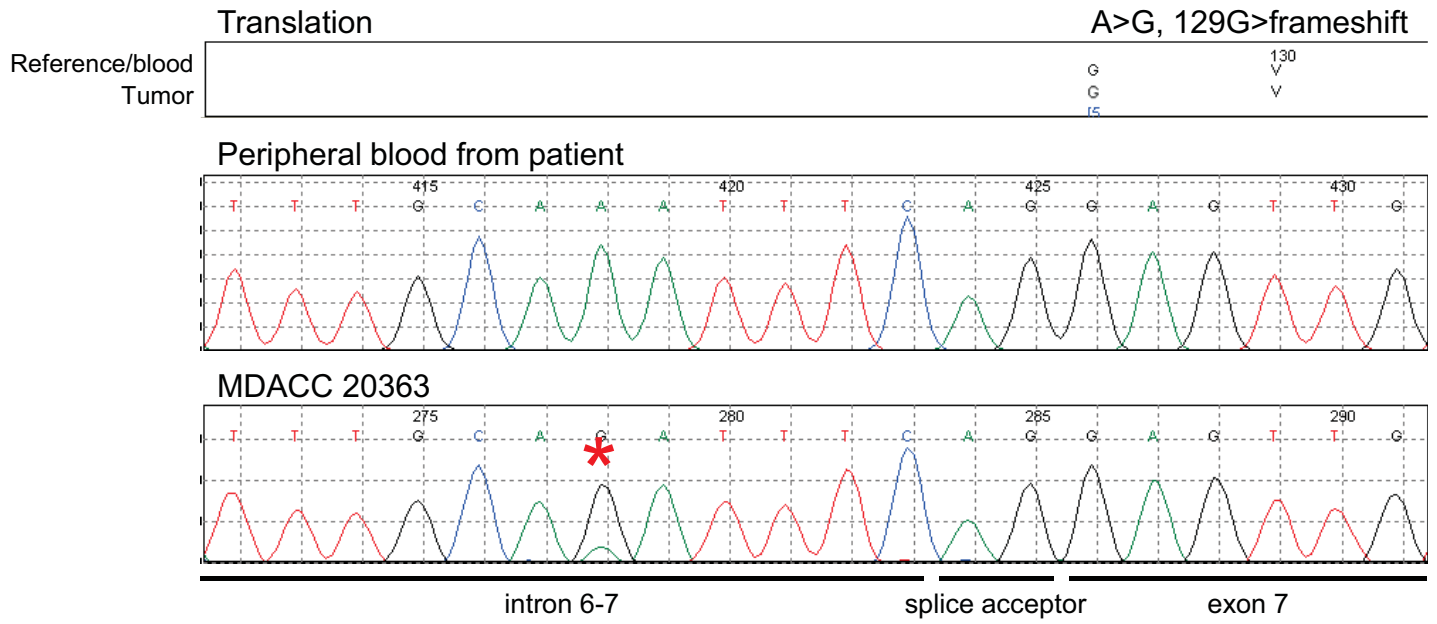


MDACC 20107

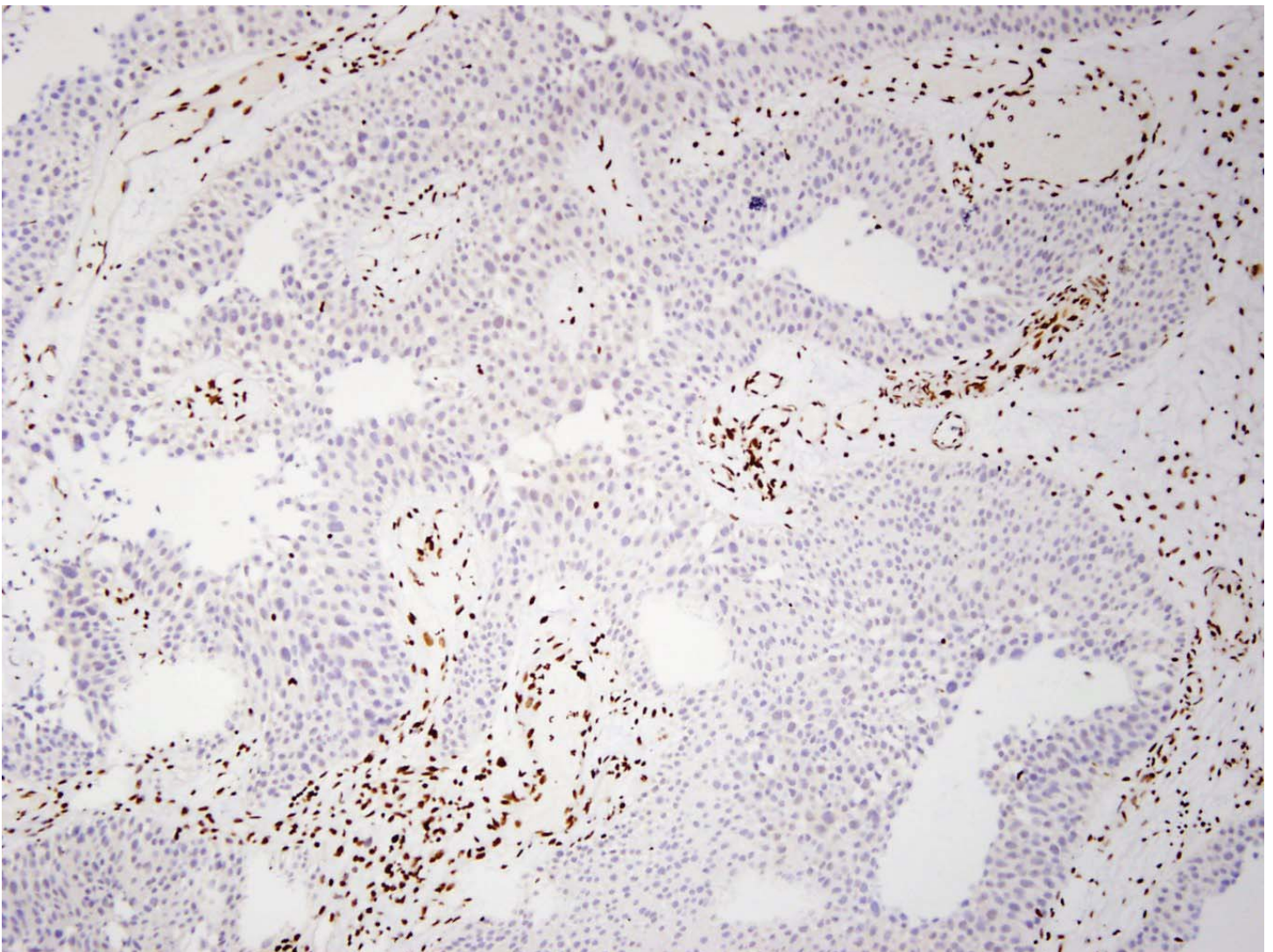


# Supplementary Figure 10 continued

F

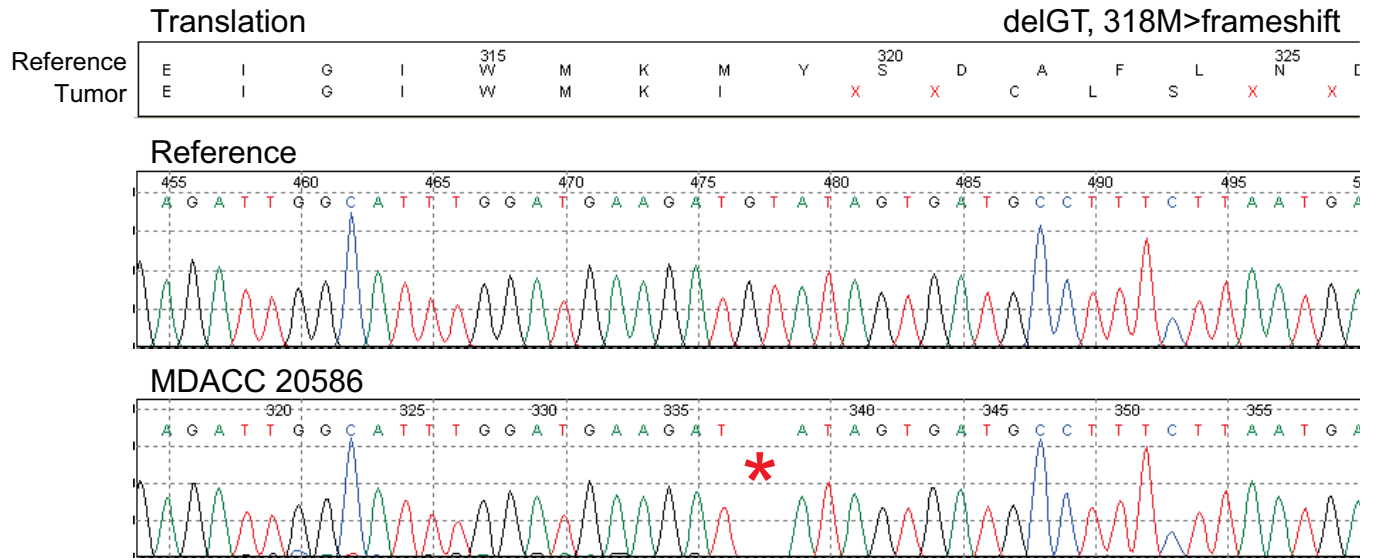


MDACC 20363

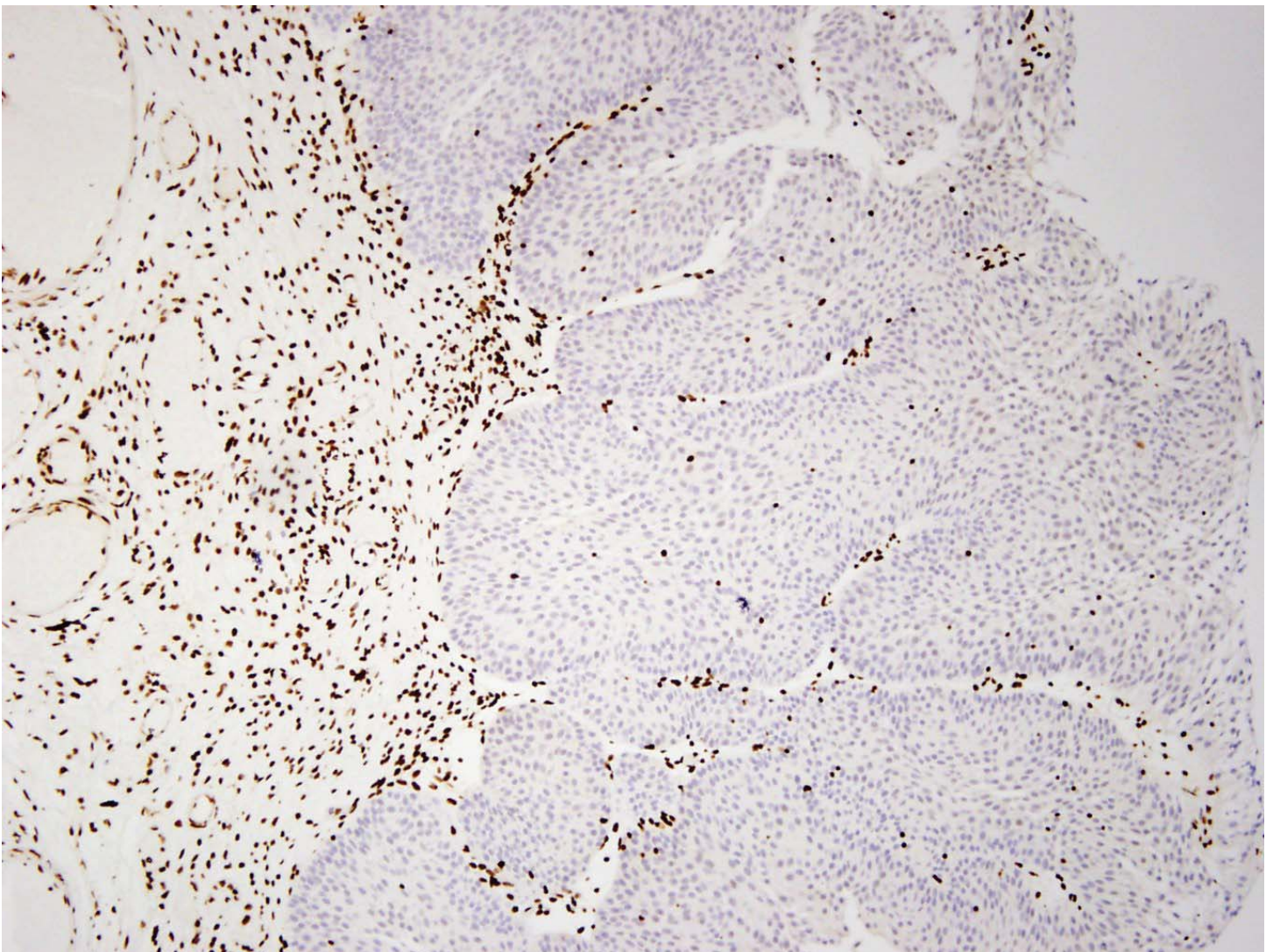


# Supplementary Figure 10 continued

G

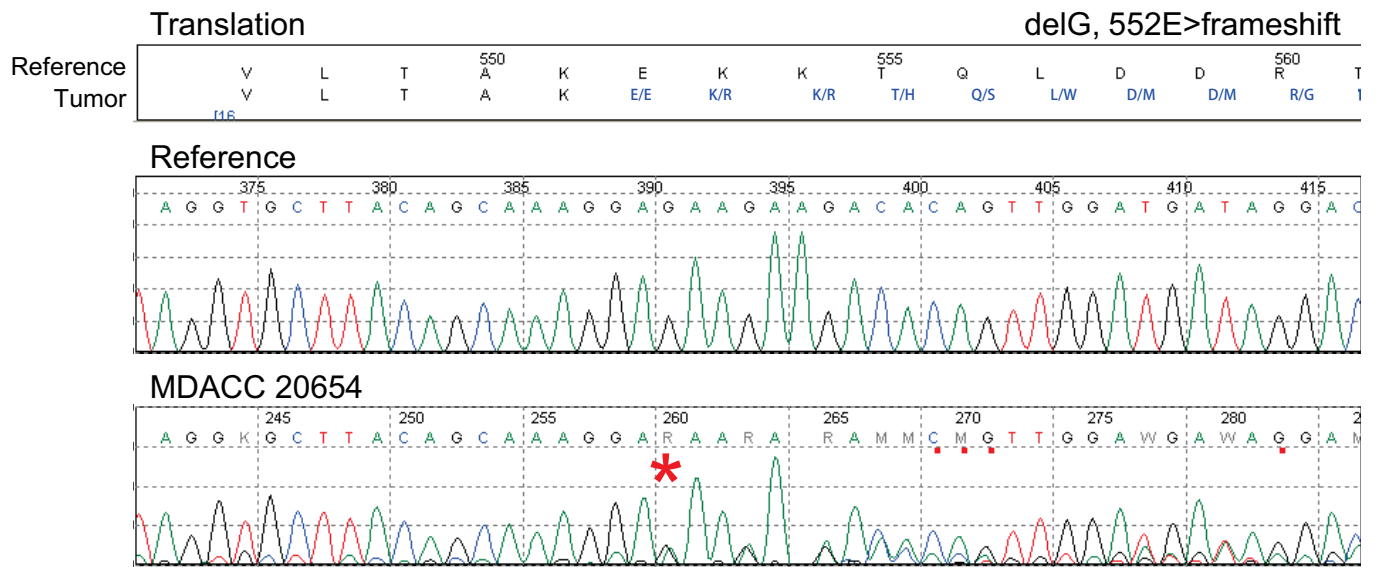


MDACC 20586

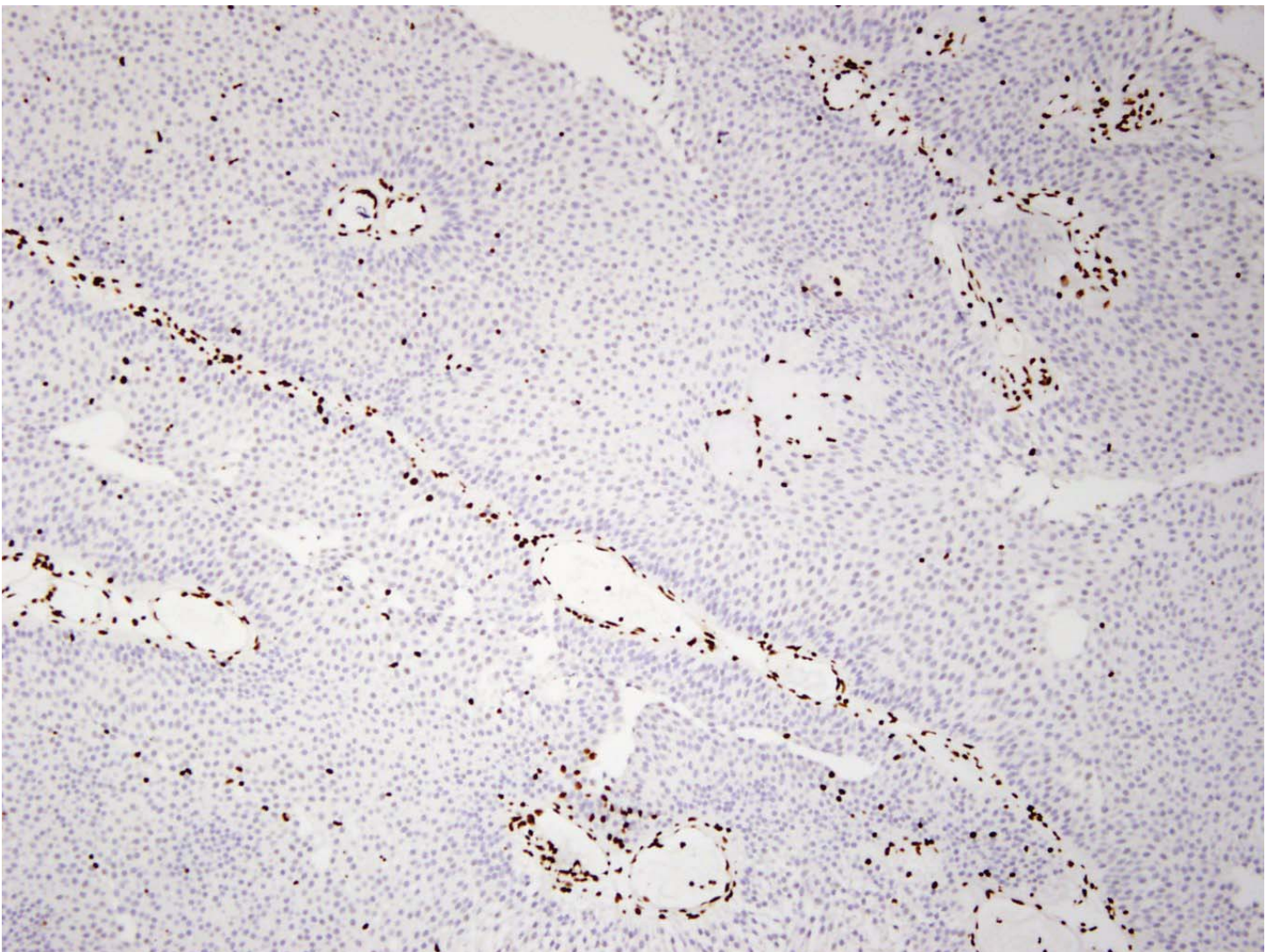


# Supplementary Figure 10 continued

## H



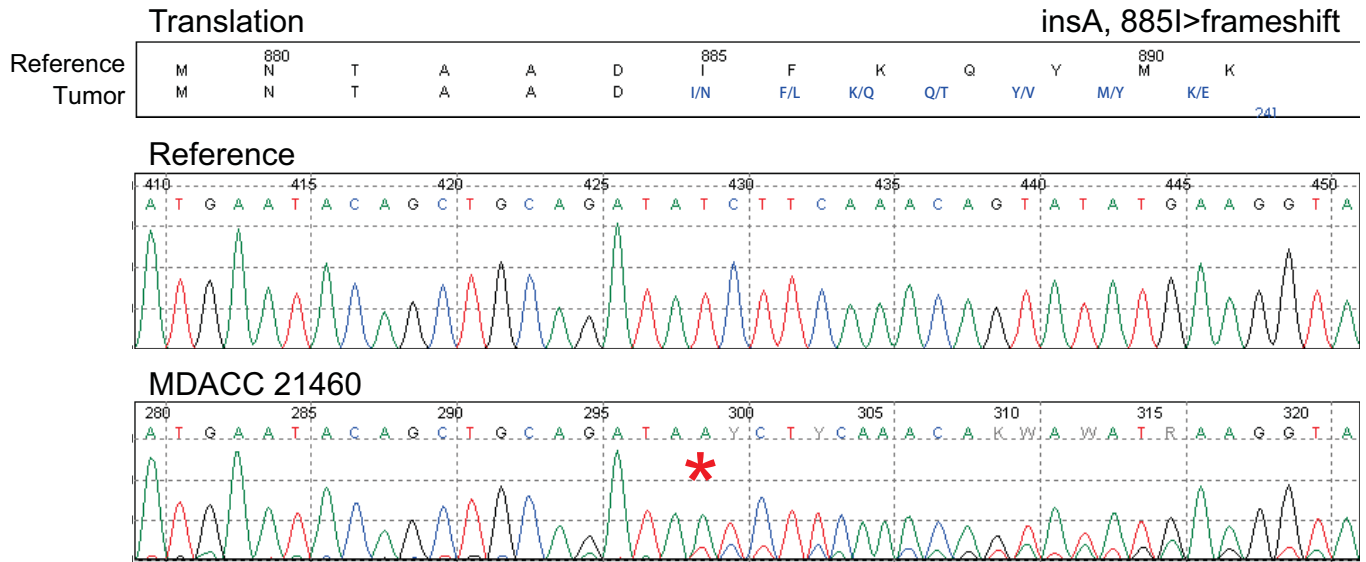
MDACC 20654



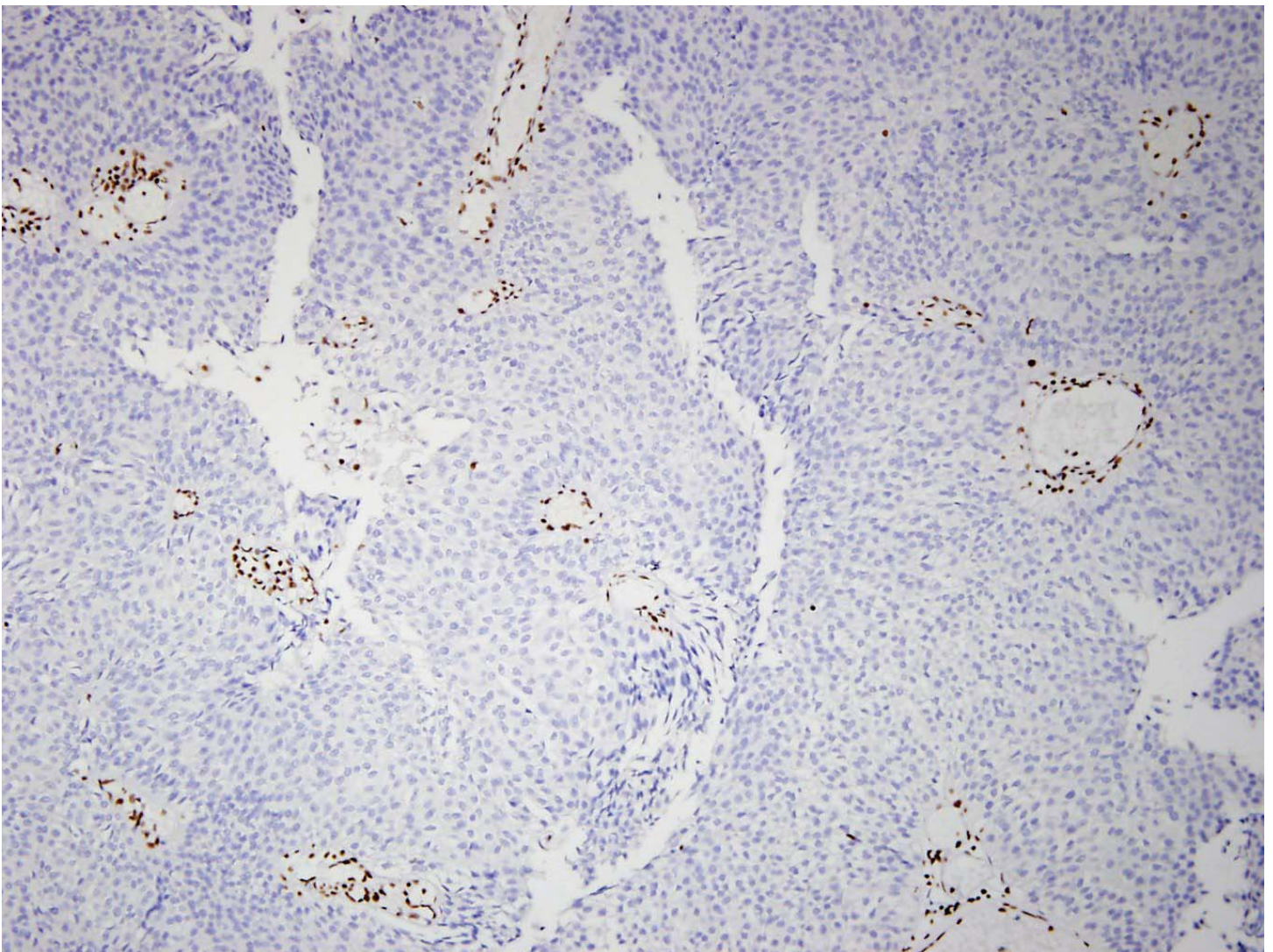


# Supplementary Figure 10 continued

J

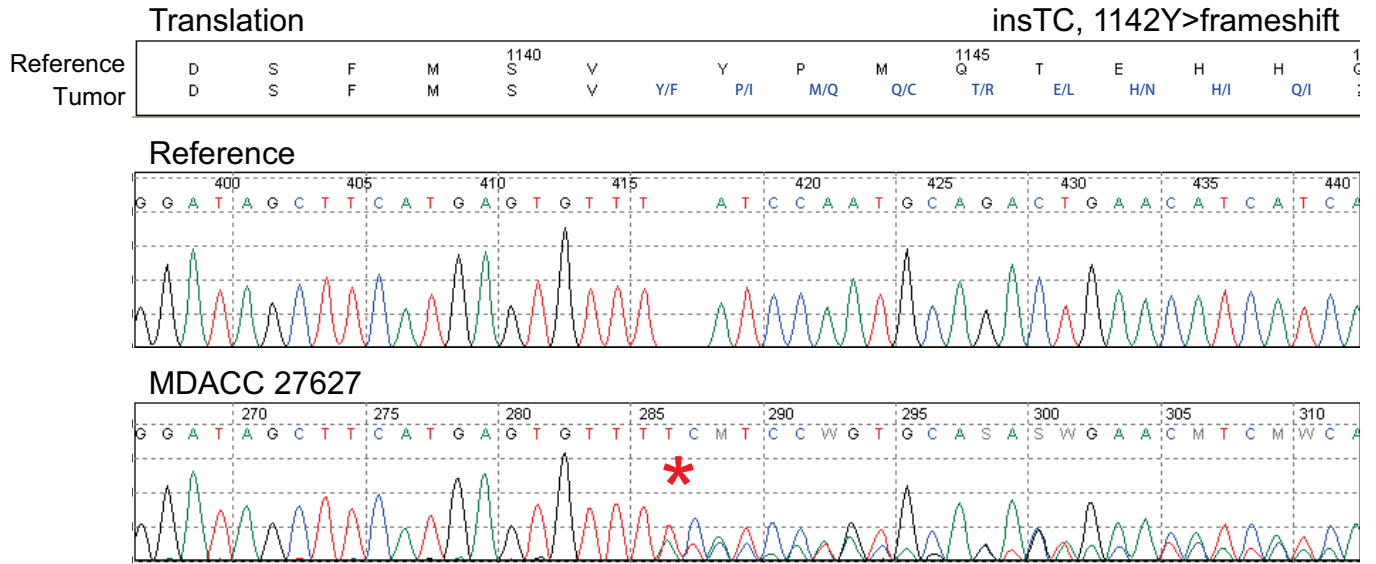


MDACC 21460

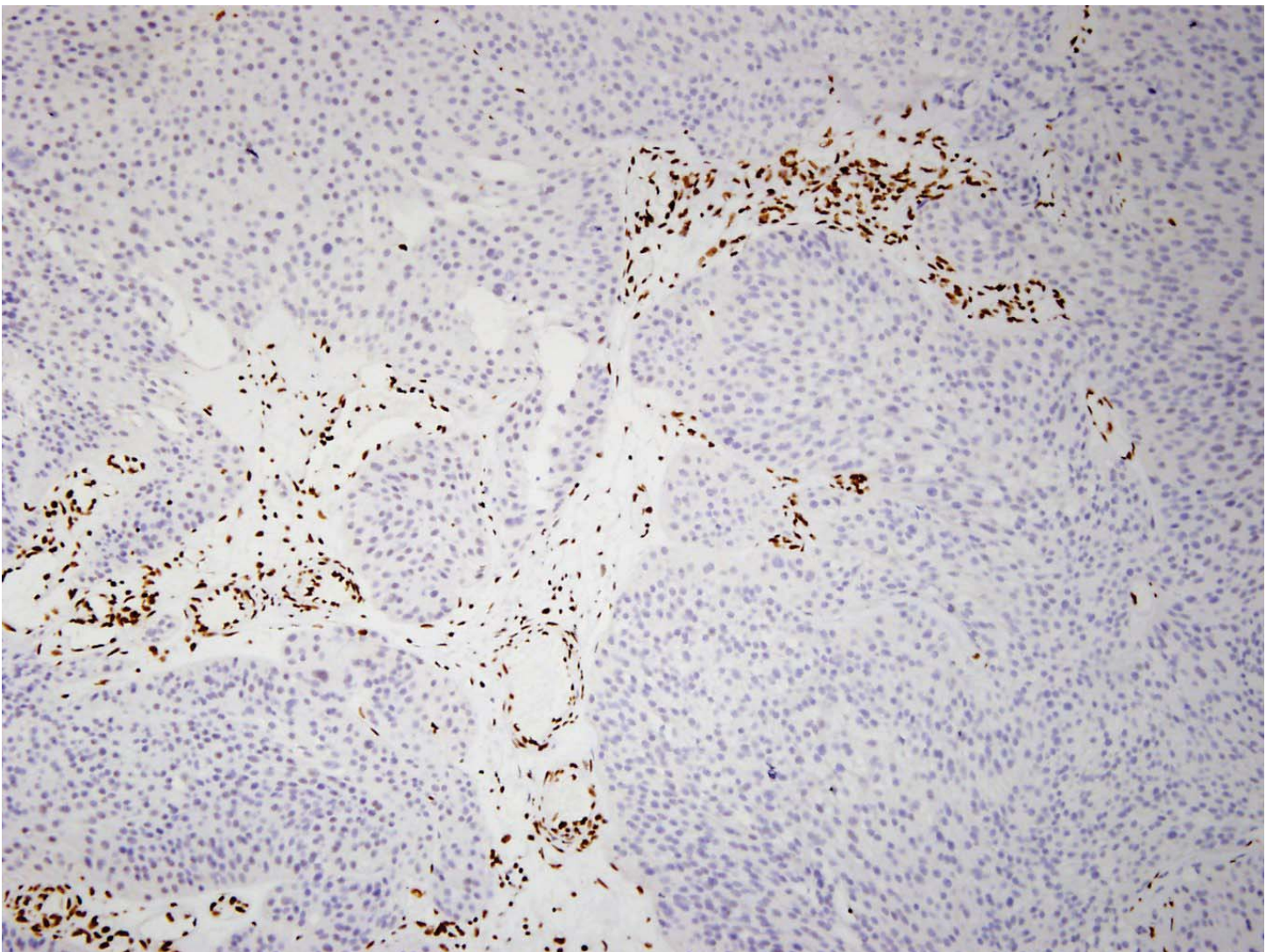


# Supplementary Figure 10 continued

K



MDACC 27627

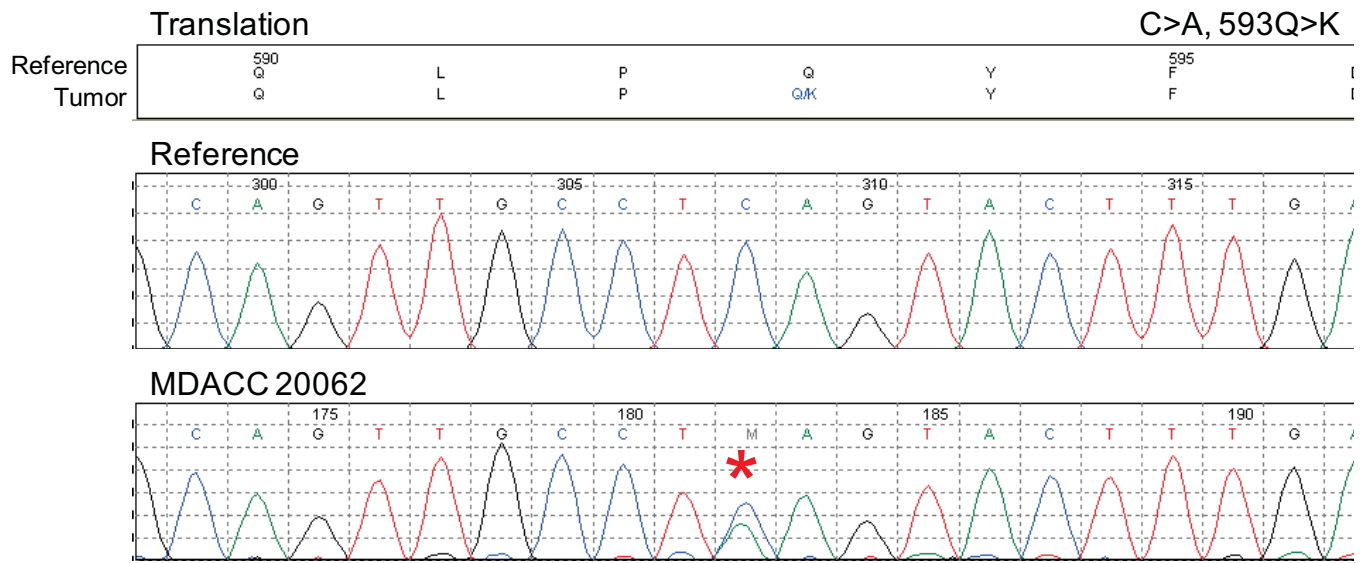


## Supplementary Figure 10 continued

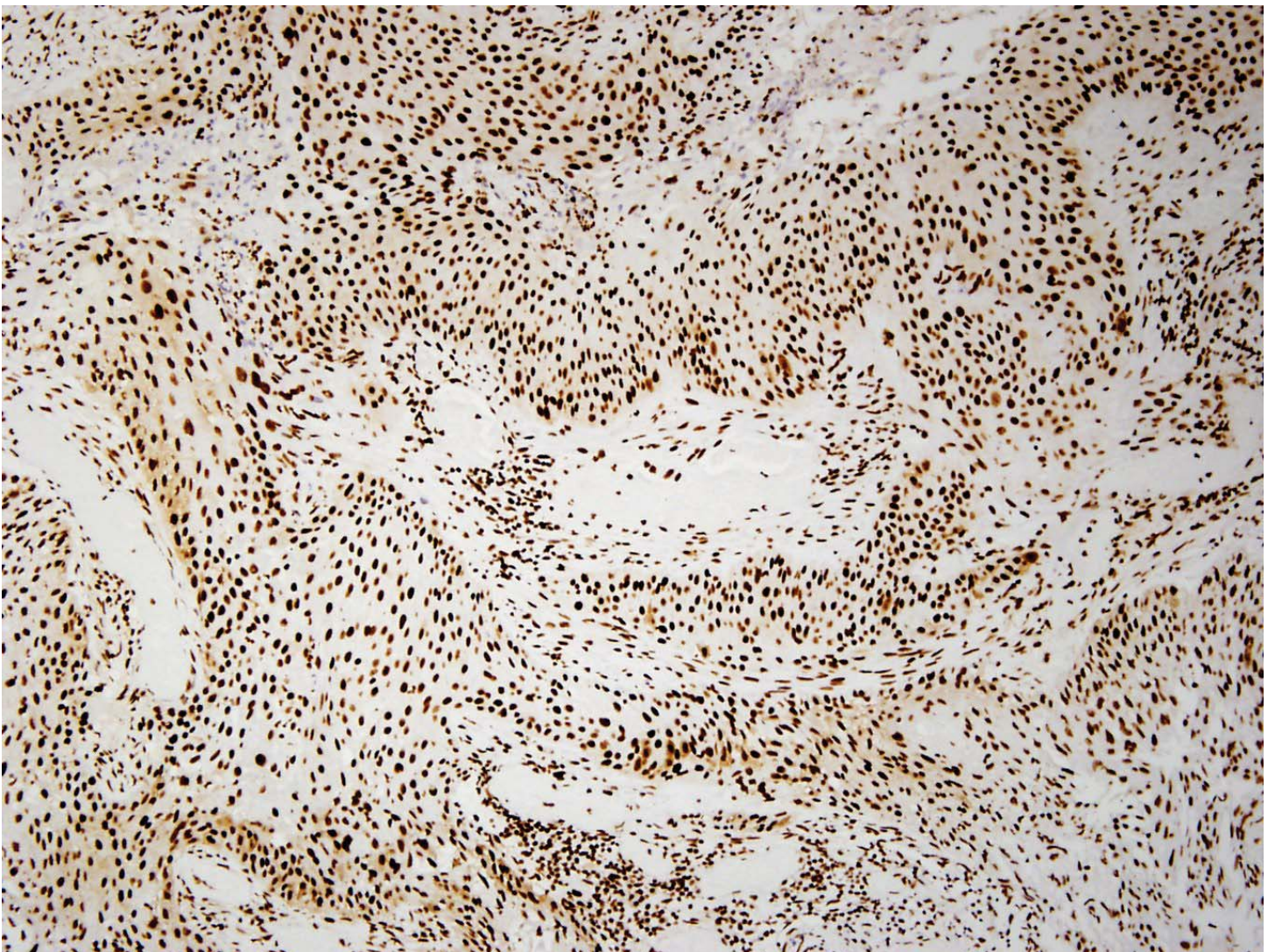
**Supplementary Figure 10.** Somatic truncating mutations drive loss of STAG2 expression in urothelial carcinomas. Examples of STAG2 immunohistochemistry and sequence traces from human urothelial carcinomas harboring truncating mutations of the STAG2 gene (A-K).

# Supplementary Figure 11

A



MDACC 20062

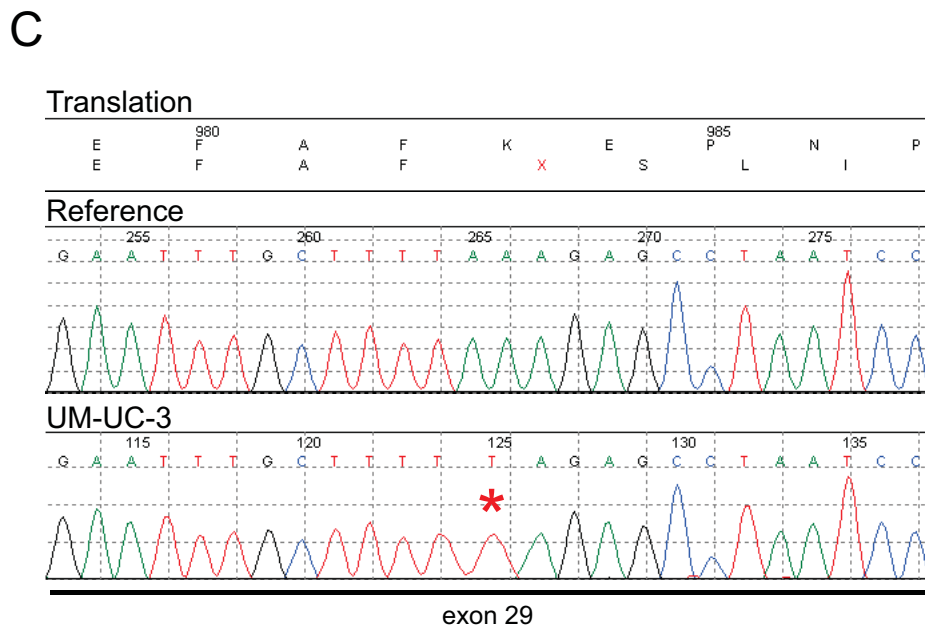
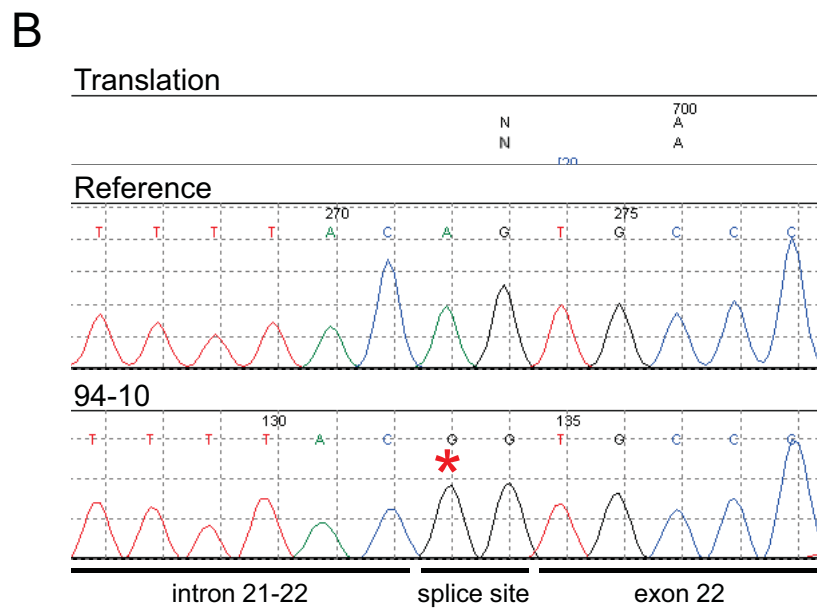
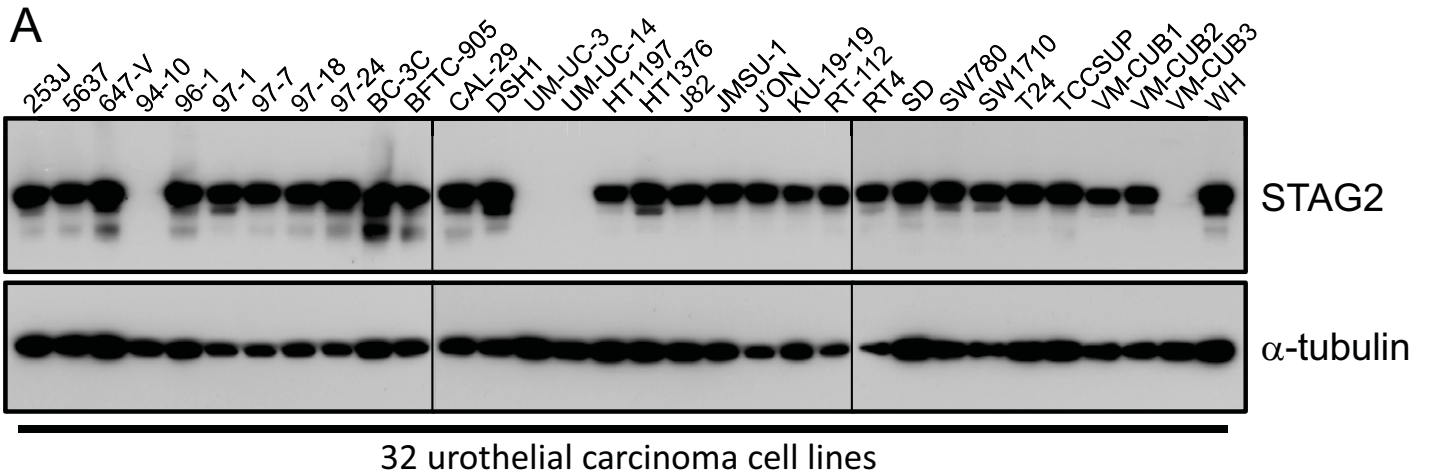




## Supplementary Figure 11 continued

**Supplementary Figure 11.** STAG2 expression is retained in the subset of urothelial carcinomas with STAG2 missense mutations. Examples of STAG2 immunohistochemistry and sequence traces from human urothelial carcinomas harboring missense mutations of the STAG2 gene.

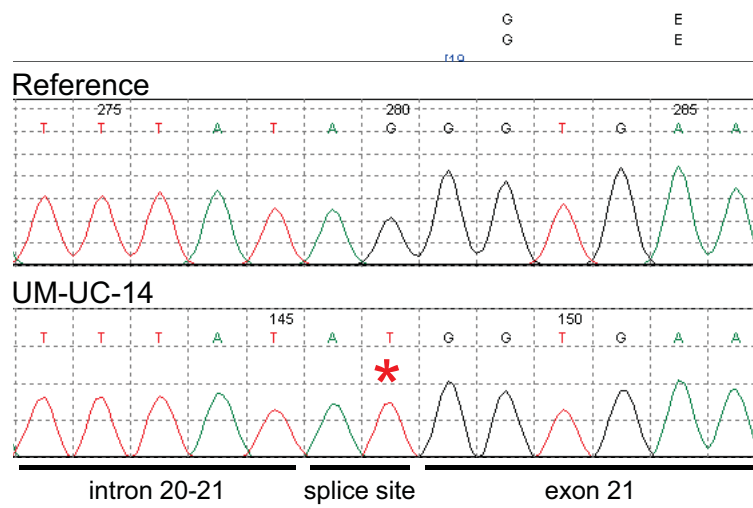
# Supplementary Figure 12



# Supplementary Figure 12 continued

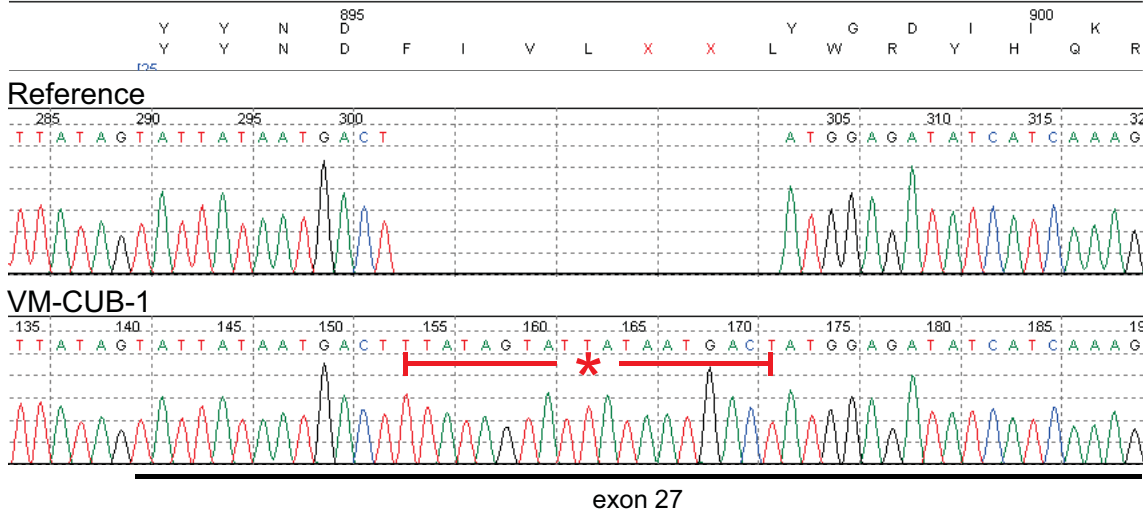
D

Translation



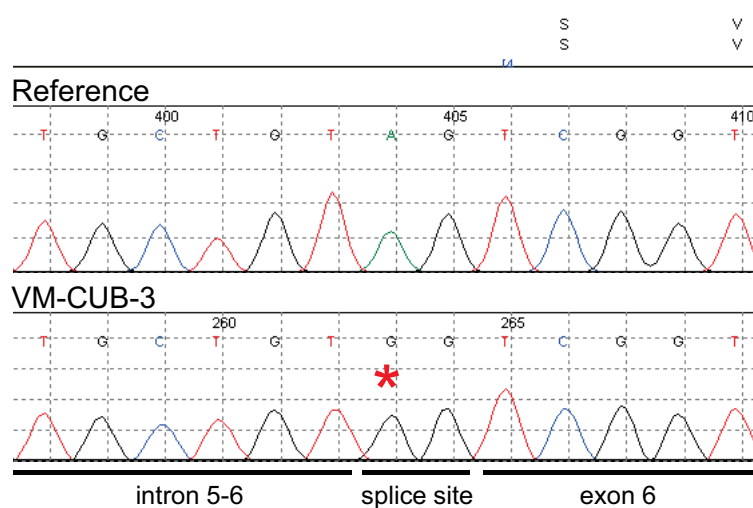
E

Translation



F

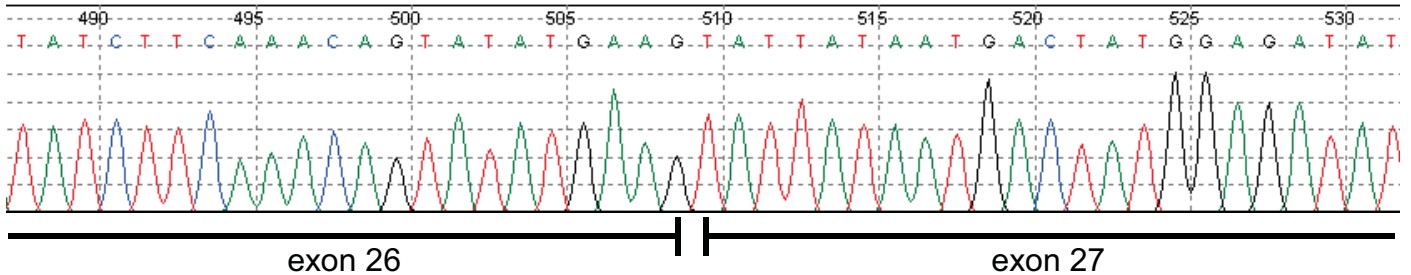
Translation



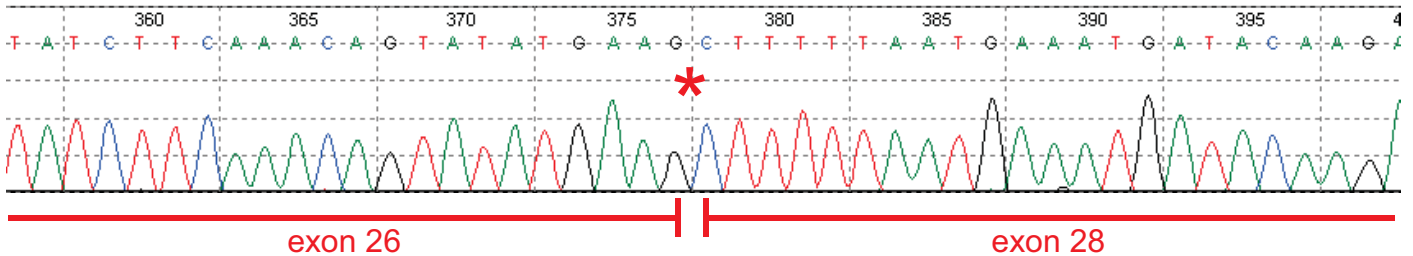
# Supplementary Figure 12 continued

G

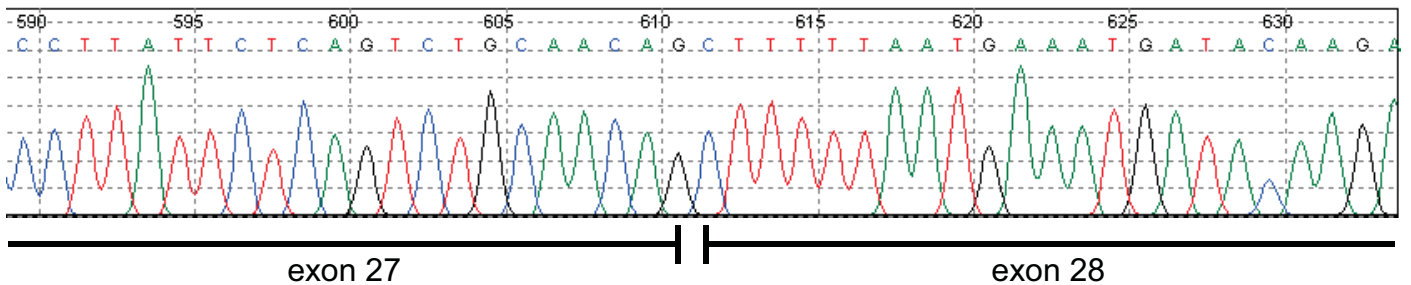
## Reference STAG2 mRNA



## VM-CUB-1 mRNA



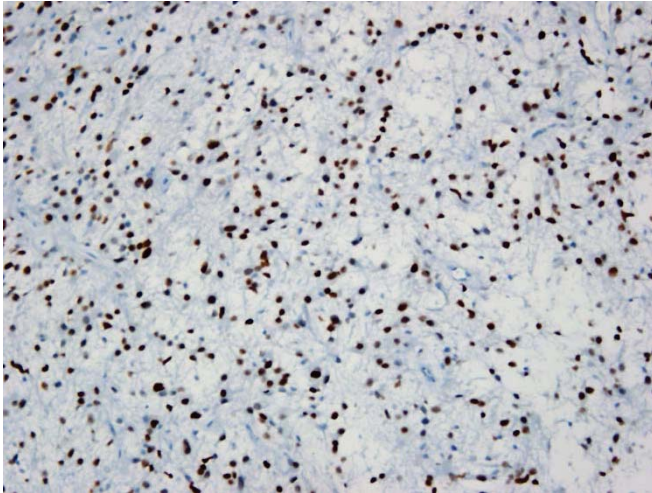
## Reference STAG2 mRNA



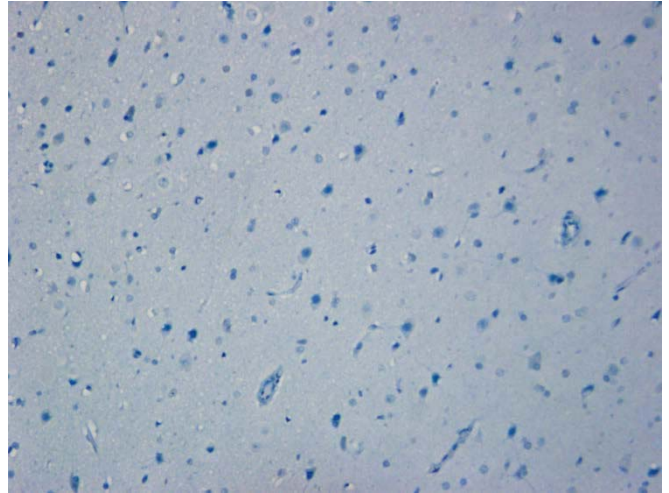
**Supplementary Figure 12.** Truncating mutations of STAG2 in 5 out of 32 human urothelial carcinoma cell lines. (A) Western blot demonstrates absence of STAG2 protein in four cell lines (94-10, UM-UC-3, UM-UC-14, VM-CUB-3) and a lower molecular weight isoform in cell line VM-CUB-1. (B-F) Truncating mutations in the STAG2 gene identified in these five cell lines with altered/absent STAG2 protein. (G) Sequencing of the STAG2 mRNA from VM-CUB-1 cells identifies that exon 27 containing the duplication/insertion is spliced out of the mature mRNA causing translation of a lower molecular weight isoform of STAG2 protein in these cells.

## Supplementary Figure 13

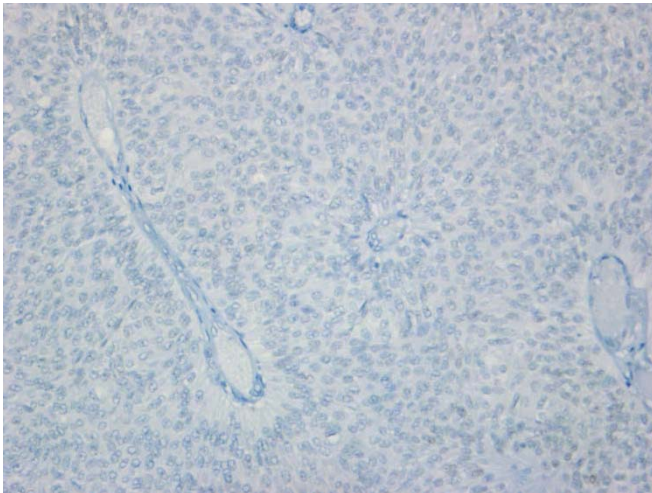
Malignant glioma with known TP53 mutation



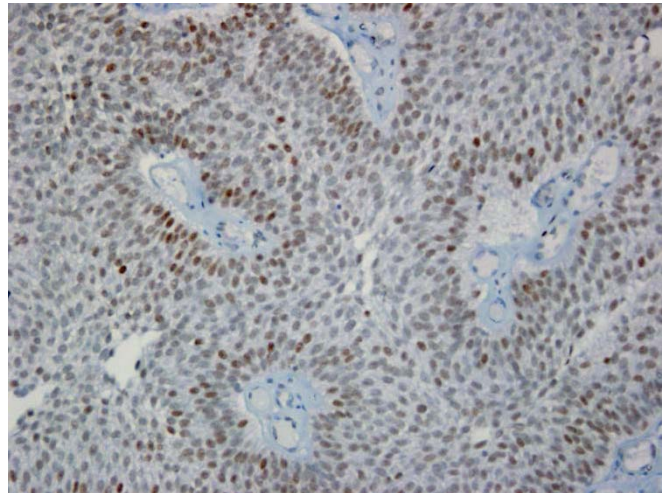
Normal brain



Urothelial carcinoma MDACC 21460

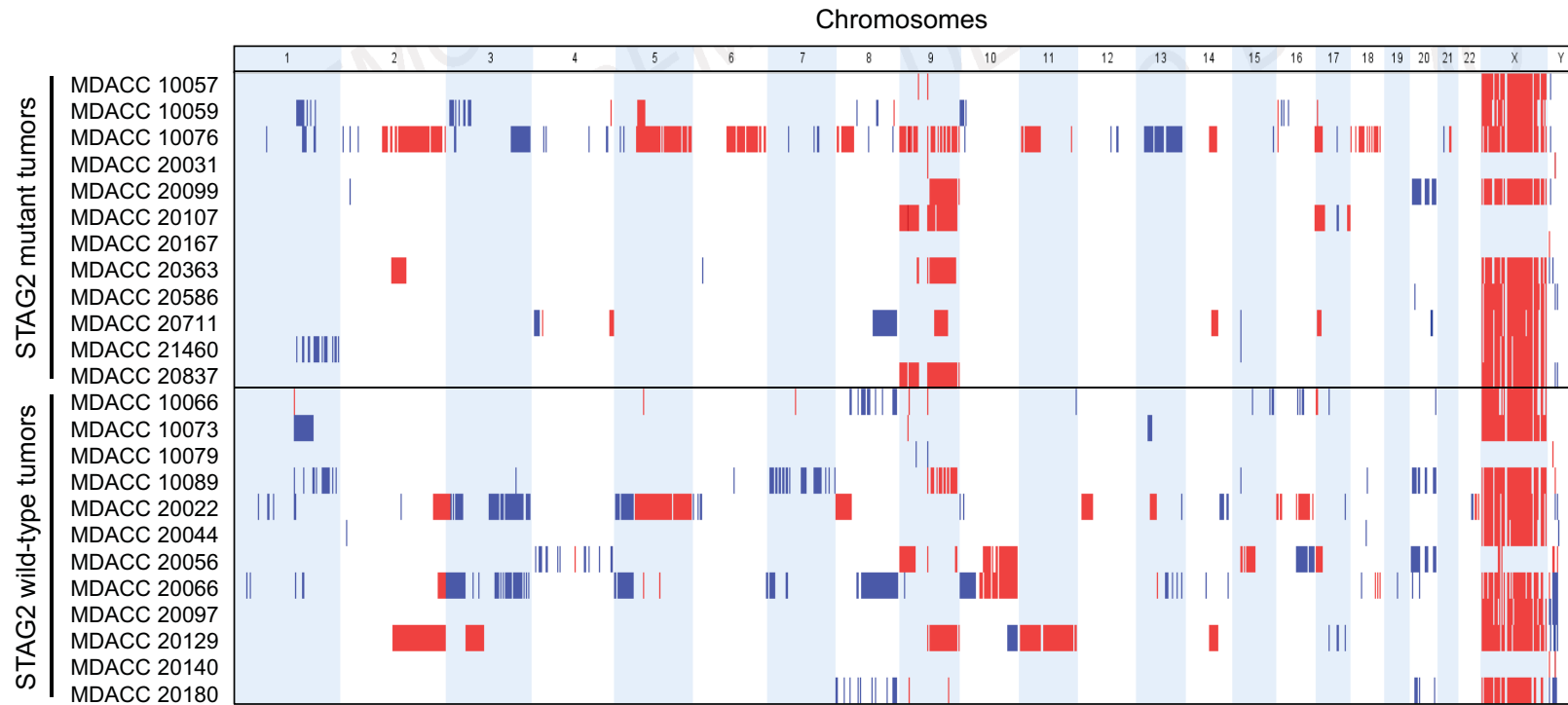


Urothelial carcinoma MDACC 20031



**Supplementary Figure 13.** Determination of p53 status of STAG2 mutant urothelial carcinomas by immunohistochemistry. A malignant glioma with known TP53 missense mutation is positive for p53 overexpression, whereas normal brain from an epilepsy patient is negative for p53 overexpression. Shown are an example of a urothelial carcinoma that is negative for p53 overexpression and a urothelial carcinoma with p53 overexpression (indicative of TP53 mutation or other alteration in the p53 signaling pathway).

## Supplementary Figure 14



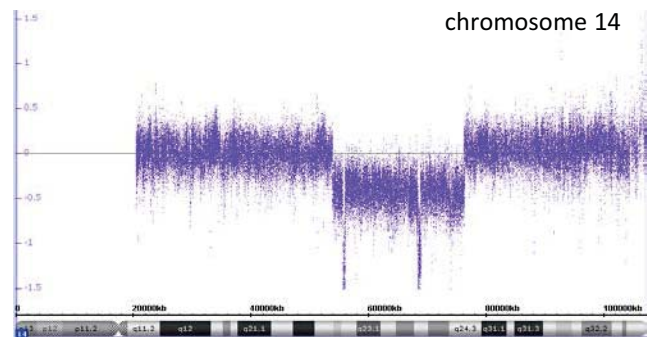
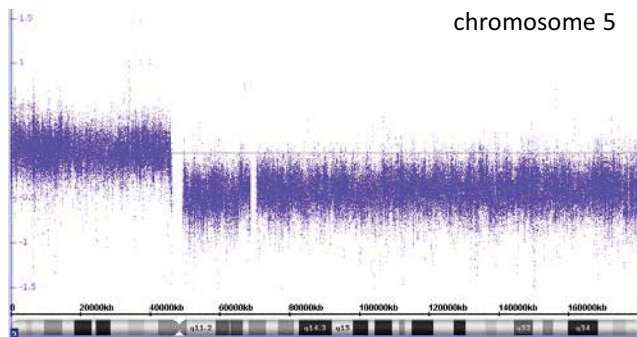
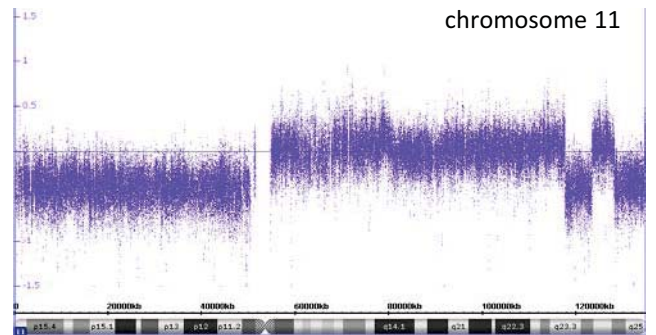
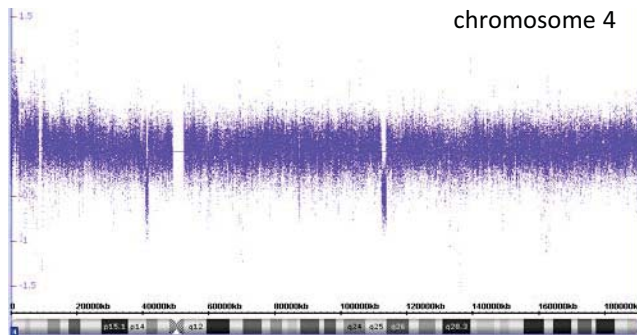
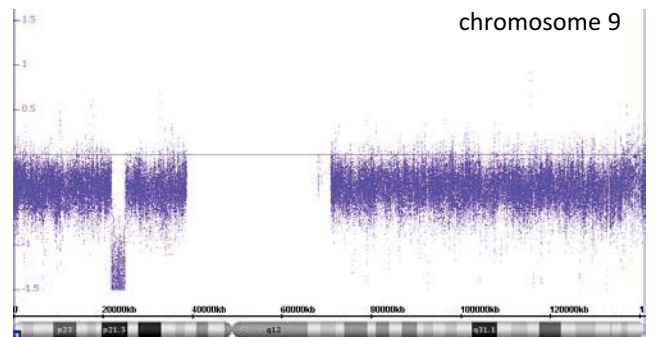
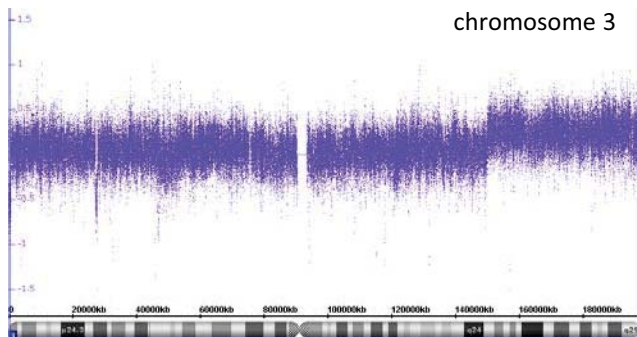
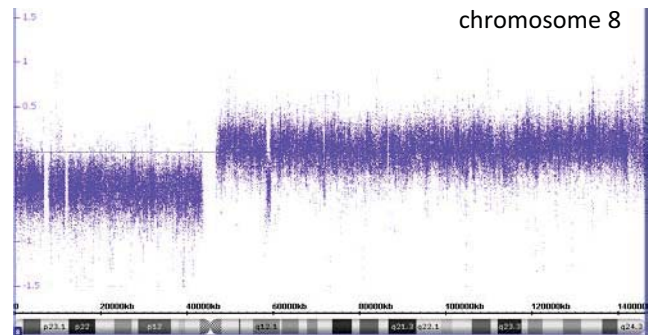
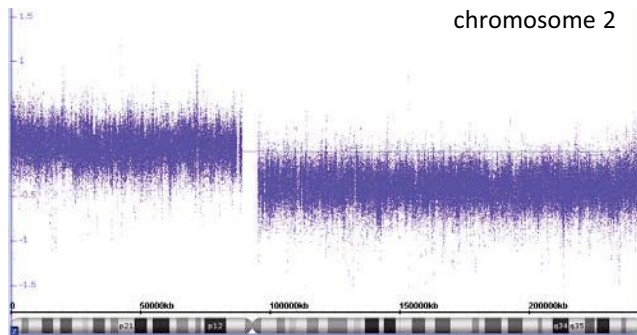
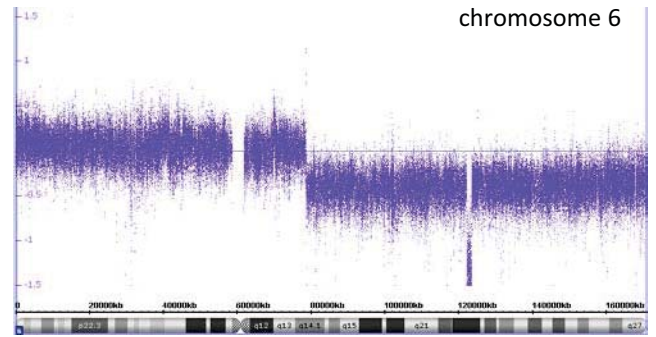
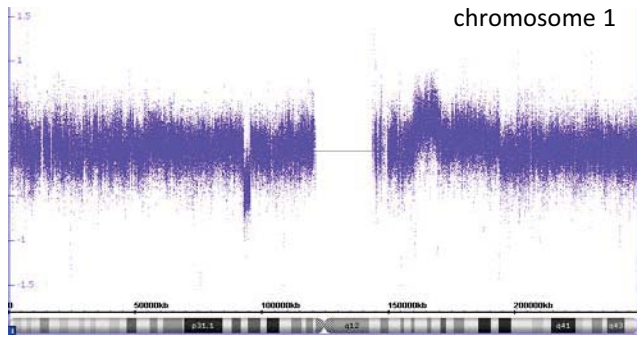
**Supplementary Figure 14.** Whole genome copy number plots for 12 STAG2 mutant and 12 STAG2 wild-type urothelial carcinomas of the bladder. Chromosomal copy number gains are shown in blue and losses are shown in red.



# Supplementary Figure 15 continued

B

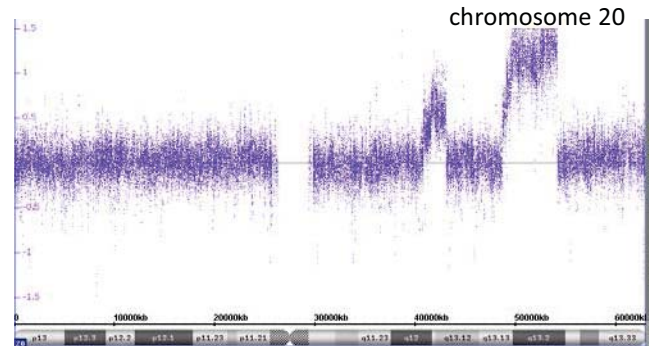
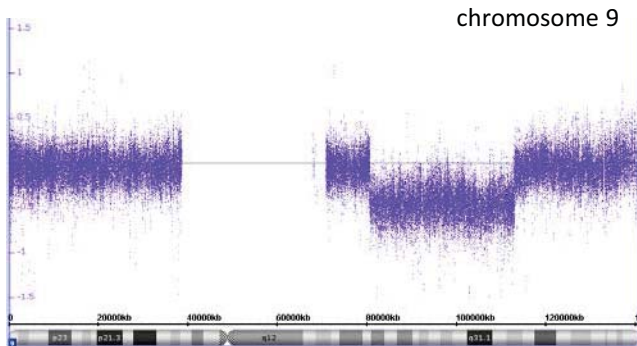
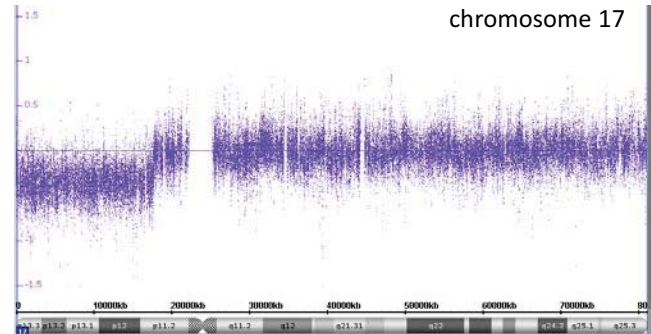
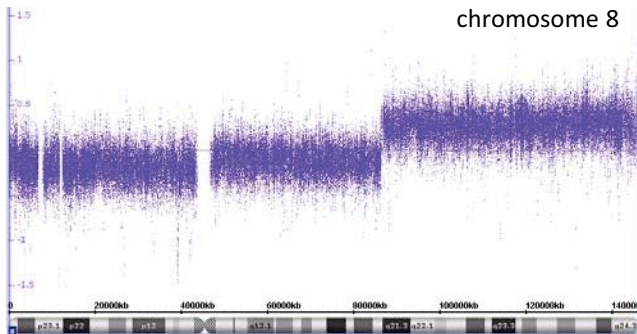
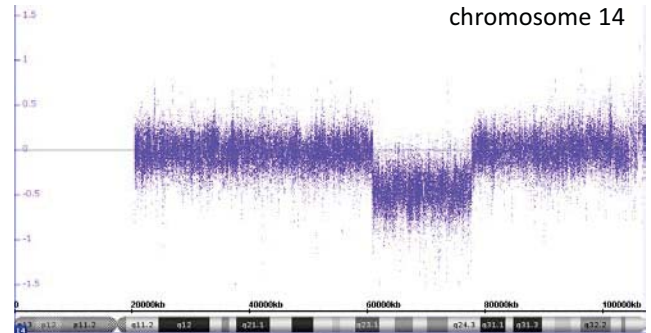
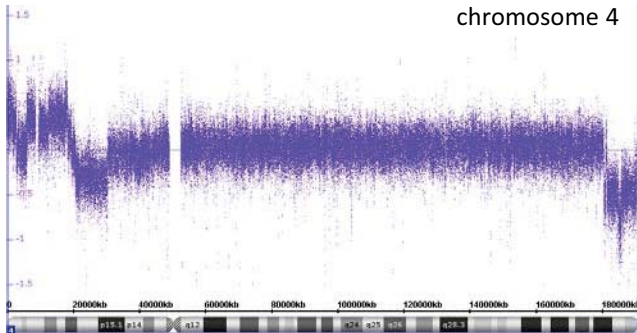
## MDACC 10076



# Supplementary Figure 15 continued

C

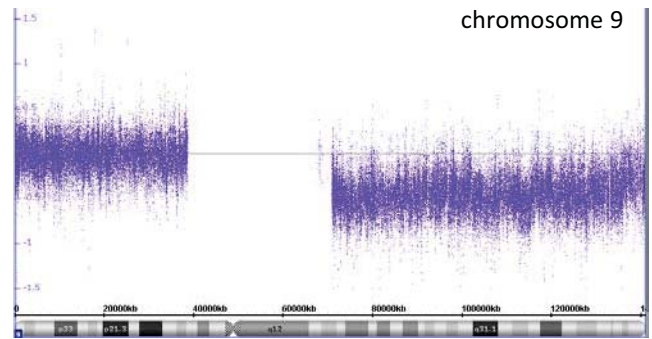
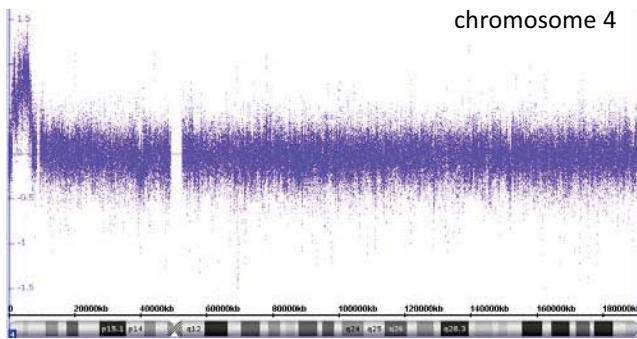
## MDACC 20711



# Supplementary Figure 15 continued

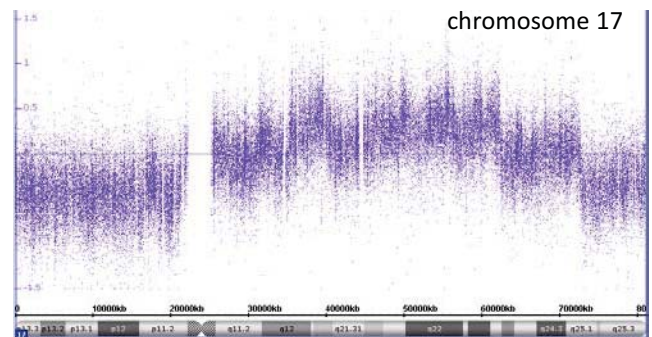
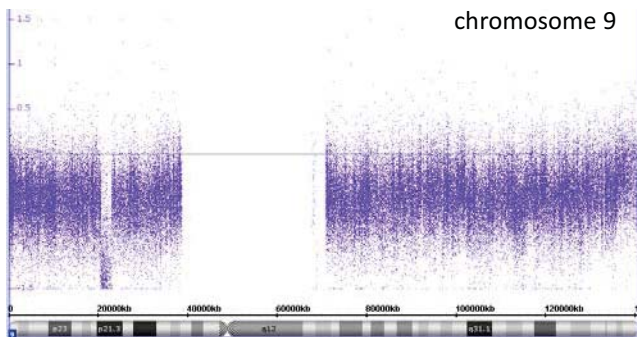
D

## MDACC 20099



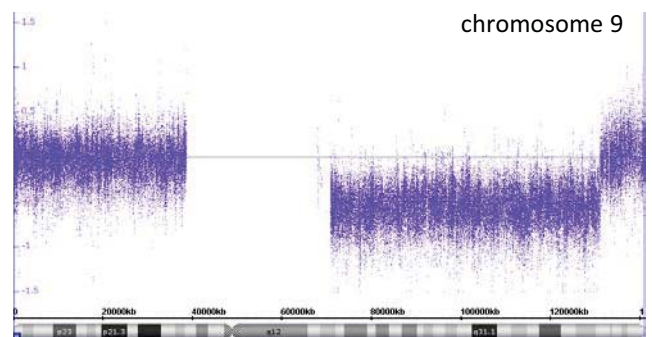
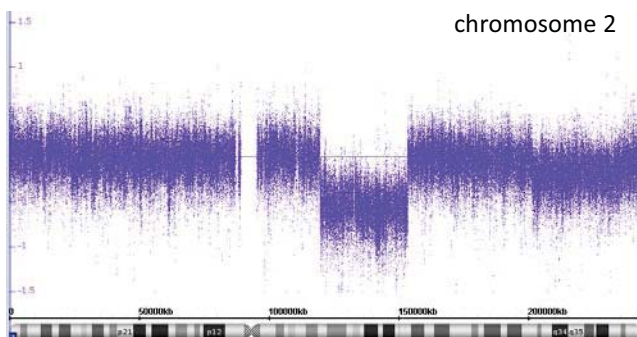
E

## MDACC 20107



F

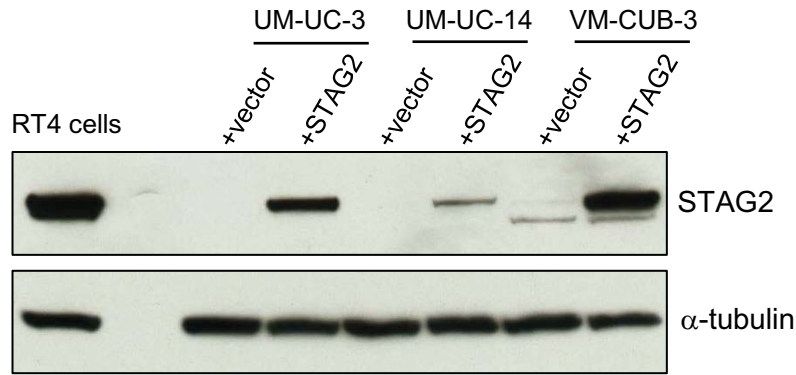
## MDACC 20363



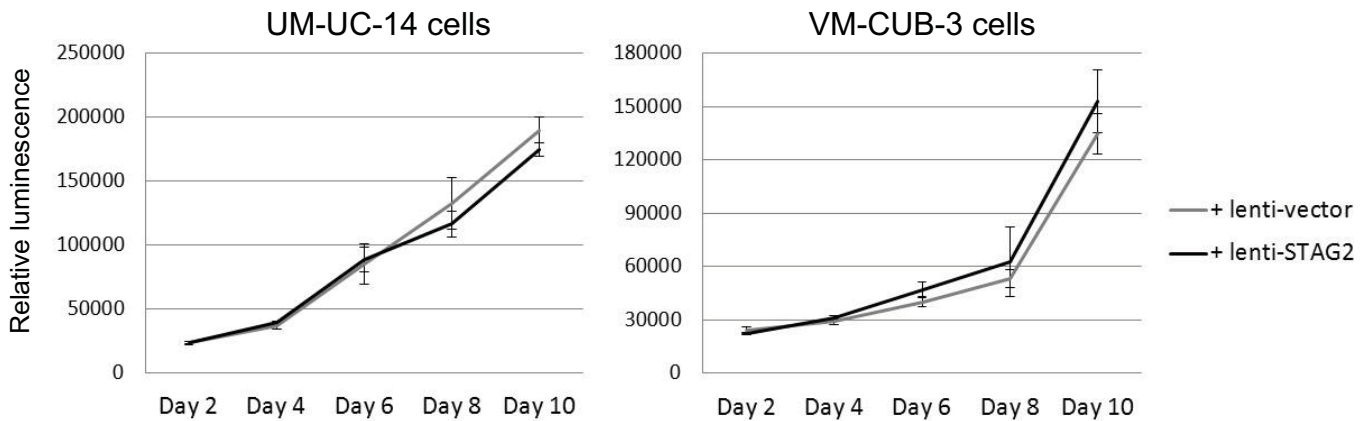
**Supplementary Figure 15.** Examples of clonal chromosome copy number aberrations identified in STAG2 mutant urothelial carcinomas.

# Supplementary Figure 16

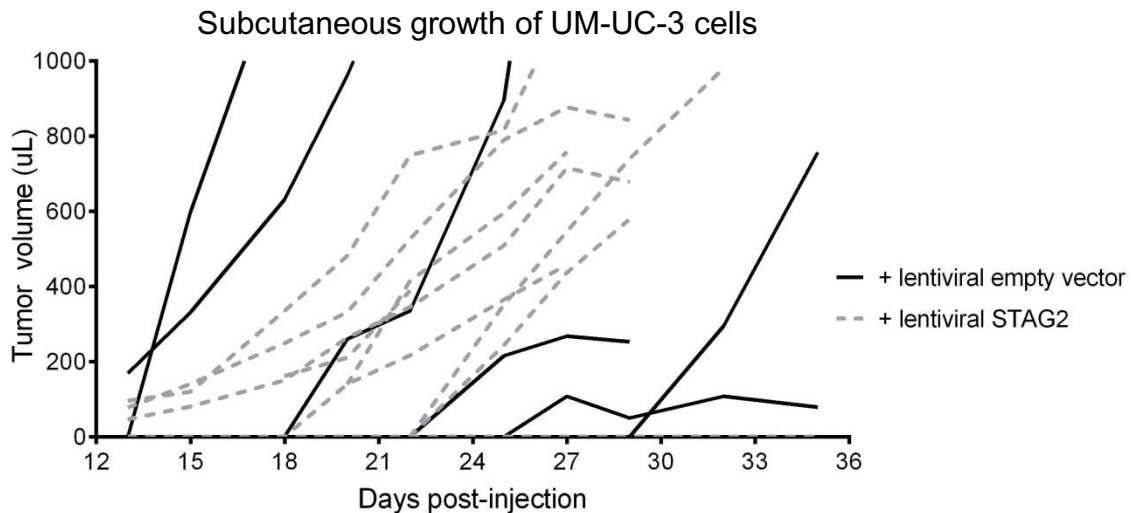
A



B



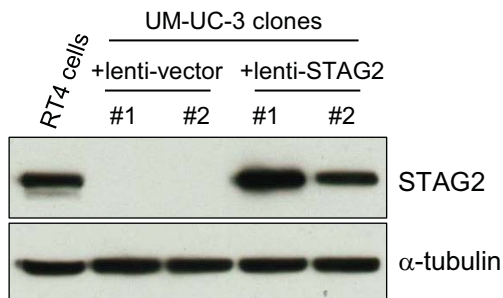
C



**Supplementary Figure 16.** Lentiviral re-expression of wild-type STAG2 in STAG2 mutant urothelial cancer cells does not affect cellular proliferation or *in vivo* xenograft growth. (A) Western blot demonstrating lentiviral re-expression of wild-type STAG2 in UM-UC-3, UM-UC-14, and VM-CUB-3 cells, which all harbor endogenous truncating mutations of STAG2. The level of re-expression is similar to the endogenous levels of STAG2 protein in RT4 cells, which harbor a wild-type STAG2 gene. (B) Proliferation of UM-UC-14 and VM-CUB-3 pooled clones infected with either lentiviral-STAG2 or lentiviral-empty vector after five days of selection in puromycin, measured via CellTiter-Glo assay. (C) Subcutaneous growth of UM-UC-3 pooled clones infected with either lentiviral-STAG2 (n=10) or lentiviral-empty vector (n=10) after injection into nude mice. Tumor volume was measured three times weekly starting at day thirteen post-injection.

# Supplementary Figure 17

A



B

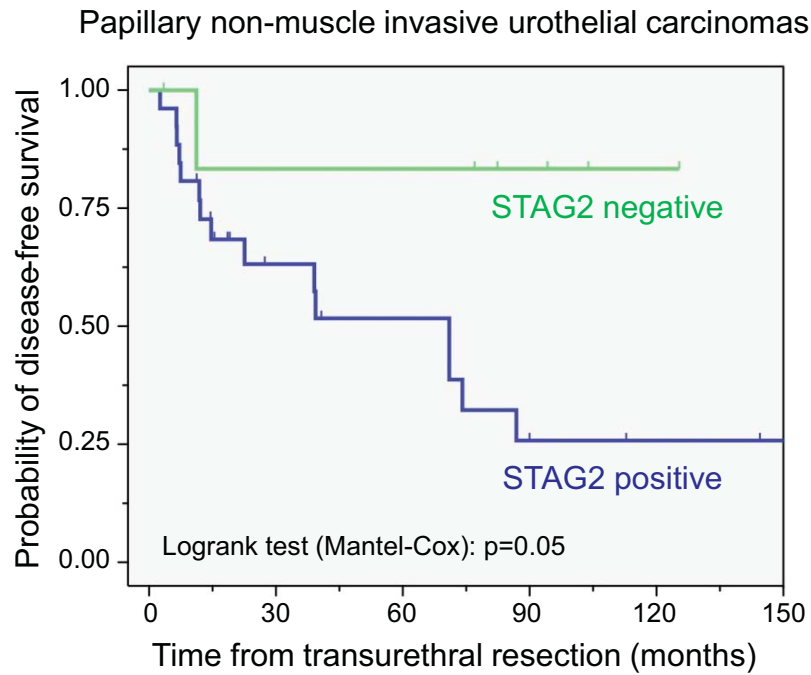
Chromosome count	Number of cells with indicated chromosome count			
	+lenti-vector		+lenti-STAG2	
	#1	#2	#1	#2
60		1		
61				
62			1	
63				
64			1	1
65				
66		1	2	
67				
68		1	1	
69				
70	1	4	4	
71				
72	1	8	9	1
73		1		
74	8	10	8	1
75	6	7	6	3
76	68	62	49	47
77	4	1	4	5
78	12	3	13	37
79			1	2
80		1		3

**Supplementary Figure 17.** Re-expression of wild-type STAG2 in STAG2-mutant UM-UC-3 urothelial carcinoma cells does not significantly alter chromosome counts. (A) Western blot of two independent single cell clones of UM-UC-3 cells following infection with lentiviral-empty vector or lentiviral-STAG2 and puromycin selection. (B) Chromosome counts from 100 cells from the two independent single cell clones of lentiviral-empty vector and lentiviral-STAG2 infected UM-UC-3 cells depicted in A are shown.

## Supplementary Figure 18

Chromosome count	Number of cells with indicated chromosome count			
	+ empty vector		+ STAG2 shRNA	
	#1	#2	#1	#2
66			2	
67				1
68	1	3		1
69				
70				3
71				
72			1	1
73				
74			3	
75				
76			1	1
77				
78			5	
79				
80		2	1	6
81				2
82	2	2	3	
83	1		2	
84	4	2	6	8
85	1	3	4	3
86	5	6	9	6
87	6	7	1	2
88	9	7	31	45
89	38	44	5	6
90	18	17	9	4
91	1			
92	9	4	7	4
93		1	2	
94	4	2	5	3

**Supplementary Figure 18.** Lentiviral shRNA depletion of endogenous wild-type STAG2 expression in RT4 urothelial carcinoma cells leads to alteration in modal chromosome count per cell. Chromosome counts from 100 cells from the two independent single cell clones of lentiviral-empty vector and lentiviral-STAG2 shRNA infected RT4 cells depicted in Figure 2C-D are shown.

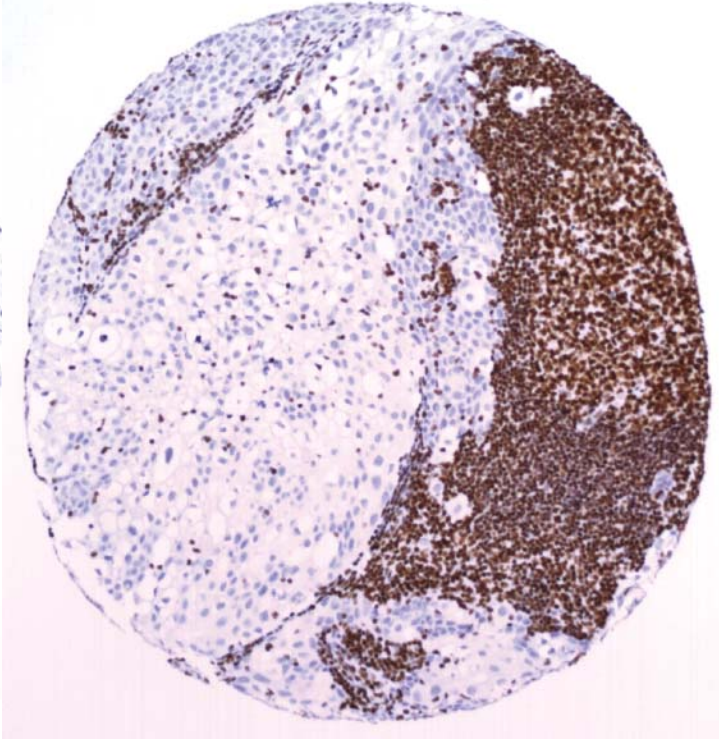
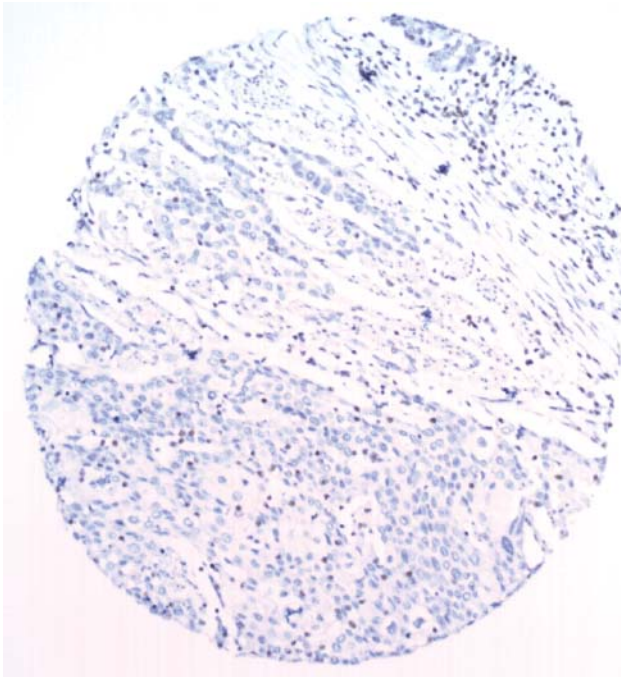


**Supplementary Figure 19.** Kaplan-Meier plot of disease-free survival for 34 patients with non-muscle invasive papillary urothelial carcinoma of the bladder following transurethral resection, with patients stratified into two subgroups according to tumor STAG2 status as determined by IHC. Clinicopathologic characteristics of this patient cohort are detailed in Supplementary Table 5.

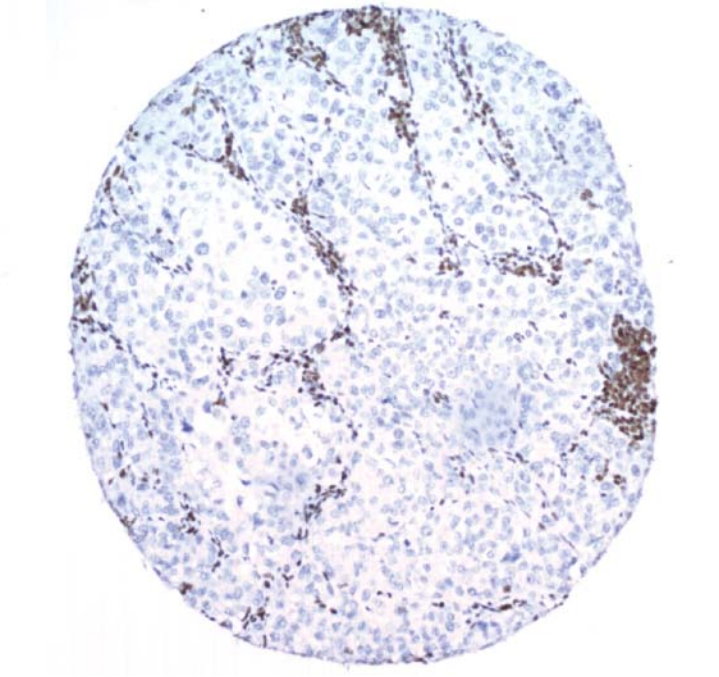
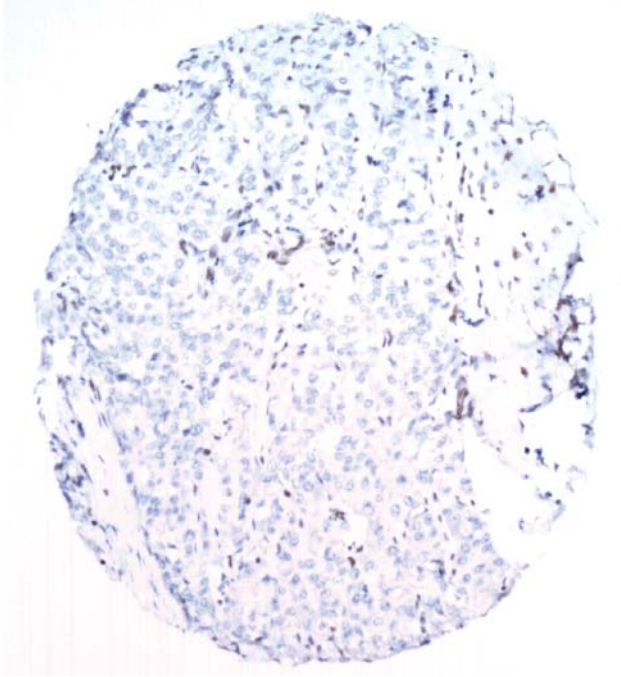
primary tumor

lymph node metastasis

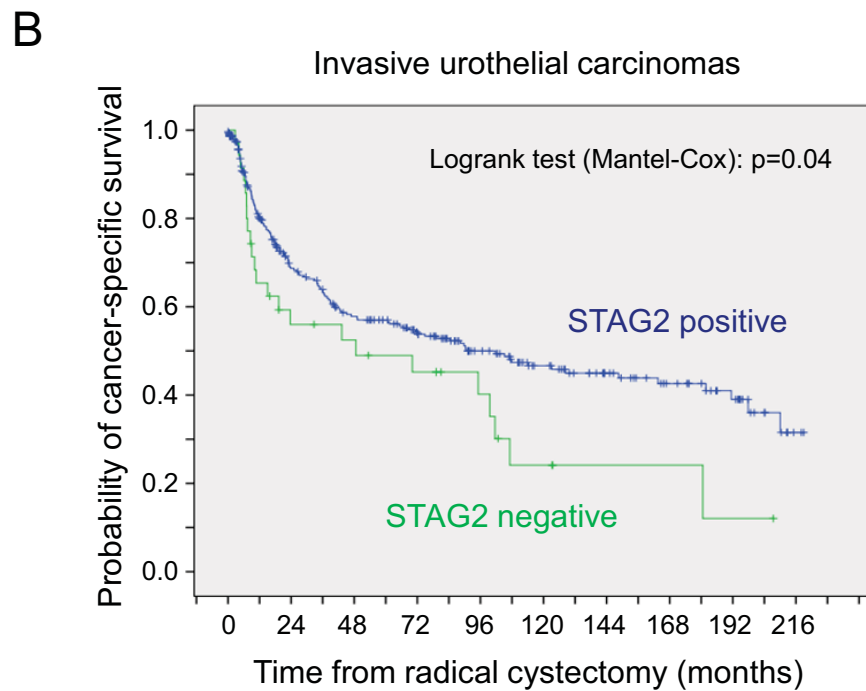
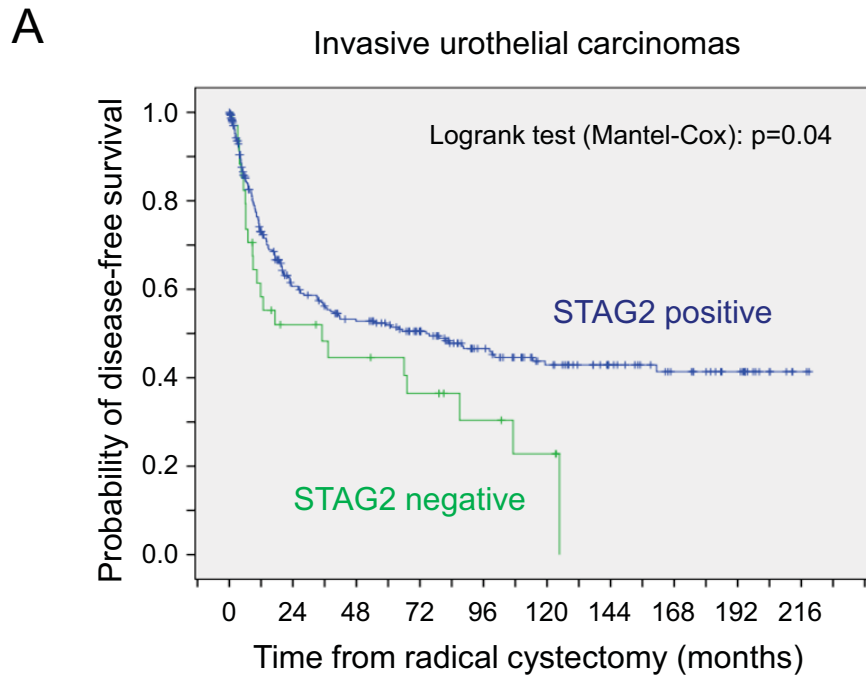
B5848/02



B8535/02



**Supplementary Figure 20.** STAG2 loss is present in urothelial carcinoma primary tumors before lymphovascular invasion. Shown are two cases of urothelial carcinoma lymph node metastases and the primary tumors in the bladder from which they originated.



**Supplementary Figure 21.** Kaplan-Meier plot of disease-free survival (A) and cancer-specific survival (B) is shown for 349 patients with invasive urothelial carcinoma of the bladder treated with radical cystectomy, with patients stratified into two subgroups according to tumor STAG2 status as determined by IHC. Clinicopathologic characteristics of this patient cohort are detailed in Supplementary Table 6.

Supplementary Table 1. IHC screen of diverse human tumors for somatic STAG2 loss.

<b>Tumor type</b>	<b>Negative</b>	<b>Total</b>	<b>% Loss</b>
<b>Brain, Head and neck</b>			
Brain, meningioma	0	46	
Larynx, sarcomatoid carcinoma	0	11	
Larynx, squamous cell carcinoma	0	34	
Nose, adenocarcinoma	0	5	
Nose, Schneiderian papilloma	0	7	
<b>Endocrine/Reproductive</b>			
Adrenal gland, adrenocortical carcinoma	0	11	
Breast, ductal carcinoma	0	52	
Breast, lobular carcinoma	0	18	
Breast, mucinous adenocarcinoma	0	7	
Endometrium, adenocarcinoma	0	21	
Ovary, adenocarcinoma	2	112	2%
Ovary, Brenner tumor	0	3	
Parathyroid, adenoma/carcinoma	0	29	
Testis, embryonal carcinoma	0	22	
Testis, seminoma	0	33	
Thyroid, papillary carcinoma	0	42	
Uterine cervix, squamous cell carcinoma	0	24	
Uterus, cellular leiomyoma/leiomyosarcoma	1	53	2%
<b>Gastrointestinal</b>			
Colon, adenocarcinoma	2	99	2%
Esophagus, adenocarcinoma	0	2	
Esophagus, squamous cell carcinoma	0	28	
Gastrointestinal stromal tumor	1	131	1%
Liver, cholangiocarcinoma	0	19	
Pancreas, adenocarcinoma	0	36	
Pancreas, neuroendocrine tumor	0	13	
Small intestine, sarcomatoid carcinoma	0	18	
Stomach, adenocarcinoma	1	49	2%
<b>Genitourinary</b>			
Bladder, adenocarcinoma	0	18	
Bladder, squamous cell carcinoma	0	15	
Bladder, urothelial carcinoma	52	295	18%
Kidney, renal cell carcinoma	0	24	
Prostate, adenocarcinoma	0	58	
Renal pelvis, urothelial carcinoma	0	12	
<b>Hematologic</b>			
Bone marrow, acute myeloid leukemia	1	12	8%
Lymphoma, follicular	0	53	
Lymphoma, Hodgkin's	0	22	
Lymphoma, large B cell	0	78	
Lymphoma, small B cell	0	32	
Lymphoma, T cell	0	48	
Spleen, chronic myelogenous leukemia	0	4	
<b>Pulmonary</b>			
Lung, adenocarcinoma	0	102	
Lung, small cell carcinoma	0	16	
Lung, squamous cell carcinoma	1	108	1%
Lung, undifferentiated large cell carcinoma	0	36	
<b>Skin</b>			
Basal cell carcinoma	0	26	
Melanoma, malignant	3	48	6%
Squamous cell carcinoma	0	10	
<b>Soft tissue</b>			
Angiosarcoma	0	24	
Chordoma	0	23	
Ewing's sarcoma	3	35	9%
Kaposi sarcoma	0	33	
Malignant peripheral nerve sheath tumor	1	46	2%
Mesothelioma, malignant	0	22	
Synovial sarcoma	0	64	
Undifferentiated pleomorphic sarcoma	0	25	
<b>Total</b>	<b>68</b>	<b>2214</b>	<b>3%</b>

Supplementary Table 4. Clonal chromosome copy number aberrations identified in 12 STAG2 mutant and 12 STAG2 wild-type urothelial carcinomas.

Tumor	STAG2 status	Pathologic stage, grade	Total # of aberrations	Chromosomal aberrations		
				chromosome	amp/gain/loss/del	coordinates (MB)
MDACC 10057	MUT	pTa, G2	0	-	-	-
MDACC 10059	MUT	pT2, G3	36	1p	gain	68-72
				1p	gain	105-120
				1q	gain	144-194
				1q	loss	194-248
				3pq	gain	0-194
				3q	loss	130-135
				3q	loss	194-196
				4pq	loss	0-134
				4q	loss	148-190
				4q	del	182-186
				5q	loss	50-180
				5q	del	156-157
				8pq	gain	0-99
				8q	loss	83-87
				8q	gain	99-105
				8q	gain	112-115
				8q	loss	115-145
				8q	del	133-135
				9p	loss	0-38
				9p	del	21-22
				10p	gain	0-15
				10q	loss	52-135
				10q	del	131-132
				11p	loss	0-44
				11p	gain	44-46
				13q	loss	27-56
				13q	gain	73-74
				16p	loss	2-8
				16p	amp	8-9
				16p	amp	10-21
				16p	gain	27-32
				17p	loss	0-22
				17q	gain	25-32
				18q	gain	42-57
				19q	gain	28-59
				20q	gain	0-63
MDACC 10076	MUT	pT1, G2	31	1p	loss	92-94
				1q	gain	161-170
				2q	loss	95-242
				3q	gain	150-197
				4p	gain	0-3
				4p	loss	41-42
				4q	loss	113-114
				5q	loss	49-181
				6q	loss	79-171
				6q	del	121-123
				8p	loss	0-47
				8q	loss	58-59
				9pq	loss	0-141
				9p	del	21-25
				11p	loss	0-51
				11q	loss	118-123
				11q	loss	128-135
				12p	loss	13-14
				13pq	gain	0-115
				14q	loss	54-76
				14q	del	68-69
				14q	del	55-56
				16p	loss	1-2
				16p	loss	3-6
				16p	loss	34-35
				17p	loss	0-22

				17q	loss	55-56
				18pq	loss	0-78
				21q	loss	25-27
				21q	loss	29-34
				22q	loss	27-29
MDACC 20031	MUT	pTa, G2	0	-	-	-
MDACC 20099	MUT	pT1, G2	4	2q	gain	107-108
				4p	gain	1-6
				9q	loss	70-140
				20pq	gain	0-63
MDACC 20107	MUT	pTa, G2	6	9pq	loss	0-140
				9p	del	20-23
				17p	loss	0-22
				17q	gain	35-40
				17q	gain	44-62
				17q	loss	73-81
MDACC 20167	MUT	pTa, G2	0	-	-	-
MDACC 20363	MUT	pT1, G3	7	2q	loss	120-153
				4p	loss	0-3
				6p	gain	0-34
				7p	gain	16-17
				9q	loss	69-131
				14q	loss	101-105
				Y	gain	0-19
MDACC 20586	MUT	pTa, G2	2	4q	loss	177-178
				15q	loss	50-51
MDACC 20711	MUT	pT1, G3	13	1q	gain	244-246
				3q	gain	174-175
				4p	gain	0-3
				4p	gain	6-18
				4p	loss	21-30
				4q	loss	181-191
				4q	del	184-185
				8q	gain	86-146
				9q	loss	81-113
				14q	loss	61-78
				17p	loss	0-17
				20q	gain	41-43
				20q	amp	49-54
MDACC 20837	MUT	pT2, G3	3	4q	loss	73-74
				9pq	loss	0-141
				9p	del	20-22
MDACC 21460	MUT	pTa, G2-3	1	1q	gain	144-249
MDACC 10066	WT	pTa, G2	9	4p	gain	0-12
				4p	loss	38-40
				8pq	gain	0-146
				9p	loss	22-24
				15pq	gain	0-102
				16q	gain	79-90
				17p	loss	0-16
				17q	gain	31-33
				18pq	loss	0-71
MDACC 10073	WT	pT1, G3	8	1q	gain	146-189
				1q	gain	153-180
				8q	amp	102-103
				9p	loss	22-24
				11q	gain	69-71
				13q	gain	31-38
				13q	loss	38-56
				17p	loss	0-22
MDACC 10079	WT	pTa, G3	1	10q	loss	84-128
MDACC 10089	WT	pT2, G3	14	1p	loss	0-120
				1q	gain	144-248

4pq	loss	0-190
4q	loss	175-177
5q	loss	55-56
7pq	gain	0-158
8pq	loss	0-146
9p	del	17-18
9p	del	21-22
9q	loss	70-140
14pq	loss	0-107
16pq	loss	0-90
18p	loss	9-10
20pq	gain	0-63

MDACC 20022	WT	pT3, G3	36	1p	gain	0-100
				1q	gain	144-154
				1q	gain	154-181
				2q	loss	214-242
				3p	loss	0-11
				3p	amp	11-14
				3p	gain	14-19
				3p	loss	19-21
				3p	gain	21-42
				3q	gain	100-197
				4p	loss	29-48
				5p	gain	0-37
				5q	loss	49-180
				5q	del	96-108
				6p	gain	0-24
				6q	loss	62-101
				8p	loss	0-36
				8p	gain	36-42
				10p	gain	0-12
				11p	gain	10-17
				12p	loss	9-35
				12q	loss	77-82
				13q	loss	34-54
				13q	del	48-51
				14q	gain	75-107
				16p	loss	0-15
				16q	loss	47-90
				17q	gain	61-81
				18q	gain	22-23
				19p	loss	0-24
				20p	loss	0-26
				20q	loss	32-41
				20q	amp	41-43
				20q	gain	43-52
				22q	gain	25-39
				22q	loss	39-51

MDACC 20044	WT	pT1, G3	4	1q	gain	148-152
				6p	gain	21-24
				8q	gain	100-106
				17q	gain	30-33

MDACC 20056	WT	pTa, G2	16	1p	loss	91-93
				4pq	gain	0-79
				4q	loss	79-111
				4q	del	100-102
				4q	gain	111-190
				6q	loss	92-141
				9p	loss	0-38
				9p	del	8-9
				9q	loss	130-134
				10q	loss	53-135
				15q	loss	23-56
				15q	loss	75-76
				16pq	gain	0-90
				17p	loss	0-19
				20pq	gain	0-63
				Xp	loss	42-45

MDACC 20066	WT	pT1, G3	34	1p	gain	31-43
-------------	----	---------	----	----	------	-------

1q	gain	146-169
2p	del	15-16
2q	gain	156-161
2q	loss	206-242
3p	gain	0-32
3p	gain	32-45
3q	gain	110-198
4pq	loss	8-74
5p	gain	0-46
5q	loss	49-180
6pq	loss	39-170
7p	gain	0-57
8p	loss	20-21
8pq	gain	35-146
9p	gain	12-16
9q	loss	103-104
10p	gain	0-38
10q	loss	42-135
12p	gain	0-44
12q	loss	47-133
13q	gain	41-115
13q	del	49-53
14q	gain	47-48
16pq	loss	0-90
17q	gain	65-81
18pq	gain	8-20
18q	loss	20-22
18q	gain	22-30
18q	loss	30-78
19q	gain	28-35
20p	gain	0-26
22q	loss	41-51
Y	del	3-5

MDACC 20097	WT	pTa, G2	0	-	-	-
-------------	----	---------	---	---	---	---

MDACC 20129	WT	pTa, G2	9	2q	loss	120-243
				3p	loss	47-90
				9q	loss	69-140
				10q	gain	110-135
				11pq	loss	0-135
				14q	loss	56-78
				17p	loss	0-21
				17pq	gain	21-81
				Y	gain	3-29

MDACC 20140	WT	pTa, G2	0	-	-	-
-------------	----	---------	---	---	---	---

MDACC 20180	WT	pTa, G2	11	2p	amp	9-10
				5p	loss	12-13
				5q	loss	140-180
				8pq	gain	0-145
				9p	del	22-25
				9q	loss	70-128
				11q	amp	69-70
				13q	loss	69-70
				20pq	gain	0-63
				Xq	gain	114-154
				Y	gain	3-29

**Supplementary Table 5.** Clinicopathologic characteristics of 34 patients treated with transurethral resection for papillary non-muscle invasive urothelial carcinoma of the bladder.

	All (n; %)	STAG2 status of tumor		p-value
		Positive (n; %)	Negative (n; %)	
<b>Number of patients</b>	34 (100)	26 (76)	8 (24)	
<b>Age</b>				0.06
Median (years)	67	69	63	
<b>Gender</b>				0.36
Male	29 (85)	23 (88)	6 (75)	
Female	5 (15)	3 (12)	2 (25)	
<b>Pathologic stage</b>				0.73
pTa	23 (68)	18 (69)	5 (63)	
pT1	11 (32)	8 (31)	3 (37)	
pT2-T4	0 (0)	0 (0)	0 (0)	
<b>Pathologic grade</b>				0.94
Low	30 (88)	23 (88)	7 (88)	
High	4 (12)	3 (12)	1 (12)	
<b>Intravesical therapy</b>				0.36
Yes	24 (71)	19 (73)	5 (63)	
No	8 (24)	5 (19)	3 (37)	
Unknown	2 (6)	2 (8)	0 (0)	
<b>Recurrence during follow-up</b>				
Yes	16 (47)	15 (58)	1 (12)	
No	18 (53)	11 (42)	7 (88)	
<b>Highest stage of recurrence</b>				
Local, non-invasive	10 (63)	9 (60)	1 (100)	
Local, invasive	2 (12)	2 (13)	0 (0)	
Distant metastasis	4 (25)	4 (27)	0 (0)	

Pathologic grading and staging in accordance with the 2004 WHO/ISUP classification of bladder cancer: Ta, non-invasive papillary carcinoma; T1, tumor invades subepithelial connective tissue; T2, tumor invades muscularis propria; T3, tumor invades perivesical tissue; T4, tumor invades prostatic stroma, uterus, vagina, pelvic or abdominal wall. Intravesical therapy included either BCG, mitomycin C, or thiotepa. All p-values reported in this table are two-tailed unpaired t-test comparisons of the indicated variables in STAG2 positive versus negative tumors.

**Supplementary Table 6.** Clinicopathologic characteristics of 349 patients treated with radical cystectomy for invasive urothelial carcinoma of the bladder.

	All (n; %)	STAG2 status of tumor		p-value
		Positive (n; %)	Negative (n; %)	
<b>Number of patients</b>	349	314 (90)	35 (10)	
<b>Age</b>				0.94
Median (years)	66	65	66	
<b>Gender</b>				0.12
Male	283 (81)	258 (82)	25 (71)	
Female	66 (19)	56 (18)	10 (29)	
<b>Pathologic stage</b>				0.97
pT1	38 (11)	36 (11)	2 (6)	
pT2	75 (21)	65 (21)	10 (26)	
pT3	147 (42)	132 (42)	15 (43)	
pT4	89 (25)	81 (26)	8 (23)	
<b>Lymph node status</b>				0.09
LN negative	211 (60)	194 (62)	17 (49)	
LN positive	138 (40)	120 (38)	18 (51)	
				<b>0.03</b>
pN0	211 (61)	194 (62)	17 (49)	
pN1	50 (14)	46 (15)	4 (11)	
pN2	84 (24)	72 (23)	12 (34)	
pN3	4 (1)	2 (1)	2 (6)	

Pathologic staging in accordance with the 2004 WHO/ISUP classification of bladder cancer: T1, tumor invades subepithelial connective tissue; T2, tumor invades muscularis propria; T3, tumor invades perivesical tissue; T4, tumor invades prostatic stroma, uterus, vagina, pelvic or abdominal wall; N0, no LN metastasis; N1, single regional LN metastasis; N2, multiple regional LN metastases; N3, metastasis to LN outside of pelvis. All p-values reported in this table are two-tailed unpaired t-test comparisons of the indicated variables in STAG2 positive versus negative tumors.